universität wien

MASTERARBEIT / MASTER'S THESIS

Titel der Masterarbeit / Title of the Master's Thesis

„DNA Methylation Analysis of Potential Molecular Markers in Glioblastoma“

verfasst von / submitted by

Daniel Berger, BSc

angestrebter akademischer Grad / in partial fulfilment of the requirements for the degree of

Master of Science (MSc)

Wien, 2023 / Vienna 2023

Studienkennzahl lt. Studienblatt / degree programme code as it appears on the student record sheet:	A 066 862
Studienrichtung lt. Studienblatt / degree programme as it appears on the student record sheet:	Masterstudium Chemie UG2002, Version 2019W
Betreut von / Supervisor:	Univ.-Prof. Mag. Dr. Margit Cichna-Markl

Acknowledgement

First, I would like to express my sincere gratitude to Univ.-Prof. Mag. Dr. Cichna-Markl who supervised and supported me throughout my work. Thank you for always being patient and motivating, and letting me be a part of this exciting project.

Next, I would like to thank my colleagues in the Cichna-Markl working group. I specifically want to point out Katja Zappe, MSc whose great knowledge and laboratory expertise was an immense help to my project. Special thanks go to Katharina Pühringer und Simon Pflug who made my introduction to the required lab work easy and enjoyable. I would also like to thank Stefanie Pezelj whose fellowship made my time in the working group much more enjoyable.

Finally, I would like to thank all the people who contributed to this thesis in any way. Deep thanks to Marina Kujundzic who supported me throughout my academic journey and suggested a number of improvements, thus helping to make this work a little better. I would also like to thank Jana Korbach and my brother Alexander Berger for proofreading this work and still discovering mistakes that had been overlooked before. Last but not least I would like to thank my core family, including my parents and grandparents, for always supporting me during my studies.

Table of Contents

Acknowledgement i
1 Introduction 1
1.1 Cancer 1
1.2 Glioblastoma multiforme 2
1.3 Temozolomide 3
1.3.1 GBM treatment with temozolomide 3
1.3.2 Temozolomide resistance 4
1.3.3 Temozolomide and MGMT 6
1.4 Epigenetics 7
1.4.1 DNA methylation 7
1.4.2 DNA methylation in cancer 8
1.5 Genes and corresponding proteins 9
1.5.1 MGMT enhancers 9
1.5.2 ATP-binding cassette transporters (ABC-transporters) 10
1.5.3 Cyclin-dependent kinase inhibitor 2A (CDKN2A, p16) 11
1.5.4 Gastrulation brain homeobox 2 (GBX2) 11
1.6 Theoretical background 12
1.6.1 Bisulfite conversion 12
1.6.2 Polymerase chain reaction (PCR) 13
1.6.3 Pyrosequencing (PSQ) 15
1.6.4 Primer design 17
2 Aims of the Thesis 18
3 Materials and Methods 19
3.1 General setup 19
3.2 Samples 19
3.3 Method development and optimization 23
3.3.1 Primer design 23
3.3.2 Polymerase chain reaction (PCR) 24
3.3.3 Pyrosequencing (PSQ) 25
3.3.4 Data analysis 26
4 Results & Discussion 28
4.1 Development and optimization of PSQ assays 28
4.1.1 MGMT enhancers 28
4.1.2 ABC-transporters 30

4.1.3 p16 ... 32
4.1.4 GBX2 ... 34
4.2 Analysis of the DNA methylation status in GBM samples ... 41
4.2.1 Methylation of the MGMT promoter ... 41
4.2.2 Methylation of the MGMT enhancers ... 44
4.2.3 Methylation of ABC-transporters ... 52
4.2.4 Methylation of p16 ... 57
5 Conclusion ... **64**
6 References ... **66**
7 Appendix ... **78**
7.1 Abstract ... 78
7.2 Zusammenfassung ... 79
7.3 Supplementary information ... 80
7.3.1 Overview of methods ... 80
7.3.2 Raw data ... 93
7.3.3 Chemicals and kits ... 121
7.3.4 Disposables ... 121
7.3.5 Laboratory equipment ... 122
7.3.6 Webtools and databases ... 122
7.3.7 Software ... 123
7.4 List of abbreviations ... 124
7.5 List of figures ... 127
7.6 List of tables ... 130

1 Introduction

1.1 Cancer

Cancer ranks as a leading cause of death with estimates of 19.3 million new cases and almost 10 million deaths worldwide in 2020. At the time, it was reported that female breast cancer was the most common type of cancer, with an estimated 2.3 million new cases (11.7%), closely followed by lung cancer (11.4%). However, lung cancer still is the leading cause of cancer death, with an estimated 1.8 million deaths (18%), whereas female breast cancer is the fifth leading cause of cancer death worldwide. Based on the GLOBOCAN (Global Cancer Observatory) estimates, 28.4 million cases are to be expected in 2040 globally, a 47% increase from 2020. This projection is mostly due to the general growth and continued aging of the population. This rising trend of cancer frequency and mortality suggests the burden of cancer as a major public health problem worldwide and indicates the need to improve the current strategies for cancer diagnosis and treatment.[1,2]

Cancer can be understood as a collection of diseases in which abnormal cells grow uncontrollably and spread to nearby tissues or other parts of the body.[3] The process of conversion from normal cells to cells capable of autonomous proliferation and invasion is called carcinogenesis. These abnormal cells are then able to form tumors, which disrupt the tissue they originated in or spread to other parts of the body, a process that is called metastasis. Carcinogenesis is caused by *e.g.* mutations in crucial genes that control the way our cells function. These mutations usually happen as a consequence of DNA damage and can be found in all daughter cells due to an inheritable change in DNA. Possible changes in the genome include: frame-shift or point mutations, overexpression or loss of a gene, and epigenetic modifications of which methylation of cytosine in CpG islands is the most important. It is essential to note that cancer does not develop all at once. Instead, multiple successive changes need to occur in critical cellular genes, each of them contributing to the malignant state.[4,5]

Two classes of genes have been found to play a major role in the process of triggering cancer: Proto-oncogenes increase cell division, whereas tumor suppressor genes suppress it. Together, these genes help control the cell cycle and coordinate the regulated growth of tissues. In their mutated form, proto-oncogenes become oncogenes and stimulate excessive cell division, which leads to an increase in the activity of proteins. Mutated tumor suppressor genes lose their function to encode critical tumor suppressor proteins, which normally inhibit excessive growth.[5]

1.2 Glioblastoma multiforme

Glioblastoma multiforme (GBM), a World Health Organization (WHO) grade IV glioma, is the most common and aggressive primary brain tumor, accounting for more than 60% of all brain tumors in adults and having a 5-year survival rate of 5%.[6,7] Patients with GBM usually suffer from headaches, seizures, confusion, memory loss or personality changes.[8] Despite rigorous therapeutic research and recent advances in therapy, there are no curative treatment options for GBM and the survival rate remains low. The median overall survival (OS) is less than 2 years.[9,10]

90% of all GBM cases occur *de novo* and are therefore known as primary GBM. They typically arise in older patients. In contrast to primary GBM, secondary GBM progress from precursors, such as low-grade astrocytoma. They make up 10% of all cases and usually have a better prognosis than primary GBM.[11,12] Since primary and secondary GBM show characteristic genetic alterations, they can be distinguished through molecular signatures. Typical alterations for primary GBM include the overexpression of the epidermal growth factor receptor (EGFR), phosphatase and tensin homolog (PTEN) mutations, and loss of chromosome 10. Isocitrate dehydrogenase-1 (IDH1) mutations, tumor protein p53 (TP53) mutations, as well as loss of chromosome 19 are commonly seen in secondary GBM. The most reliable molecular indicator to accurately differentiate primary from secondary GBM is the IDH1 mutation. The WHO classifies GBM into IDH-wildtype (primary GBM), IDH-mutant (secondary GBM), and glioblastoma not otherwise specified (NOS).[13–15]

Another important biomarker for GBM is the methylation status of the promoter of the repair protein MGMT (O^6-methylguanine-DNA methyltransferase). Methylation of the MGMT promoter and as a result epigenetic silencing of the repair protein is associated with an increase in OS of patients who received radiation therapy and alkylator chemotherapy with temozolomide (TMZ).[16–18] In 2005 Hegi *et. al.* showed that among patients, whose tumor contained a methylated MGMT promotor, the longest median OS of 21.7 months was observed when they were treated with both TMZ and radiotherapy. Access to only radiotherapy resulted in a median OS of 15.3 months, respectively. In contrast, the difference in OS of patients with an unmethylated MGMT promoter was only marginally significant between the two treatment options. Assignment to radiotherapy and TMZ offered a median OS of 12.7 months and 11.8 months with only radiotherapy as treatment, respectively. Since patients benefited from the concomitant treatment with TMZ, this therapeutic approach is currently the standard treatment option for GBM.[19]

1.3 Temozolomide

1.3.1 GBM treatment with temozolomide

TMZ is a small lipophilic molecule with a molecular weight of 194 Da. It is an orally available alkylating agent of the imidazotetrazine class and is also known by its tradenames Temodal® and Temodar®. The addition of TMZ to surgery and radiotherapy in order to treat GBM was demonstrated to extend the median OS of patients and thus TMZ received approval by the United States Food and Drug Administration (FDA) in 2005. It acts as a prodrug and is stable at acidic pH values, but labile at pH levels above 7.[20,21] Consequently, this process only occurs within a narrow pH window close to the physiological pH. Since the alkaline pH value within brain tumors is more favorable for TMZ prodrug activation, TMZ is mostly used to treat glioma.[22]

TMZ can be administered orally and is rapidly absorbed intact, but then breaks down spontaneously to monomethyl triazene 5-(3-methyltriazin-1-yl)-imidazole-4-carboxamide (MTIC) at alkaline pH values. MTIC reacts with water, forming 5-aminoimidazole-4-carboxamide (AIC) and the methyldiazonium cation. The highly reactive methyldiazonium cation transfers its methyl group to guanine and adenine residues and thereby elicits the cytotoxic effect of TMZ (see **Figure 1**).[22–24]

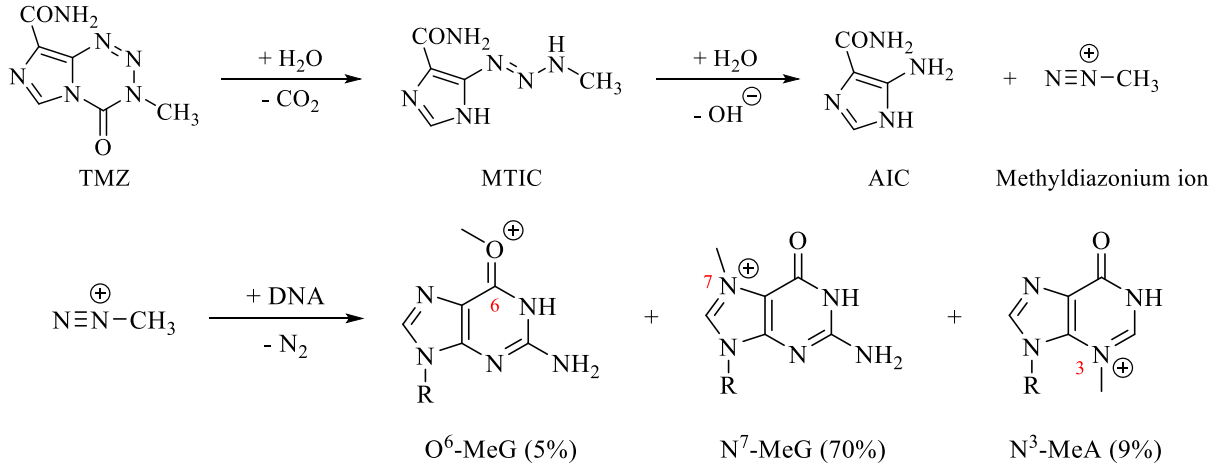

Figure 1: Prodrug activation of temozolomide and its effects on DNA.

Methylation of DNA caused by TMZ occurs at several nucleophilic sites, generating approximately 70% N^7-methylguanine (N^7-MeG), 9% N^3-methyladenine (N^3-MeA), and 5% O^6-methylguanine (O^6-MeG).[25,26] Although N-methylation is more abundant than O^6-MeG, its therapeutic value is not as pronounced since the associated lesions are successfully excised by the base excision repair (BER) pathway. The effectiveness of TMZ as an anti-cancer agent is

solely attributed to the formation of O^6-MeG, which mispairs with thymine instead of cytosine. This mutation is recognized by the mismatch repair (MMR) system, which only excises newly synthesized DNA strands, keeping the original O^6-MeG intact. Consequently, repetitive futile MMR cycles lead to double-strand breaks (DSB) during subsequent DNA replication, inducing cytotoxicity and finally apoptosis. Therefore, a functional MMR mechanism is needed for the pharmacological effect of TMZ. However, increasing evidence shows that tumors can become resistant to TMZ, allowing tumor progression during treatment.[27–29]

1.3.2 Temozolomide resistance

Even though TMZ has shown benefits in the treatment of GBM patients, inherent or acquired resistances still present major obstacles for successful treatment. DNA repair mechanisms that are impacting the mechanism of action and cytotoxicity are: direct repair (by MGMT), mismatch repair (MMR), and base excision repair (BER).[28,29]

The removal of methyl groups from O^6-MeG lesions by the DNA repair protein MGMT is the best-documented mechanism of TMZ resistance. The methyl group attached to the O^6-position can be transferred to the cysteine residue in the active center of MGMT. There, the C-O bond is cleaved in a substitution reaction resulting in a mixed thioether product, repairing DNA in the process. Thus, the methylated repair protein is now inactive and subsequently degraded through the ubiquitin/proteasomal system (see **Figure 2**). For that reason, MGMT is consumed stoichiometrically during this mechanism, a process known as suicide inhibition. Consequently, the inactivation of the repair protein has a beneficial effect on TMZ treatment.[30,31]

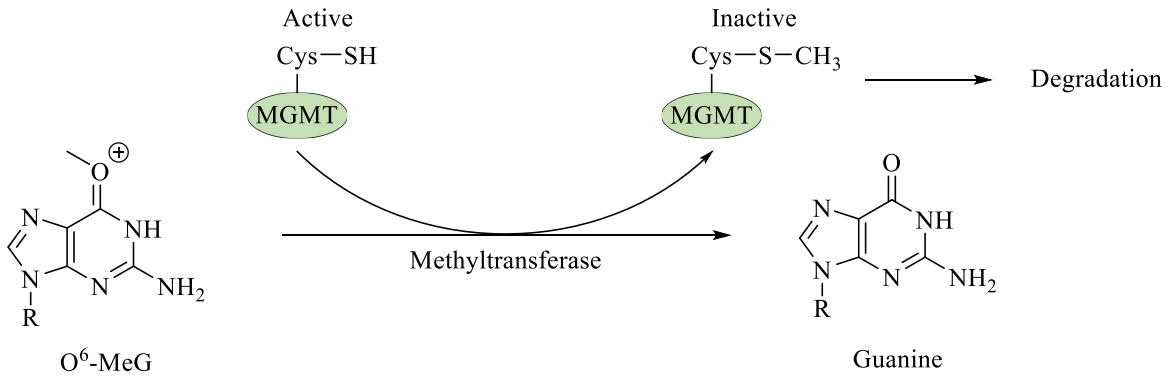

Figure 2: MGMT repair mechanism of O^6-MeG.

In contrast, when MGMT is not able to successfully repair O^6-MeG, it is instead recognized by the MMR system. As previously stated, an intact MMR apparatus is required for a good response to TMZ, along with low levels of MGMT. MMR repairs damage to DNA by correcting base substitution mutations and small insertions/deletions arising during replication. These

mismatches are first recognized by the heterodimers MSH2 and MSH6, and then repaired by another heterodimeric complex consisting of MLH1 and PMS2. However, MMR-deficient cells tolerate these mismatches and do not induce apoptosis as a result. O^6-MeG remains undisturbed, and the cells survive TMZ treatment, increasing the risk of mutagenesis. Mutations of MMR genes like MSH2, MSH6, MLH1, and PMS2 lead to an impaired MMR pathway.[32,33] For instance, Hunter *et. al.* discovered MSH6 mutations in recurrent GBM tissues after TMZ treatment, indicating that MSH6 mutations mediate TMZ resistance.[34]

The BER system is a major pathway that repairs single nucleotide modifications generated by alkylating agents, ionizing radiation, and reactive oxygen species. TMZ-induced N^7-MeG and N^3-MeA are recognized by the BER pathway and subsequently repaired. If the BER apparatus is disrupted, these lesions become highly cytotoxic instead. Since N^7-MeG is the primary lesion caused by TMZ, an active BER plays a key role in TMZ resistance. DNA glycosylases, such as alkyl adenine DNA glycosylase (AAG), recognize and excise modified bases, thereby initiating the BER pathway. The damaged end is then cleaved, and the single nucleotide filled, completing the repair process.[35,36] **Figure 3** gives an overview of the mentioned DNA repair mechanisms commonly related to TMZ resistance.

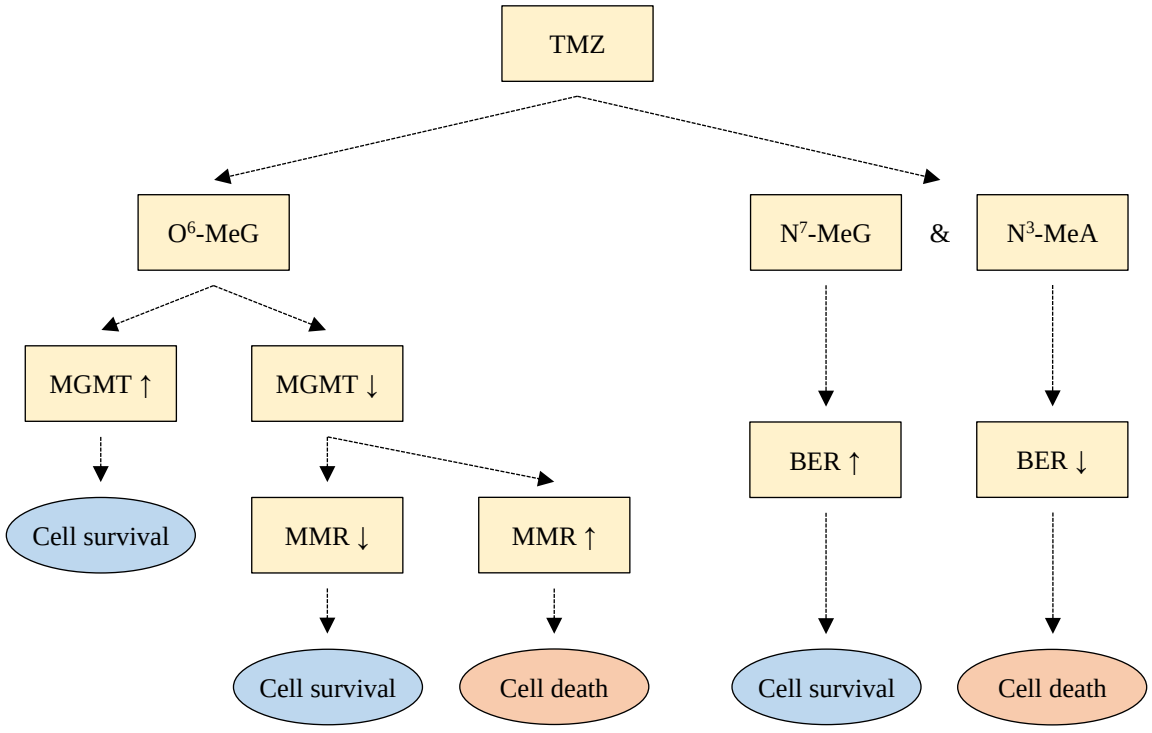

Figure 3: Representative scheme of DNA repair mechanisms related to TMZ resistance.

1.3.3 Temozolomide and MGMT

Promotor methylation and as a result epigenetic silencing of the MGMT gene have been associated with a longer OS median in GBM-patients, who received TMZ during and after the completion of radiotherapy.[37] The MGMT gene is located on chromosome 10q26 and encodes a DNA-repair protein that usually prevents the genotoxic effects of O^6-alkylguanine adducts by removing the alkyl groups from guanine, a target site for TMZ. This repair mechanism is suppressed by epigenetic silencing of the MGMT protein by promoter methylation.[38,39] Furthermore, MGMT promoter methylation has been detected in many different tumor types, which is consistent with the observation that gene silencing by DNA methylation is an early and common mechanism by which tumor suppressor genes are inactivated during malignant progression. Consequently, MGMT promoter methylation and MGMT expression have emerged as important prognostic biomarkers for the success of TMZ treatment.[40–42]

However, conflicting data have been reported and thus the best method to determine the MGMT status in patients is still a matter of debate. Even though a negative correlation between promoter methylation and expression has been demonstrated in a multitude of studies, there are still inconsistencies between MGMT promoter methylation status, MGMT protein/gene expression, and patient outcome.[43–46] Butler *et. al.* suggested the combined use of promoter methylation and expression status as an accurate prediction of patient outcome, especially for patients with inconsistent MGMT methylation and expression.[47] Hegi *et. al.* questioned whether MGMT promoter methylation provides clinical use yet and argued that it should not be used presently to determine whether to use TMZ on a patient or not. Additionally, there are currently no effective alternative treatment options for patients with an unmethylated MGMT promoter, making it not clinically relevant as of now.[48] Spiegl-Kreinecker *et. al.* emphasized the use of MGMT expression as the superior predictive marker for TMZ response in GBM-patients. In their study, several tumor cell samples did not follow the typical negative correlation between promoter methylation and expression. Tumors of several patients with methylated MGMT promoters showed MGMT expression and vice versa. The reasons for this discrepancy are unclear so far.[49]

Although the MGMT status has been used as a biomarker in clinical trials for some time, its clinical utility suffers from a number of limitations that hinder its use for prognostic evaluation or treatment decision-making. As a result, analytical methods need to be improved to increase the utility of MGMT promoter methylation as a diagnostic tool for personalizing GBM treatment.[50]

1.4 Epigenetics

Historically, the term “epigenetics” was first coined by British biologist Conrad Waddington (1905-1975) and was used to describe events that could not be explained by genetic principles.[51,52] Epigenetics was seen as a branch of biology in which interactions between genes and their products should be studied. Today, epigenetics is defined as the study of heritable changes in the expression of the genome that are not based on changes in the primary DNA sequence. These modifications play an important role in developmental pathways. Moreover, they have also been associated with numerous diseases, including cancer. Three primary mechanisms are responsible for epigenetic modifications in mammalian cells: DNA methylation, histone modifications, and RNA-based processes.[53,54] In the following section DNA methylation and its involvement in cancer development and progression shall be explained in detail.

1.4.1 DNA methylation

DNA methylation is an epigenetic mechanism by which a methyl group is added to DNA, thereby altering gene functions and affecting gene expression. It is primarily found on the 5’ position of cytosine bases that form a CpG dinucleotide with a subsequent guanine base. As a result, 5-methylcytosine (5mC) is formed. The DNA methyltransferase (DNMT) family of enzymes catalyzes this reaction by transferring a methyl group from S-adenosyl methionine (SAM) to the fifth carbon of a cytosine residue (see **Figure 4**).[55,56]

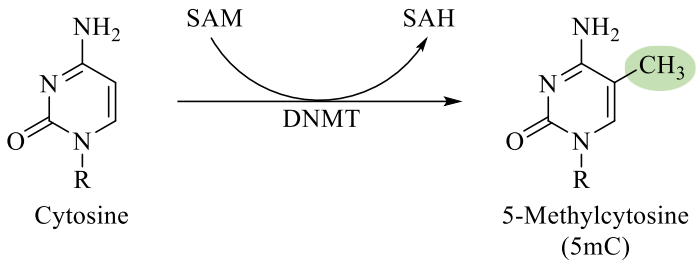

Figure 4: Methylation of cytosine by DNA methyltransferases (DNMTs).

CpG dinucleotides are actually quite uncommon, making up 1-2% of all dinucleotides in mammalian sequences, of which about 70% are methylated.[57] It is assumed that mutations have progressively depleted them over the course of evolution, which would explain their general scarcity. However, there are regions in the genome called CpG islands (CGIs) where CpGs can be found in high densities. These stretches of DNA are roughly 1000 base pairs long. CGIs reside in about 60-70% of all human gene promoters and the vast majority of them are unmethylated.[58,59] Their location and preservation have been highly conserved throughout

evolution, which implies that these regions are of functional importance, such as the control of gene expression.[60] Moreover, the methylation of promoter-associated CGIs can suppress gene expression, which leads to long-term silencing of the affected gene. This process and the resulting transcriptional regulation play an important role in many cellular processes, such as X chromosome inactivation in female mammals.[61,62]

1.4.2 DNA methylation in cancer

A characteristic methylation pattern that can be found in many types of human cancers is the hypermethylation of normally unmethylated promotor CGIs and a global hypomethylation (see **Figure 5**). Cancer cells contain approximately 20-60% less 5mC than their normal counterparts. Hypomethylation in malignant cells is usually found in the coding region, introns, and repetitive DNA sequences.[63] Hypermethylation of CGIs in promoter regions generally leads to the inactivation of tumor suppressor genes (*e.g.* MGMT), which has been reported in numerous studies. Additional examples of inactivated tumor suppressor genes include BRCA1, MLH1, p16INK4a, RB1 and VHL1.[64–69] Moreover, hypermethylation in the promoter region often involves multiple genes simultaneously, suggesting the existence of a hypermethylator phenotype. It is known as the CpG island methylator phenotype (CIMP) and was initially elucidated in colon cancer.[70] In contrast, the oncogene promoter tends to be hypomethylated during tumorigenesis resulting in transcriptional activation. This leads to overexpression of oncogenes and has been linked to the emergence of cancer in multiple studies.[71–73] Thus, hyper- and hypomethylation of CGIs in promoter regions clearly indicate that epigenetic mechanisms play a very important role in tumorigenesis.

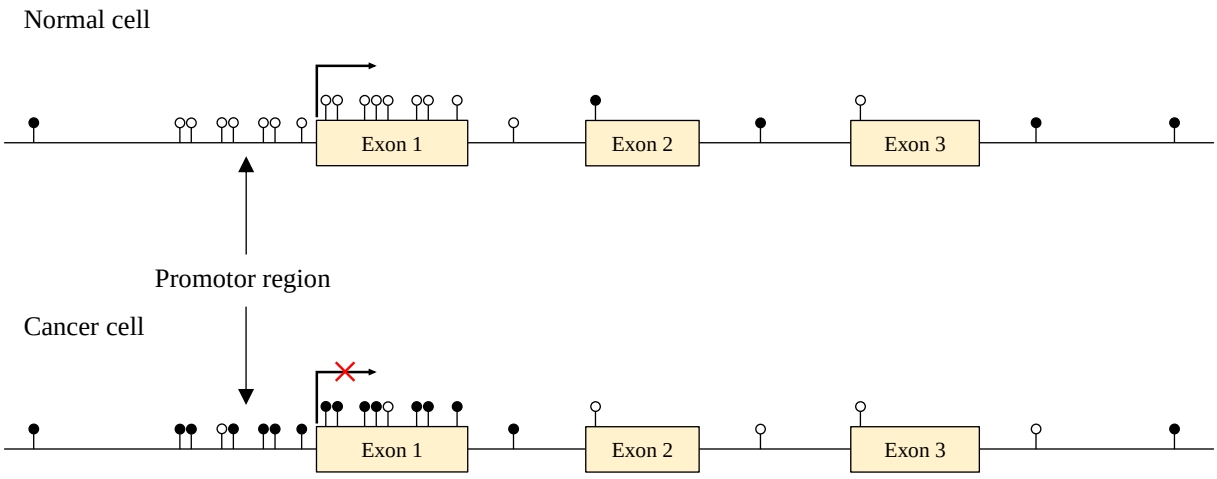

Figure 5: Methylation patterns in normal and cancer cells. White cycles represent unmethylated CpGs, black circles methylated CpGs. Transcription start site marked by a black arrow, which is repressed by hypermethylation. Modified from [53].

1.5 Genes and corresponding proteins

Over the years more and more biomarkers in GBM tumorigenesis have been identified due to advancements in genomics and proteomics. They have many potential applications, such as determination of prognosis and prediction of response to treatment. However, reliable early-stage diagnostic biomarkers for GBMs have not been identified yet.[74,75] Major biomarkers that have been associated with GBM are MGMT[76], EGFR[77], and IDH[78]. In this section the following potential biomarkers will be discussed in detail: MGMT enhancers, ATP-binding cassette transporters (ABC transporters), cyclin-dependent kinase inhibitor 2A (CDKN2A), and gastrulation brain homeobox 2 (GBX2).

1.5.1 MGMT enhancers

As previously stated, there are cases where the MGMT promoter methylation status and protein expression do not show the expected negative correlation. Furthermore, not all GBM patients showing a hypermethylated MGMT promoter benefited from TMZ treatment, whereas some patients with unmethylated promoters did. These observations indicate that other mechanisms exist that can regulate MGMT expression and grant TMZ resistance. Identifying these additional regulation factors would help to improve clinical routine analysis and could provide a new basis for therapeutic strategies.[79–81] Some studies suggest that enhancer methylation is considerably altered in tumor cells and plays a role in the emergence of cancer.[82–84] For instance, Wickström *et. al.* reported that several target genes are regulated by an active enhancer in prostate cancer, altering tumor cell proliferation and invasion.[85] Enhancers and their associated transcription factors can regulate gene expression via a long-range interaction with their related promoters. They can be located thousands of base pairs away from the promoter region, upstream or downstream from the start site.[86] However, few studies have investigated the long-range regulation network of the MGMT enhancer so far. He *et. al.* identified a novel enhancer that is located between the marker of proliferation Ki67 (MKI67) and the MGMT promoter. Ki67, a proliferation marker in GBM and other cancer types, is encoded by MKI67. Its overexpression has been linked to a significant decrease in TMZ sensitivity, suggesting its involvement in the gene network regulated by the MGMT enhancer. Activation of this enhancer led to increased MGMT expression, even if the associated promoter is hypermethylated. Moreover, deletion of the investigated enhancer reduced expression of MGMT. Additionally, brain tumor cells without the presence of the enhancer were sensitive to TMZ and showed a reduced growth rate. In summary, He *et. al.* suggest that the assessment of the novel MGMT enhancer might be useful as a predictive biomarker.[87]

1.5.2 ATP-binding cassette transporters (ABC-transporters)

Adenosine triphosphate (ATP)-binding cassette (ABC) transporters comprise a large family of selective transmembrane transporter proteins, which are involved in the transport of a variety of substrates across extra- and intracellular membranes. They consist of four core domains: two transmembrane domains (TMDs) and two ATP binding cassettes, also known as nucleotide binding domains (NBDs). Based on their sequence homology and structural organization, ABC-transporters have been divided into seven subfamilies (ABCA-ABCG).[88,89] By functioning as efflux pumps, they lower the intracellular accumulation of various anti-cancer drugs and play a crucial role in multi drug resistance (MDR) of cancers. Overexpression of ABC-transporters has been linked to a number of clinical problems, including cystic fibrosis, neurological diseases, and limited efficacy of anti-cancer drugs.[90,91]

ABCA7 is a member of the ATP-binding cassette subfamily A, which contains twelve full transporters. Its gene is located on chromosome 19p13.3 and includes 47 exons. It was first identified by Kaminski *et. al.* in 2000 who detected high ABCA7 mRNA levels predominantly in myeloid and lymphoid tissues including peripheral leukocytes, thymus, spleen, and bone marrow. Their findings suggest a role for ABCA7 in transmembrane lipid transport processes, like ABCA1, which has 54% protein sequence homology with ABCA7.[92] A few studies have pointed out an association of ABCA7 with various types of diseases.[93,94] For instance, higher ABCA7 mRNA levels have been found in ovarian cancer[95] and were linked to a poorer general survival rate.[96] In addition, ABCA7 has been identified as one of the most important risk genes of both early-onset and late-onset Alzheimer's disease.[97]

ABCB1 is one of eleven members of the ABCB subfamily, and its gene is located on chromosome 7q21.12, consisting of 29 exons and 2 promoters. The promoter located in exon 2 and intron 2 is known as the "downstream" promoter and has been identified to be the major promoter, whereas the "upstream" promoter situated upstream of exon 1 is usually inactive in normal tissues.[98,99] ABCB1 overexpression has been reported in a number of cancer types including lung, colon, liver, and kidney malignancies.[100] Furthermore, overexpression of ABCB1 is considered a major cause of MDR.[101]

ABCG2 belongs to the ABCG subfamily, along with four other transporters. The ABCG2 gene is located on chromosome 4q22.1 and includes 16 exons.[102,103] High ABCG2 levels have been observed in lung, ovarian, and breast cancer.[104] Moreover, ABCG2 gene amplification has been associated with MDR in cancer cells, such as glioblastoma.[105,106] ABCB1 and ABCG2 are commonly co-expressed, however, they have been found to function independently.[107]

1.5.3 Cyclin-dependent kinase inhibitor 2A (CDKN2A, p16)

CDKN2A or p16 is an important cyclin-dependent kinase inhibitor and a tumor suppressor gene, located on chromosome 9p21. This gene locus is a 35 kb long multigene region and encodes three major tumor suppressor genes, namely p16, p15, and the MDM2 ubiquitin ligase inhibitor p14ARF.[108] Its main role is to regulate the cell cycle by blocking the traversal from G1 to S phase as a part of a multiprotein regulatory complex. It binds to the cyclin-dependent kinases (CDK) 4 and 6, and as a result inhibits the catalytic activity of the CDK4-6/cyclin D enzyme complexes, which are required for the phosphorylation of the retinoblastoma protein (Rb). Thus, p16 inhibits the activation of pRb and consequently prevents further transition of the cell cycle past the G1/S restriction point.[109,110] Therefore, p16 is needed for the control of unregulated cell growth and its inactivation would lead to the emergence of tumors.[111,112] Deletion of the 9p21 region causes various types of tumors indicating its potential as a predictive biomarker. p16 gene deletions are associated with mesotheliomas[113], bladder cancer[114], and glioblastoma[115] among others. Hypermethylation of the regulatory regions of the p16 gene offers an alternative mechanism for p16 inactivation. Hypermethylation of the p16 promoter region was identified as a major mechanism of tumor suppressor gene silencing and was found in several different cancer types, including breast[116], oral[117], and colon[118] cancer. Additionally, hypermethylation of p16 exon 2 has been linked to oesophageal[119], breast[120], and colon[121] cancer so far.

1.5.4 Gastrulation brain homeobox 2 (GBX2)

The homeobox family of transcription factors is known for its contribution to the control of cell identity and differentiation. They all contain a common DNA sequence motif, which is termed homeobox domain, encoding a 60-amino acid residue polypeptide. These encoded transcription factors recognize and bind to specific DNA sequences, with which homeobox genes can either positively or negatively regulate the expression of target genes.[122] GBX2 is located on chromosome 2q37.2 and is expressed in the forebrain during vertebrate brain development.[123] It has been reported that the pleiotropic cytokine IL-6, located on chromosome 7p21-14, is a downstream target of the GBX2 homeobox gene. It plays an important role in mediating cellular growth and differentiation, and its overexpression has been linked to the progression of several types of cancer.[124,125] Overexpression of GBX2 results in the stimulation of malignant growth of cancer cells and it is also involved in the up-regulation of the IL-6 gene as a mediator in this molecular pathway.[126–128] Interestingly, GBX2 has been found to act as a tumor suppressor in head and neck cancer[129], while being an oncogene in breast and prostate cancer.[130,131]

1.6 Theoretical background

In order to determine the methylation status of CpG dinucleotides in the described potential biomarkers via high resolution melting (HRM) or pyrosequencing (PSQ), certain preparatory steps are required first. The following section will give an overview of the theory and principles of the experiments employed as part of this master's thesis.

1.6.1 Bisulfite conversion

To begin with, bisulfite conversion of the DNA of interest needs to be carried out before polymerase chain reaction (PCR) and PSQ analysis. This is due to the fact that the enzyme used in PCR, DNA polymerase, is not able to discern the difference between methylated and unmethylated cytosines. Therefore, cytosine and 5mC need to be made distinguishable. This is done by adding bisulfite (SO_3^{2-}) at a low pH level to single-stranded DNA, which selectively deaminates cytosine, but ignores 5mC. This reaction is followed by desulfonation of the uracil sulfonate by alkali treatment, resulting in uracil as shown in **Figure 6**.

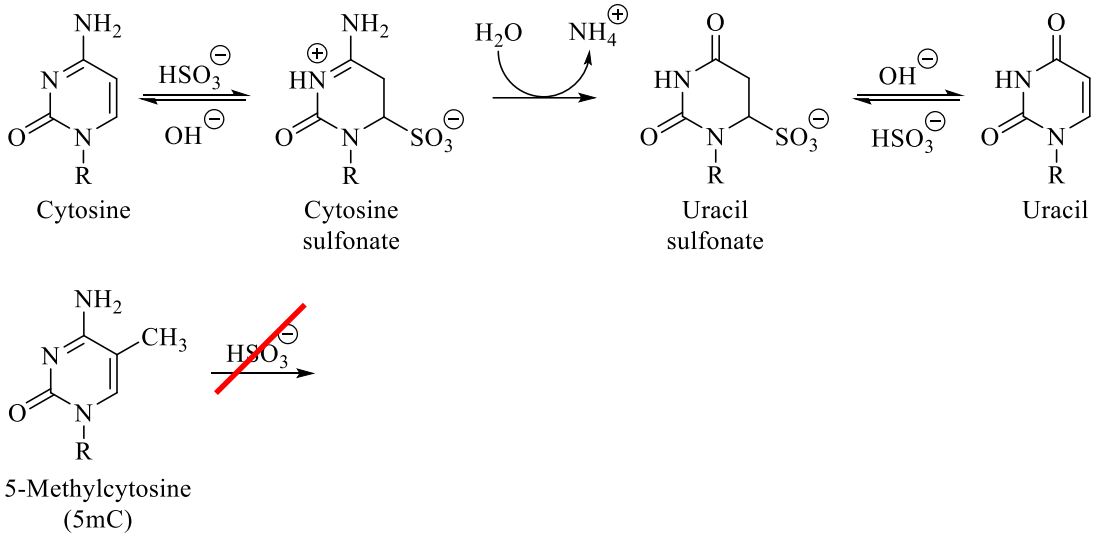

Figure 6: Bisulfite conversion of cytosine and 5-methylcytosine.

During subsequent PCR amplification the newly transformed uracil (marked red) is read as thymine and paired with adenosine, while methylated cytosine (marked blue) is read as cytosine and paired with guanine (see **Figure 7**). Since the two bisulfite converted DNA strands are not complementary anymore, four different DNA strands (a_c+a_c', b_c+b_c') could be generated during PCR amplification. Design of the primers decides if either a_c+a_c' or b_c+b_c' are produced.[132,133]

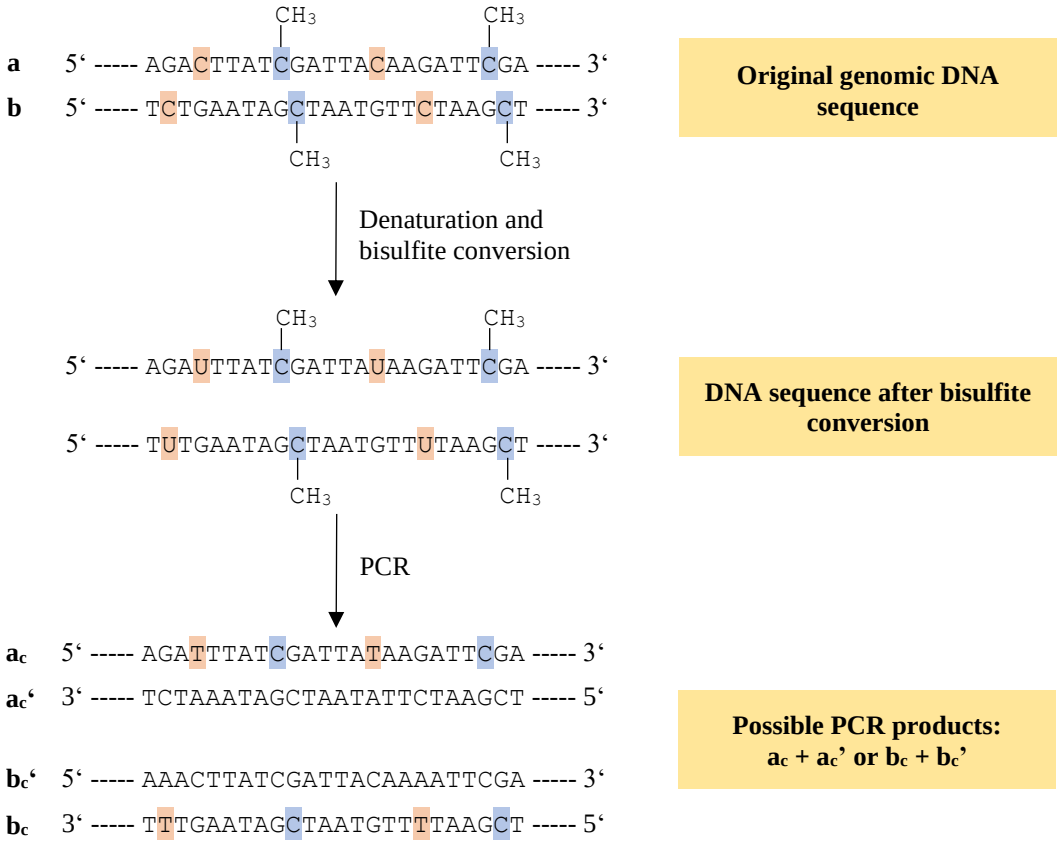

Figure 7: PCR amplification of bisulfite converted genomic DNA.

1.6.2 Polymerase chain reaction (PCR)

The polymerase chain reaction, first discovered by Kary B. Mullis in the early 1980s, is an *in vitro* technique for exponential amplification of specific DNA segments. This technique is based on the natural process of DNA replication, in which two identical DNA double strands are generated from a parental double-stranded DNA (dsDNA) template.[134]

Each PCR assay requires the following components: template DNA, oligonucleotide primers, deoxynucleoside triphosphates (dNTPs), and DNA polymerase. The nucleotides deoxyadenosine triphosphate (dATP), deoxycytidine triphosphate (dCTP), deoxyguanosine triphosphate (dGTP), and deoxythymidine triphosphate (dTTP) are used by the DNA polymerase, which connects them to the primers, building a new complementary strand according to the template. The primers, including forward (fw) and reverse (rev) primers, act as a starting point for the DNA polymerase, defining the amplified target region.[135]

A single PCR cycle consists of three steps: denaturation of the dsDNA template by heat, annealing of the primers to the single-stranded DNA (ssDNA) sequence(s), and extension of the annealed primers.[136]

1. *Denaturation.* Initially, the dsDNA template is heated above the melting point of the two complementary DNA strands of the target DNA, which leads to the separation of the two strands. The required temperature correlates positively with the G+C content of the target DNA. The denaturation is performed at 95 °C in PCRs catalyzed by Taq DNA polymerase.

2. *Annealing.* In the second step, the temperature is then lowered allowing the primers to bind to the ssDNA template via hydrogen bonding. The method-specific annealing temperature (T_a) is dependent on the length and base composition of the primers and needs to be determined for each primer pair individually. Generally, annealing is performed 3-5 °C below the melting temperature (T_m) of the used primers. If T_a is too low, mismatches may occur, which leads to nonspecific PCR amplification. Conversely, too high T_a reduces the reaction efficiency by preventing primer annealing.

3. *Extension.* Finally, the temperature is raised again, allowing the thermostable DNA polymerase to extend the primers and form the desired PCR product. The required elongation temperature (T_e) depends on the used DNA polymerase and primers. Taq DNA polymerase has its temperature optimum at 72 °C.

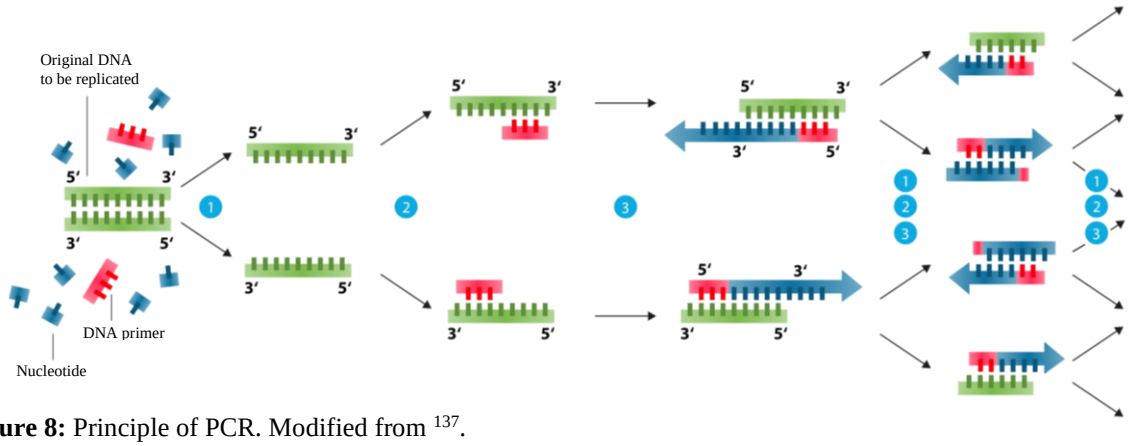

Figure 8: Principle of PCR. Modified from [137].

Although an exponential amplification of DNA (2*n* amplicons after *n* cycles) is expected in theory, this will only be achieved in an exponential phase under real conditions. The amplification efficiency will eventually drop due to product inhibition or reduced reagent concentration, bringing the reaction into a linear phase.[136]

In order to detect and quantify the desired PCR product while it is being synthesized, real-time quantitative PCR (real-time qPCR) is used. It is performed in a thermal cycler that is able to measure the emitted fluorescence through a detector module. The intensity of the measured signal reflects the current amount of DNA amplicons. The two methods for the detection and

quantification of the amplified DNA fragments are non-specific fluorescent DNA dyes and fluorescently labeled sequence-specific DNA probes.[136]

HRM is a quantitative post-PCR analysis method, enabling the quantification of DNA methylation levels in DNA fragments according to the shape of their melt curves. Intercalating fluorescent dyes, such as EvaGreen, are required in order to obtain HRM melting curves. After PCR, the amplicons are gradually heated up to around 95 °C, denaturing in the process. In the absence of dsDNA, the intercalating dye molecules are not able to bind to anything and as a result fluoresce only at a low level. This process is detected, and characteristic melting curves are generated by plotting the fluorescence signal against the temperature. Even a single base change in the targeted DNA sequence causes deviations in the HRM curve. However, in contrast to the PSQ method, HRM methylation analysis is only able to identify the overall methylation status, instead of the methylation status of individual CpG sites.[138,139]

1.6.3 Pyrosequencing (PSQ)

Pyrosequencing, a sequencing-by-synthesis technique, is commonly used for the detection of single nucleotide polymorphisms (SNPs) or bisulfite modified CpG sites in a given DNA sequence. Making use of a mixture of enzymes, this method relies on the luminometric detection of inorganic pyrophosphate (PP_i) released upon the incorporation of a single nucleotide into the growing DNA double strand. This enzymatic reaction cascade was first described by Nyrén and Hyman in the 1990's.[140,141]

The four enzymes included in the pyrosequencing system are DNA polymerase, ATP sulfurylase, luciferase, and apyrase. The reaction mixture also contains adenosine-5'-phosphosulfate (APS), luciferin, and the template, a ssDNA amplicon. Therefore, during PCR amplification one of the employed primers (fw or rev) must be marked with a biotin-label allowing the isolation of the ssDNA sequencing template. Additionally, a third primer, the sequencing (seq) primer, is needed to mark the starting point of the pyrosequencing reaction. The building blocks consist of four different dNTPs, but 2'-deoxyadenosine-5'-(alpha-thio)-triphosphate (dATPαS) is used instead of dATP, as the latter would be recognized by luciferase causing light generation and generating false signals.[141]

After isolation of the ssDNA template by binding of the biotinylated primer to streptavidin-coated beads, the sequencing primer is annealed to the template. DNA polymerase attaches to the 3' end of the primer and starts incorporating the respective dNTP complementary to the target strand. The dNTPs are sequentially dispensed and release PP_i if they can be incorporated into the growing DNA strand. The released PP_i acts as a substrate for ATP sulfurylase,

generating ATP and sulfate in the process. Then, ATP is hydrolyzed by luciferase, which in turn activates the conversion of luciferin to oxyluciferin, emitting light as part of the reaction. The emitted light intensity is proportional to the amount of produced PP_i, which is directly proportional to the number of incorporated dNTPs. Consequently, a signal is only produced if the correct nucleotide is added. Before the addition of the next dNTP, excess ATP and dNTPs are removed by the addition of apyrase (see **Figure 9**).[142]

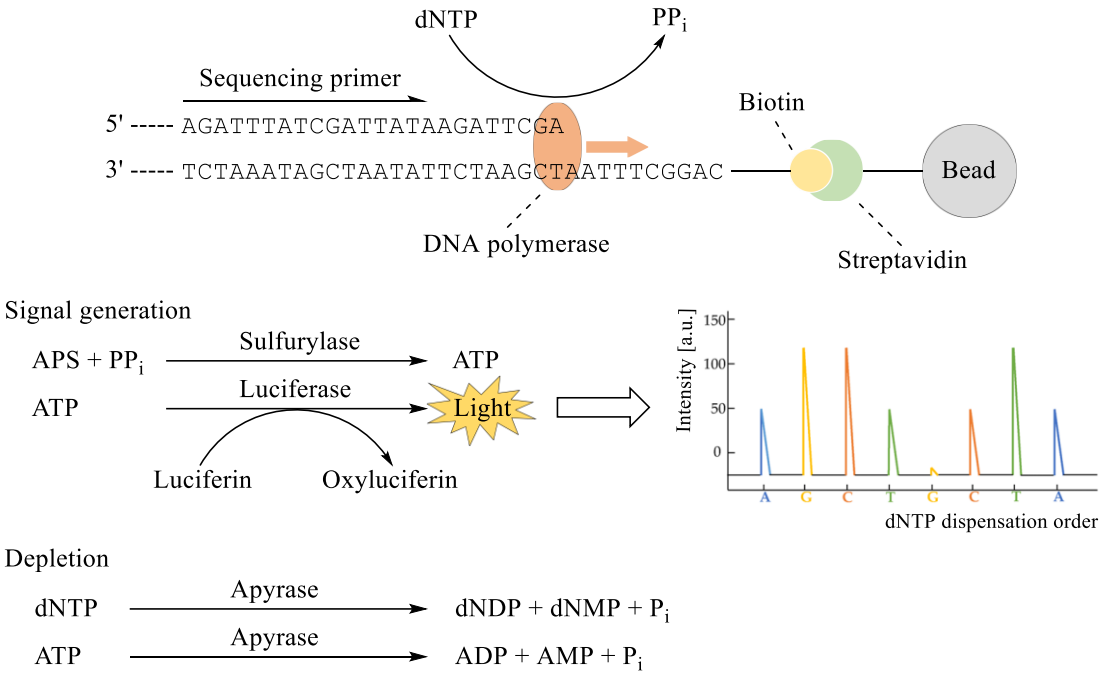

Figure 9: Overview of the enzymatic cascade during pyrosequencing. Modified from [143].

In order to analyze the CpG methylation status via PSQ, one of the primers used during PCR amplification needs to be modified with biotin at its 5' end, generating biotinylated DNA sequences. Depending on which primer is biotinylated, the associated assay is either called "forward" or "reverse" assay. If the forward primer is biotinylated, the sequencing primer is extended according to the reverse strand, and the associated assay is a reverse assay. If the reverse primer is biotinylated, the sequencing primer acts as the starting point for the forward strand, and the associated assay is a forward assay. Moreover, the primer pairs can be designed for the bisulfite-converted genomic upper or lower strand, resulting in four different potential assays for the same region of interest. Bisulfite conversion of the DNA of interest results in variable positions in former CpG sites. If a CpG cytidine was methylated, cytidine is retained, whereas thymidine indicates that the cytidine was unmethylated. Therefore, dTTP and dCTP are added in consecutive cycles for each cytidine followed by guanosine. The methylation status is then calculated from intensities of the C and T signals. It has to be noted that in reverse assays, CpG methylation is calculated from the signal intensities of A and G instead of C and T.[144,145]

1.6.4 Primer design

Primer design is an important factor in the creation of new PSQ assays, used to determine the CpG methylation levels in a target sequence. There are some general rules for primer design that should be followed in order to ensure specific binding and successful amplification of the DNA sequence of interest:[146]

- Forward and reverse primers should consist of 16-30 nucleotides and the length of sequencing primers should be 15-25 nucleotides.
- The difference in the melting temperatures of forward and reverse primers should not exceed 2 °C and their annealing temperature should be 55-65 °C.
- The 3’ ends of the primers should have strong binding affinities to the template. The presence of G or C bases at the 3’ end helps promote specific binding.
- Nucleotide repetitions longer than 4 or more in the primers should be avoided, particularly at the 3’ end.
- Regions of homology in the primers should be avoided in order to improve specificity. Primers must not amplify other DNA regions.
- The presence of secondary structures in the primers can lead to poor or no yield of the amplicon and should therefore be avoided. Common secondary structures include hairpins, homo-, and heterodimers.
- No common SNPs should be located in the primer binding sites on the template.
- CpGs in primer binding sites should be avoided.
- The amplicon length should not be longer than approximately 350 bases.
- The CG content of the PCR amplicons should be 40-60%.

2 Aims of the Thesis

Many potential biomarkers for glioblastoma patients have been identified over the years. Their applications range from prognosis to predicting the response to treatment with TMZ. The present study aimed to investigate the methylation status of several regions and regulatory elements of genes that have been associated with GBM.

Multiple studies have shown that MGMT promoter methylation inversely correlates with MGMT expression. Thus, it has been used as a predictive biomarker for the responsiveness of GBM patients to TMZ. However, more and more cases arise where MGMT promoter methylation does not correctly predict MGMT expression. Other regulatory mechanisms seem to influence this correlation. It has been reported that the activity of MGMT enhancers might be one possible cause. One aim of this thesis was to investigate a possible correlation between MGMT enhancer methylation and MGMT expression. PSQ assays to determine the methylation status of two MGMT enhancers have been developed in-house and should be employed as part of this master's thesis.

Overexpression of ABC-transporters in tumor tissues has been linked to a limited efficacy of anti-cancer drugs, among other things. In order to elucidate the role of DNA methylation changes in the acquisition of MDR, promoter methylation levels should be investigated for ABCB1, ABCG2 and ABCA7. Furthermore, the p16 promoter and exon 2 should be investigated as well. Hypermethylation of the p16 region has been found in a number of cancer types. The associated PSQ assays have been developed in-house, but not yet used on GBM samples. If necessary, optimization of the existing assays should be made to improve their applicability for the GBM sample set.

Finally, a novel assay should be developed to determine the methylation status of the GBX2 promoter in the GBM sample set. Overexpression of GBX2 has been reported to stimulate malignant growth of cancer cells.

3 Materials and Methods

3.1 General setup

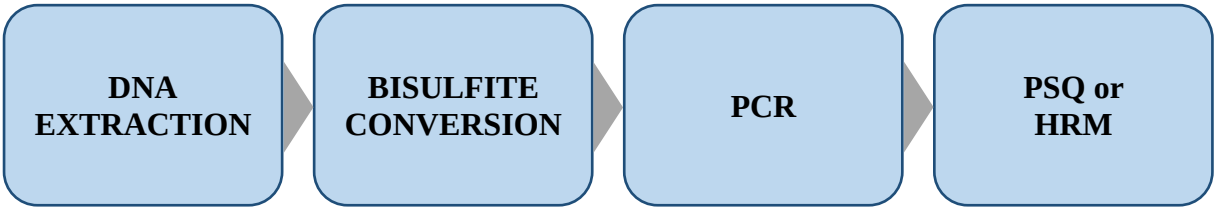

Figure 10: General workflow for DNA methylation analysis.

The basic workflow of DNA methylation analysis consisted of four steps (see **Figure 10)**. In order to minimize the risk of DNA cross-contamination, separate laboratories were used for different steps of the workflow. Laboratory 1 was used for reagent storage, separating DNA and non-DNA reagents. The preparation of the master mixes for PCR and PSQ was done in laboratory 2 inside a PCR workstation, to which DNA was added in laboratory 3 inside another PCR workstation. Laboratory 4 contained the necessary equipment for PSQ preparation and was the only place where amplicons were allowed to be handled freely. The sequencing instrument was located in laboratory 5 and the amplicons were stored in laboratory 6. Additionally, a separate lab coat was worn in each laboratory. To further minimize the contamination risk, all surfaces were cleaned with DNA-ExitusPlus IF before work. Moreover, the PCR workstations were decontaminated by irradiation with ultraviolet (UV) light for 30 minutes before each subsequent use.

3.2 Samples

The GBM sample set used as part of this master's thesis was provided by our cooperation partner Sabine Spiegl-Kreinecker from the Kepler University Hospital (Department of Neurosurgery) in Linz. The set consisted of 40 DNA extracts from *in vitro* cultured, primary cell line samples, isolated from GBM tumor tissue. Due to limited amounts of some samples, the full set was not analyzed with all assays in this project. **Table 1** gives an overview of the GBM patients, including the following information: sex, age at surgery, histology, MGMT promoter methylation and expression, therapy after surgery, overall survival (OS) time, Karnofsky performance status (KPS), and Ki67 expression. Bisulfite conversion of the extracted DNA was carried out by Katja Zappe, a PhD student of the Cichna-Markl group. Bisulfite conversion of the employed DNA standards was carried out by Katja Zappe and Katharina Pühringer, a master's student in said research group. Information about the DNA standards is listed in section 7.3.3 (**Supplementary Table 55**).

Table 1: GBM samples analyzed as part of this study. The 40 listed samples were provided by our cooperation partner Sabine Spiegl-Kreinecker from the Kepler University Hospital (Department of Neurosurgery) in Linz. They consist of DNA extracts from primary cell line samples, which were isolated from GBM tumor tissue. Clinical data of the patients is listed, along with MGMT promoter methylation, expression levels of MGMT (determined via Western blotting), and Ki67 (determined via Immunohistochemistry). f = female, m = male, GBM = Glioblastoma multiforme, GS = Gliosarcoma, wt = wildtype, mut = mutant, UM = unmethylated, M = methylated, R-Ch-Th = chemoradiotherapy, R-Th = radiotherapy, Ch-Th = chemotherapy, adj. = adjuvant, OS = overall survival, KPS = Karnofsky performance status. Not specified data is indicated with a n.s.

Sample	Sex	Age [years]	Histology	MGMT prom. meth.	MGMT expr. [a.u.]	Therapy	OS [months]	KPS [%]	Ki67
L01	f	64	GBM IDHwt	UM	0	R-Ch-Th with TMZ	7.43	60	n.s.
L02	f	43	GS	M	0	R-Th	9	80	low
L03	m	85	GBM IDHwt	M	0	n.s.	3	40	low
L04	f	53	GBM IDHwt	M	0	R-Ch-Th with TMZ	52.5	100	n.s.
L05	f	67	GBM IDHwt	M	0	R-Th	46.63	70	high
L06	f	57	GBM IDHwt	M	0	R-Th, adj. Ch-Th	10.5	100	low
L07	m	46	GBM IDHwt	M	0	R-Ch-Th & adj. Ch-Th with TMZ	30.5	90	n.s.
L08	f	50	GBM IDHwt	M	0	R-Th, adj. Ch-Th with TMZ	27.4	90	n.s
L11	f	74	GBM IDHwt	M	0	R-Ch-Th, adj. Ch-Th with TMZ	7.79	70	low
L12	m	48	GBM IDHwt	M	0	n.s.	1.55	60	n.s.
L14	m	64	GBM IDHwt	UM	0.2	R-Ch-Th & adj. Ch-Th with TMZ	11.7	80	high
L15	f	73	GBM IDHwt	UM	0.16	R-Ch-Th with TMZ	10.6	60	high
L16	m	44	GBM IDHwt	UM	1.1	R-Ch-Th & adj. Ch-Th with TMZ	13	80	high
L17	m	65	GBM IDHwt	UM	1.2	R-Th	9.27	90	low
L18	m	69	GBM IDHwt	UM	0.04	R-Th, adj. Ch-Th with TMZ	8	90	low

Sample	Sex	Age [years]	Histology	MGMT prom. meth.	MGMT expr. [a.u.]	Therapy	OS [months]	KPS [%]	Ki67
L19	f	73	GBM IDHwt	UM	1.1	n.s.	7	100	n.s.
L20	m	83	GBM IDHwt	UM	1	R-Th	9.57	90	low
L21	m	74	GBM IDHwt	UM	1.32	R-Ch-Th with TMZ	5.19	90	n.s.
L22	m	44	GBM IDHwt	UM	0.25	R-Ch-Th & adj. Ch-Th with TMZ	23.15	100	n.s.
L39	m	48	GBM IDHwt	UM	0.09	R-Ch-Th & adj. Ch-Th with TMZ	18.67	100	high
L40	m	75	GBM IDHwt	UM	0.06	Ch-Th & adj. Ch-Th with TMZ	23.9	60	low
L41	m	60	GBM IDHwt	UM	0.4	R-Ch-Th & adj. Ch-Th with TMZ	13	90	low
L42	m	53	GBM IDHwt	UM	0.54	n.s.	0.89	70	high
L43	f	47	GBM IDHwt	M	0	R-Ch-Th & adj. Ch-Th with TMZ	37.25	70	high
L44	m	64	GBM IDHwt	UM	0.49	R-Ch-Th & adj. Ch-Th with TMZ	7.73	90	low
L45	f	67	GBM IDHwt	M	0	R-Ch-Th & adj. Ch-Th with TMZ	16.8	70	high
L46	f	75	GBM IDHwt	M	0	R-Th	8.22	70	low
L47	f	52	GBM IDHwt	M	0	R-Ch-Th & adj. Ch-Th with TMZ	n.s.	90	high
L48	m	63	GBM IDHwt	M	0	R-Ch-Th & adj. Ch-Th with TMZ	21.8	n.s.	high
L49	f	79	GBM IDHwt	M	0	n.s.	1.31	40	high
L50	m	58	GBM IDHwt	M	0	R-Ch-Th & adj. Ch-Th with TMZ	16	90	high
L51	f	58	GBM IDHwt	M	0	R-Ch-Th & adj. Ch-Th with TMZ	13.3	n.s.	high
L52	m	71	GBM IDHwt	M	0	n.s.	1.25	n.s.	low

Sample	Sex	Age [years]	Histology	MGMT prom. meth.	MGMT expr. [a.u.]	Therapy	OS [months]	KPS [%]	Ki67
L53	m	57	GBM IDHwt	UM	0.2	R-Ch-Th & adj. Ch-Th with TMZ	12.7	n.s.	n.s.
L54	m	53	GBM IDHwt	M	0	R-Ch-Th & adj. Ch-Th with TMZ	32.3	n.s.	n.s.
L55	m	64	GBM IDHwt	M	0	R-Ch-Th with TMZ	10.6	40	n.s.
L56	m	62	GBM IDHwt	UM	0.9	n.s.	1.48	50	low
L57	m	32	GBM IDHmut	UM	0.25	R-Ch-Th & adj. Ch-Th with TMZ	39.9	n.s.	low
L58	m	63	GBM IDHwt	UM	0.11	R-Ch-Th & adj. Ch-Th with TMZ	19.5	80	high
L59	m	76	GBM IDHwt	UM	0.29	n.s.	4.44	30	low

3.3 Method development and optimization

As part of this master's thesis, the DNA methylation status of the genes MGMT, ABCB1, ABCG2, ABCA7, p16, and GBX2 should be examined. Except for GBX2, PSQ assays for the regions of interest were already established by former students. Consequently, the following section gives an overview about method development and optimization only for GBX2. Reaction setups and parameters for the pre-established PSQ assays can be found in section 7.3.1.

3.3.1 Primer design

Primer design for the PSQ assays was done using the *PyroMark Assay Design 2.0* software. First, the respective target sequence, including flanking sequences of approximately 1000 bases, was loaded into the software. Either the upper or lower strand was selected for bisulfite conversion, generating the specific bisulfite converted upper or lower strand. A target region containing several CpGs of interest was chosen and 100 primer sets (fw, rev, seq) were generated automatically according to preset parameters (see **Table 2**).

Table 2: *PyroMark Assay Design* software settings used for automatic primer design.

PCR primer	
Min Primer Length [nt]	16
Max Primer Length [nt]	30
Opt. Amplicon Length From [nt]	50
Opt. Amplicon Length To [nt]	100
Max Amplicon Length [nt]	400
Allow Primer Over Variable Pos.	✓
Melting Temperature Algorithm	NN Mismatch
Primer Concentration [µM]	0.2
Min Melting Temperature [°C]	50
Max Melting Temperature [°C]	72
Max Allowed Tm Difference [°C]	10
Max GC Difference [%]	50

Sequencing primer	
Min Primer Length [nt]	15
Max Primer Length [nt]	25
Min Distance from Target [nt]	0
Max Distance from Target [nt]	10
Allow Primer Over Variable Pos.	✓
Melting Temperature Algorithm	NN Mismatch
Min Melting Temperature [°C]	29
Max Melting Temperature [°C]	59

The proposed primer sets were checked manually and optimized according to the general rules of primer design described in section 1.6.4. For that reason, a number of browser applications were used to determine and test additional parameters, summarized in section 7.3.6 (see **Supplementary Table 58**). The salt adjusted melting temperatures of the primers were

calculated by the webtool *Oligonucleotide Properties Calculator* (OligoCalc). The possible formation of secondary structures was checked by the *RNAfold* web server. The online tool *OligoAnalyzer* was used to predict the probability of homo- and heterodimer formation. Possible off-target products were searched for on the *BiSearch* web server. The primer binding sites were searched for any SNPs with the *Primer Design and Search Tool* on the genome browser *Ensembl*. Suitable primer sets were ordered from *Sigma-Aldrich* and delivered in lyophilized form. Each primer was dissolved in RNase-free water to a concentration of 100 µM and stored in 10 µL aliquots at -20 °C.

3.3.2 Polymerase chain reaction (PCR)

PCR reactions can be optimized by changing various essential parameters, including primer concentrations, cycle number, PCR reaction times, and reaction temperatures, the type of DNA polymerase and its concentration. This optimization process for GBX2 is explained in detail in section 4.1.4. Next, the general workflow for performing PCRs will be described.

The PCR reagents and DNA samples were all stored at -20 °C. For GBX2, the *EpiTect HRM PCR Kit* was used, and the employed PCR conditions were based on the manufacturer's instructions.[147] The purchased kit included the 2x EpiTect HRM Master Mix (MM), containing HotStarTaq Plus DNA Polymerase, EpiTect HRM PCR Buffer (including EvaGreen dye), and a dNTP mix. The master mix was prepared by adding RNase free water and both the forward and reverse primer to the 2x EpiTect HRM Master Mix according to the reaction setup described in **Table 3**. Then, 18 µL of the master mix was distributed into each PCR tube, which were kept cold in a cooling block. These steps were performed inside a PCR workstation in laboratory 2.

Table 3: General PCR reaction setup – *EpiTect HRM PCR Kit*[147].

	Final primer concentration	
	0.2 µM	**0.4 µM**
Component	**Volume per reaction [µL]**	
2x EpiTect HRM PCR MM	10.0	10.0
RNAse-free water	7.2	6.4
Fw primer [10 µM]	0.4	0.8
Rev primer [10 µM]	0.4	0.8
Volume [µL]	18	18
DNA [2.5 ng/µL]	2	2
Total volume [µL]	20	20

2 µL of the bisulfite converted DNA was added to the PCR tubes inside a second PCR workstation in laboratory 3. This was either methylated or unmethylated DNA standards or the DNA extracts of the GBM samples. Additionally, each PCR run also contained two PCR tubes, where the template DNA was replaced with RNase-free water. These no-template controls (NTCs) served to detect possible contaminations or non-specific amplifications. After adding the DNA template, the reaction mixtures were transferred to the thermocycler (Rotor-Gene Q, Qiagen) and programmed according to **Table 4**. After amplification, the PCR tubes were stored at -20 °C.

Table 4: Modified thermal cycling program using the *EpiTect HRM PCR Kit*[147]. Annealing and elongation temperatures are method dependent.

	Step	Time	Temperature
	Activation	5 min	95 °C
50x	Denaturation	10 sec	94 °C
	Annealing	20 sec	variable
	Elongation	20 sec	variable
	Final elongation	10 min	variable
	Denaturation	1 min	95 °C
	Hybridization	1 min	40 °C
	HRM	-	65-95 °C

3.3.3 Pyrosequencing (PSQ)

PSQ was performed using the *PyroMark Q24 Advanced System*. The necessary chemicals (nucleotides, enzymes, substrates, buffers) were included in the *PyroMark Q24 Advanced CpG Reagents Kit*, which was used according to the manufacturer's protocol.[148] The master mix was prepared inside the PCR workstation in laboratory 2, as shown in **Table 5**. It included MilliQ water, PyroMark Binding Buffer, and Streptavidin Sepharose High Performance beads. Since the streptavidin coated sepharose beads tend to sediment quickly, the bead suspension was homogenized thoroughly before use. Additionally, the master mix was vortexed every time after filling four wells on the 24-well plate. The sequencing primers were diluted to a concentration of 0.375 µM with PyroMark Annealing Buffer. The lyophilized enzyme and substrate mixtures were dissolved in 660 µL of MilliQ water. The following steps were performed in laboratory 4, as they involved working with highly concentrated DNA. The PyroMark Q24 Cartridge was filled with the enzyme and substrate mixtures, as well as the nucleotide solutions. The required volumes were calculated by the *PyroMark Advanced Software* on basis of the PSQ target sequence. After the cartridge was loaded, it was placed into

the PyroMark Q24 sequencer. Next, the biotinylated PCR products were added to the respective wells and the plate sealed with an adhesive foil. The sealed 24-well plate was then vortexed for 10 min at approximately 1400 rpm, causing the streptavidin coated beads to bind to the biotinylated amplicons. Meanwhile, the PyroMark Q24 Vacuum Workstation was set up and 20 µL of the respective sequencing primers were transferred into the wells of a PyroMark Q24 plate. After vortexing, the sealing foil was quickly removed and the beads containing the immobilized template were captured with the vacuum tool. Then, washing and denaturation steps were performed by flushing the vacuum tool in three different solutions provided by Qiagen for a predefined time (5 s in 70% ethanol, 5 s in denaturation solution, and 10 s in washing buffer). Afterwards, the vacuum tool was dried for 5 s, placed into the plate containing the diluted sequencing primers, and slewed gently. This plate was then put on a heating block and heated for 5 min at 80 °C. After incubation, the plate was immediately placed in the PyroMark Q24 sequencer and the PSQ analysis was started.

Table 5: Master mix setup used for pyrosequencing using the *PyroMark Q24 Advanced CpG Reagents Kit*[148].

	Volume per reaction [µL]				
Component	**0.6x**	**1x**	**1.26x**	**1.5x**	**2x**
Streptavidin Sepharose HP	0.6	1	1.26	1.5	2
PyroMark Binding Buffer	24	40	50.4	60	80
MilliQ water	14.4	24	30.24	36	48
Reaction mix [µL]	39	65	81.9	97.5	130
Biotinylated PCR product	9	15	18.9	22.5	30
Total volume [µL]	48	80	100.8	120	160

3.3.4 Data analysis

In order to determine the methylation status via HRM, a calibration curve needed to be established. Raw data of the employed DNA standards (0%, 25%, 50%, 75%, and 100% methylation) and GBM samples was analyzed using the *Rotor-Gene Q Series Software* (version 2.3.1). The resulting fluorescence signals were normalized and exported to *Microsoft Excel*. Then, the mean values of the fluorescence signals in the defined interval of analysis were standardized by applying **Equation 1** (SF: standardized fluorescence, NF: normalized fluorescence, $\overline{NF}$: mean value of normalized fluorescence).

$$SF_{sample}[\%] = \frac{NF_{sample} - \overline{NF}_{(0\%\ standard)}}{\overline{NF}_{(100\%\ standard)} - \overline{NF}_{(0\%\ standard)}} * 100 \quad (1)$$

The standardized data was transferred to *OriginPro 2022b* (version 9.95) and the calibration curve was created by plotting the standardized fluorescence of the DNA standards against the respective methylation levels. Using this calibration curve, the overall methylation levels of the GBM samples were calculated.

PSQ raw data was examined with the *PyroMark Q24 Advanced Software* (version 3.0.1). The quality of each analyzed CpG was evaluated by its internal quality control and ranked as either "passed" (blue), "check" (yellow) or "failed" (red). For calculating mean values of the technical replicates, the data was exported to *Microsoft Excel*. The lower limit of quantification (LLOQ) was set to 5% and the upper limit of quantification (ULOQ) was set to 95%. Methylation values lower than the LLOQ were replaced with 2.5% and values higher than the ULOQ were replaced with 97.5% instead. If possible, two technical replicates from two independent PSQ experiments were used to calculate mean values.

Statistical analysis was carried out using both *OriginPro 2022b* and *IBM SPSS Statistics* (version 28). Statistical correlations between DNA methylation levels and other variables of interest were examined by employing nonparametric measures, *e.g.* the Spearman-Rho correlation coefficient and p-values (two-tailed). Parametric measures were not used as part of this master's thesis, since most of the available data did not fulfill the necessary requirements. Tests for normal distribution were carried out both graphically and analytically by using the Shapiro-Wilk and Kolmogorov-Smirnof test. Statistically significant results were marked with asterisks depending on their p-value, indicating the level of significance: $p < 0.05$ (*), $p < 0.01$ (**), and $p < 0.001$ (***). The Mann-Whitney U test, which is also nonparametric, was used in order to compare the means of two groups.

4 Results & Discussion

The aim of this master's thesis was to determine the DNA methylation status of several regions and regulatory elements associated with the genes MGMT, ABCB1, ABCG2, ABCA7, p16, and GBX2 in GBM-related DNA extracts by PSQ. Furthermore, the present study aimed to investigate the biomarker potential of the analyzed regions.

4.1 Development and optimization of PSQ assays

PSQ assays for the MGMT enhancers, ABC-transporters, and p16 were already established by previous master or PhD students and adopted from their theses. However, some optimization experiments had to be done to these assays, which will be outlined, along with the development of GBX2 assays, in the following section.

4.1.1 MGMT enhancers

4.1.1.1 MGMT enhancer E

Four PSQ assays for the MGMT enhancer E, which were designed and established by Katharina Pühringer as part of her master's thesis, were employed in this study.[149] The enhancer of interest, named human element (hs696), was found on the *VISTA Enhancer browser*, but designated as MGMT enhancer E for the sake of simplicity. It is located within the MGMT gene (Accession number: NG_052673.1) and has the coordinates chr10: 129605804-129607046 (GRCh38.p13). The PSQ assays 1D, 3C, 4F, and 5E cover 14 CpG sites in total (see **Figure 11**) and were applied without any changes, except for assay 1D.

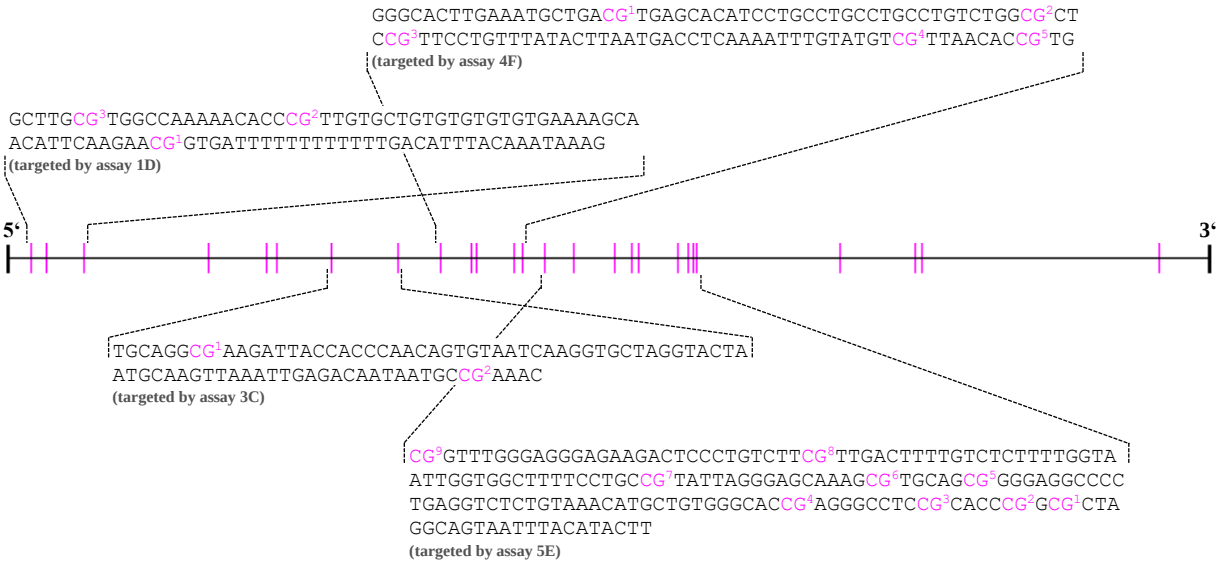

Figure 11: Assays for MGMT enhancer E employed in this thesis.

Since PSQ analysis with assay 1D was unsuccessful in the original thesis, a new sequencing primer was developed by Katja Zappe and employed as part of this master's thesis. As an example, the PSQ results for the PCR product of the 50% methylated DNA standard are shown in **Figure 12**. All three CpGs were analyzed successfully with the *PyroMark Q24 Advanced* software, making it possible to use this PSQ assay to determine the methylation status of the GBM samples.

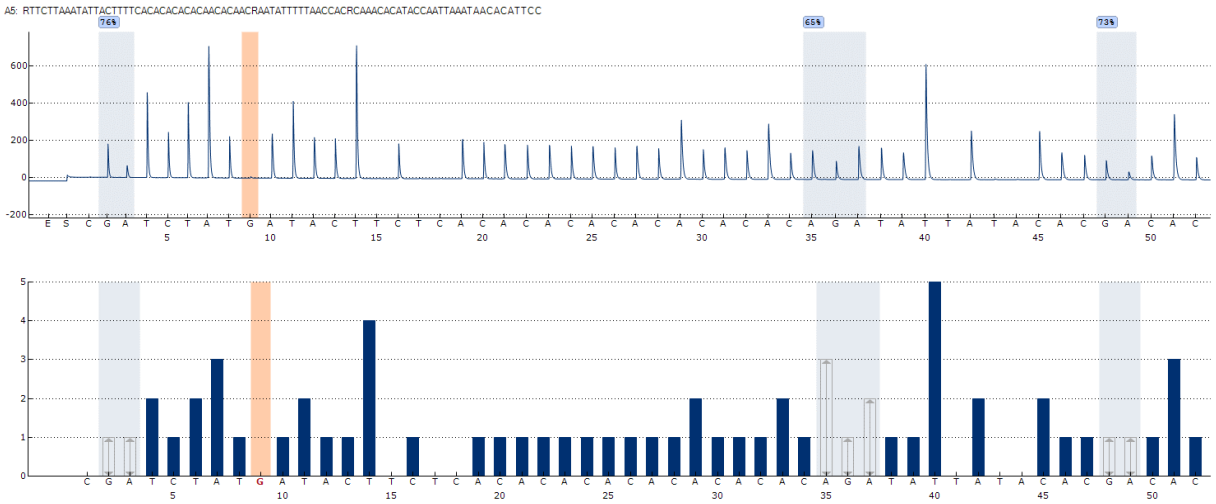

Figure 12: Representative pyrogram (top) and histogram (bottom) of assay 1D with 50% methylated standard DNA.

4.1.1.2 MGMT enhancer K-M

In his master's thesis, Simon Pflug established four PSQ assays for the analysis of the K-M enhancer, which was first characterized by Chen *et. al.* in 2018.[150,151] This novel enhancer is located upstream of the MGMT gene (Accession number: NG_052673.1) and has the coordinates chr10: 128906630-128909942 (GRCh38.p13). The four PSQ assays cover 19 of the 46 CpGs located in the region of interest (see **Figure 13**) and were applied without any changes, except for assay 3.

Since the fourth CpG was not included in the original PSQ analysis for assay 3 and the third CpG was always marked as "failed", the assay file was modified by Katja Zappe and employed as part of this master's thesis. Additionally, the 2-fold reaction setup of the PSQ analysis was reduced to 0.6 (see **Table 5**). With these new settings the analysis of the third CpG was improved and the fourth CpG could be included in this assay. Unfortunately, the fourth CpG could not be evaluated reliably, but was still considered in the analysis of the GBM samples. The results have to be taken with caution though. **Figure 14** shows an exemplary pyrogram for the PCR product of the 50% methylated DNA standard.

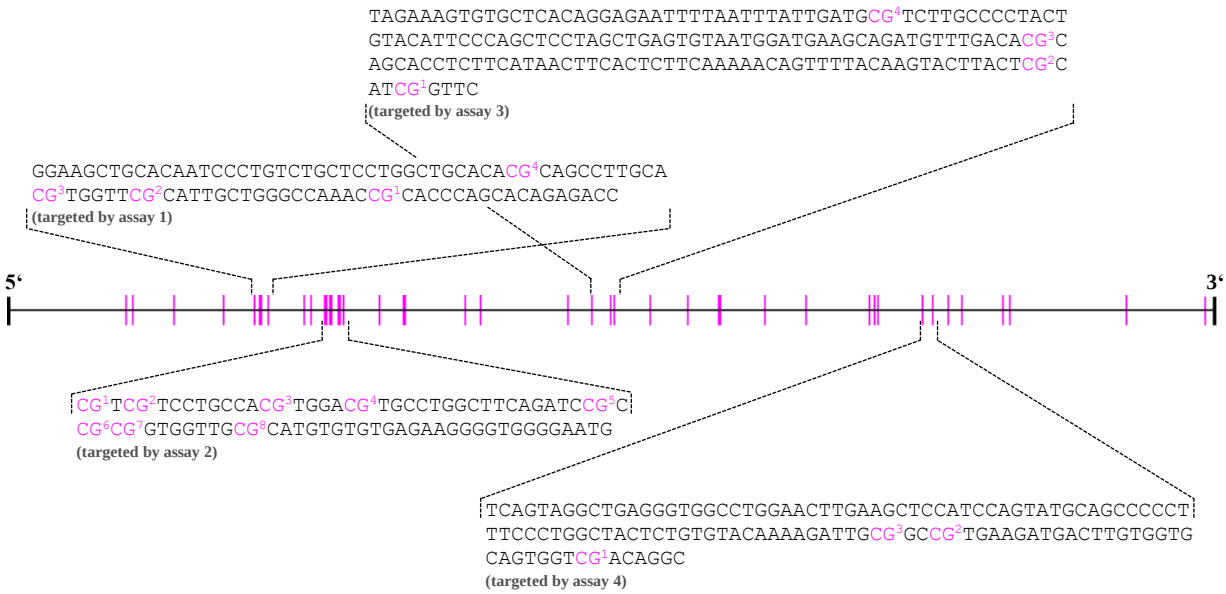

Figure 13: Assays for MGMT enhancer K-M employed in this thesis.

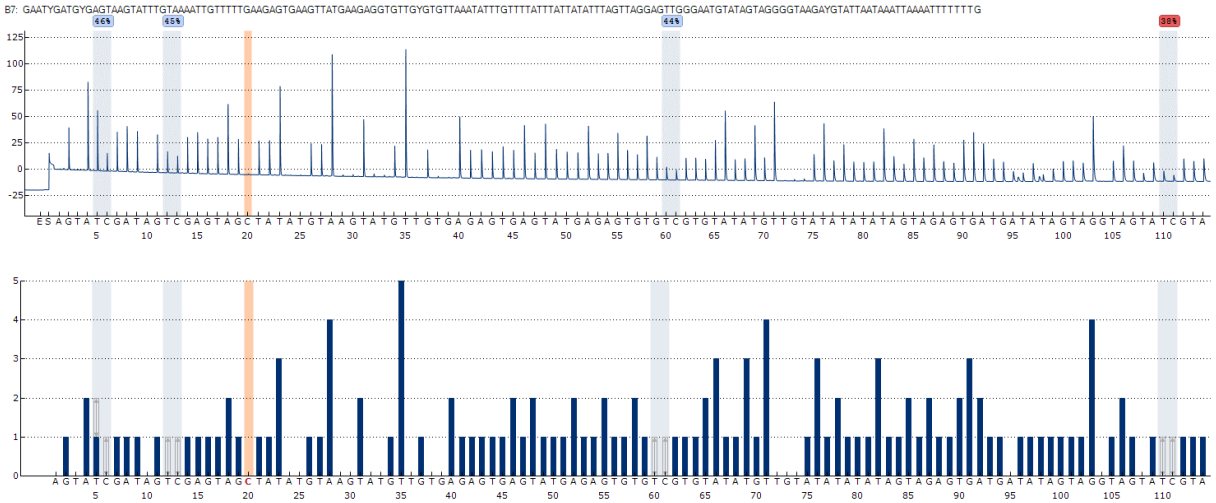

Figure 14: Representative pyrogram (top) and histogram (bottom) of assay 3 with 50% methylated standard DNA.

4.1.2 ABC-transporters

PSQ assays for the ABCB1 and ABCG2 promoter regions were developed by Melanie Spitzwieser as part of her PhD thesis.[152] The corresponding nucleotide sequences were taken from the *National Center for Biotechnology Information* (NCBI) *Nucleotide* database (Accession number: NG_011513.1 and NG_028268.1), and the promoter regions were identified using the *Transcriptional Regulatory Element Database* (TRED). The ABCB1 assay allows the determination of the methylation status of seven CpGs in the promoter region (chr7: 87598600-87601400 (GRCh38.p13)) and the ABCG2 assay targets eight CpGs in the promoter region (chr4: 88156801-88159801 (GRCh38.p13)), as seen in **Figure 15**.

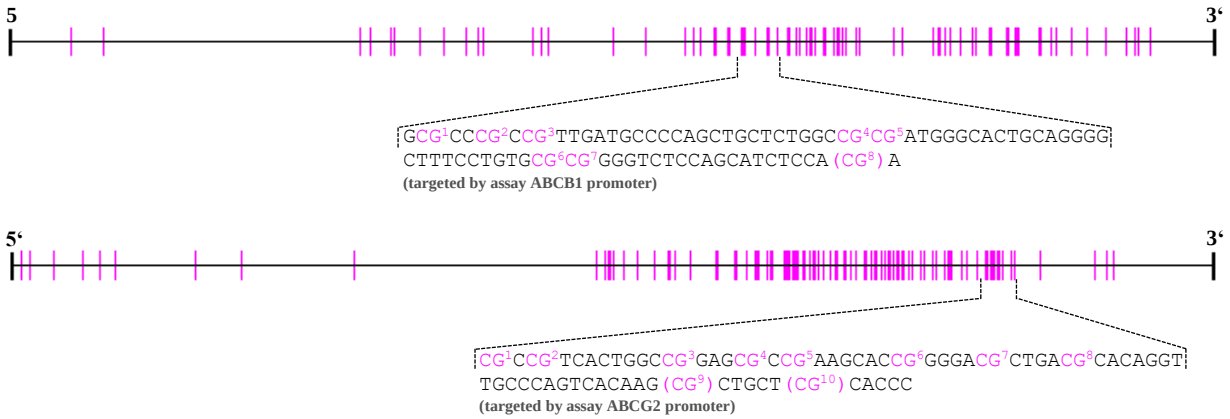

Figure 15: Assay ABCB1 (top) and ABCG2 (bottom) employed in this thesis.

The reaction parameters were adopted from the original literature, except for the composition of the PCR master mix. The fluorescent nucleic acid EvaGreen dye was added to the mixture for its use in real-time PCR and HRM analysis (see **Figure 16**).

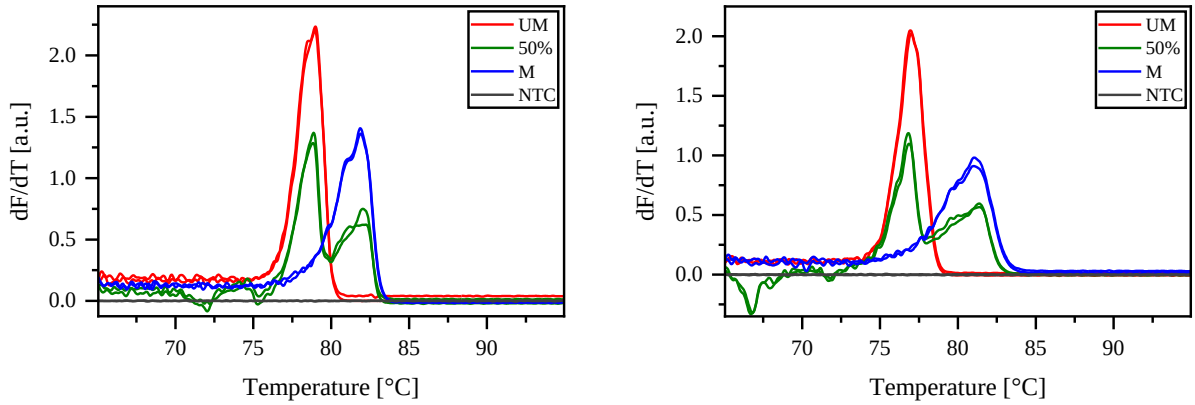

Figure 16: Derivative HRM plot obtained for assay ABCB1 (left) and assay ABCG2 (right). UM = unmethylated standard DNA, 50% = 50% methylated standard DNA, M = methylated standard DNA, NTC = no-template control.

The PSQ assay encompassing the ABCA7 exon 5 / intron 5 boundary was designed by Alexandra Scheichel.[153] Ann-Katrin Schier was responsible for the establishment of the PSQ assay analyzing the ABCA7 exon 6 / intron 6 boundary.[154] The nucleotide sequence of ABCA7 and exon / intron annotation were taken from the *NCBI* database (Accession number: NG_046909.1). The ABCA7 ex 5 / in 5 assay encompasses seven CpGs in chr19: 1042063-1042314 (GRCh38.p13) and the ABCA7 ex 6 / in 6 assay allows the determination of the methylation status of nine CpGs in chr19: 1042315-1042745 (GRCh38.p13). **Figure 17** shows the boundaries for exon 5 / intron 5 and exon 6 / intron 6, the position of the CpGs targeted by pyrosequencing and the sequence to analyze for ABCA7. For both assays, EvaGreen dye was added to the PCR master mix as well (see **Figure 18**). The rest of the reaction parameters and conditions were applied as already established.

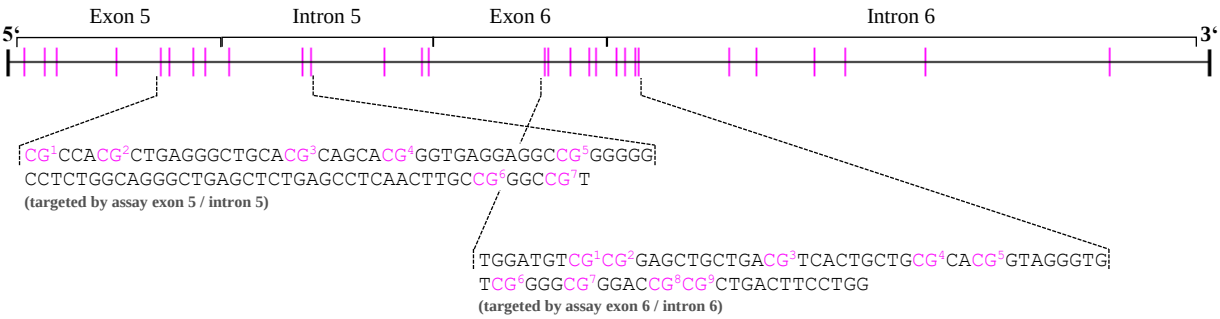

Figure 17: Assay ABCA7 ex 5 / in 5 and ex 6 / in 6 employed in this thesis.

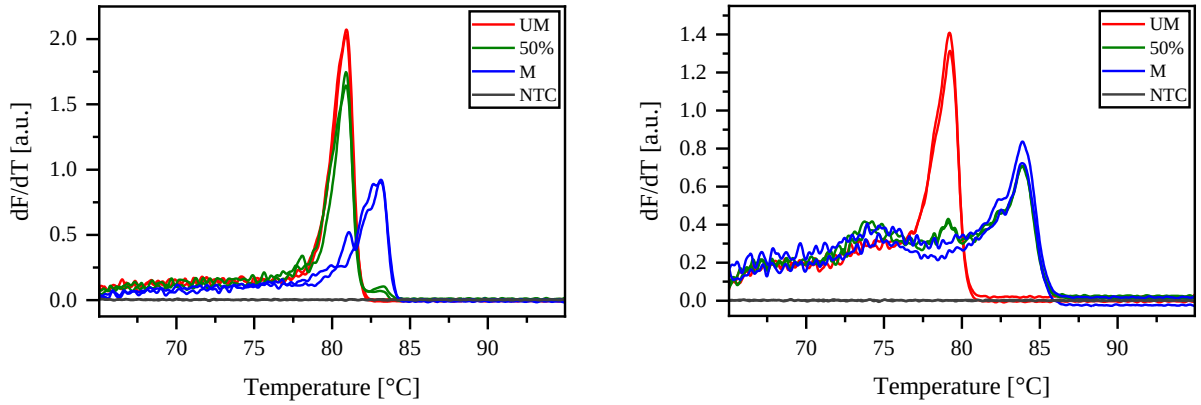

Figure 18: Derivative HRM plot obtained for assay ABCA7 ex 5 / in 5 (left) and assay ABCA7 ex 6 / in 6 (right). UM = unmethylated standard DNA, 50% = 50% methylated standard DNA, M = methylated standard DNA, NTC = no-template control.

4.1.3 p16

As part of his diploma thesis, Andreas Jenik developed and employed two PSQ assays for the p16 gene region.[155] The corresponding nucleotide sequence was taken from the *NCBI* database (Accession number: NG_007485.1). The first assay covers seven CpGs in the p16 promoter region in chr9: 21972200-21976201 (GRCh38.p13), whereas the second assay encompasses 24 CpGs in the exon 2 region, located in chr9: 21974678-21975134 (GRCh38.p13), as seen in **Figure 19**. The reaction parameters for the p16 promoter assay were adopted from the original literature, except for the PCR master mix. Instead of the 2x PyroMark PCR Master Mix, the 2x EpiTect HRM Master Mix was employed as part of this study. The original PSQ assay for p16 exon 2 encompassed only 21 CpGs, however, two newly designed sequencing primers by Katja Zappe were used instead, bringing the total number of analyzable CpGs to 24. In fact, 26 CpGs alone were targeted by the first sequencing primer. However, since pyrosequencing offers usable data only for short to medium length DNA sequences, just the first 14 analyzed CpGs were considered. The following 10 CpGs were targeted by the second sequencing primer. The sequences of these primers can be found in section 7.3.1 (**Supplementary Table 29**). An

exemplary pyrogram for both sequencing primers for the PCR product of the 50% methylated DNA standard is shown in **Figure 20**.

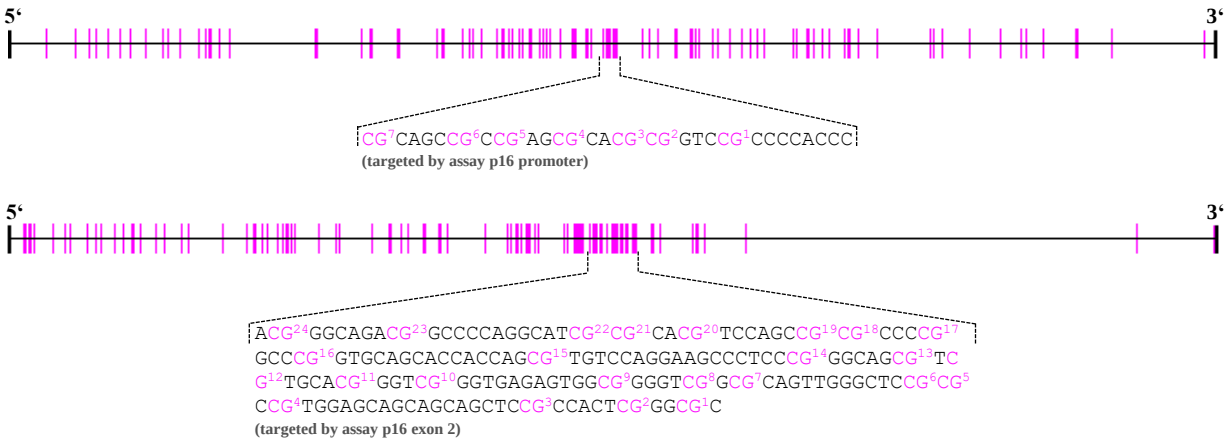

Figure 19: Assay p16 promoter (top) and p16 exon 2 (bottom) employed in this thesis.

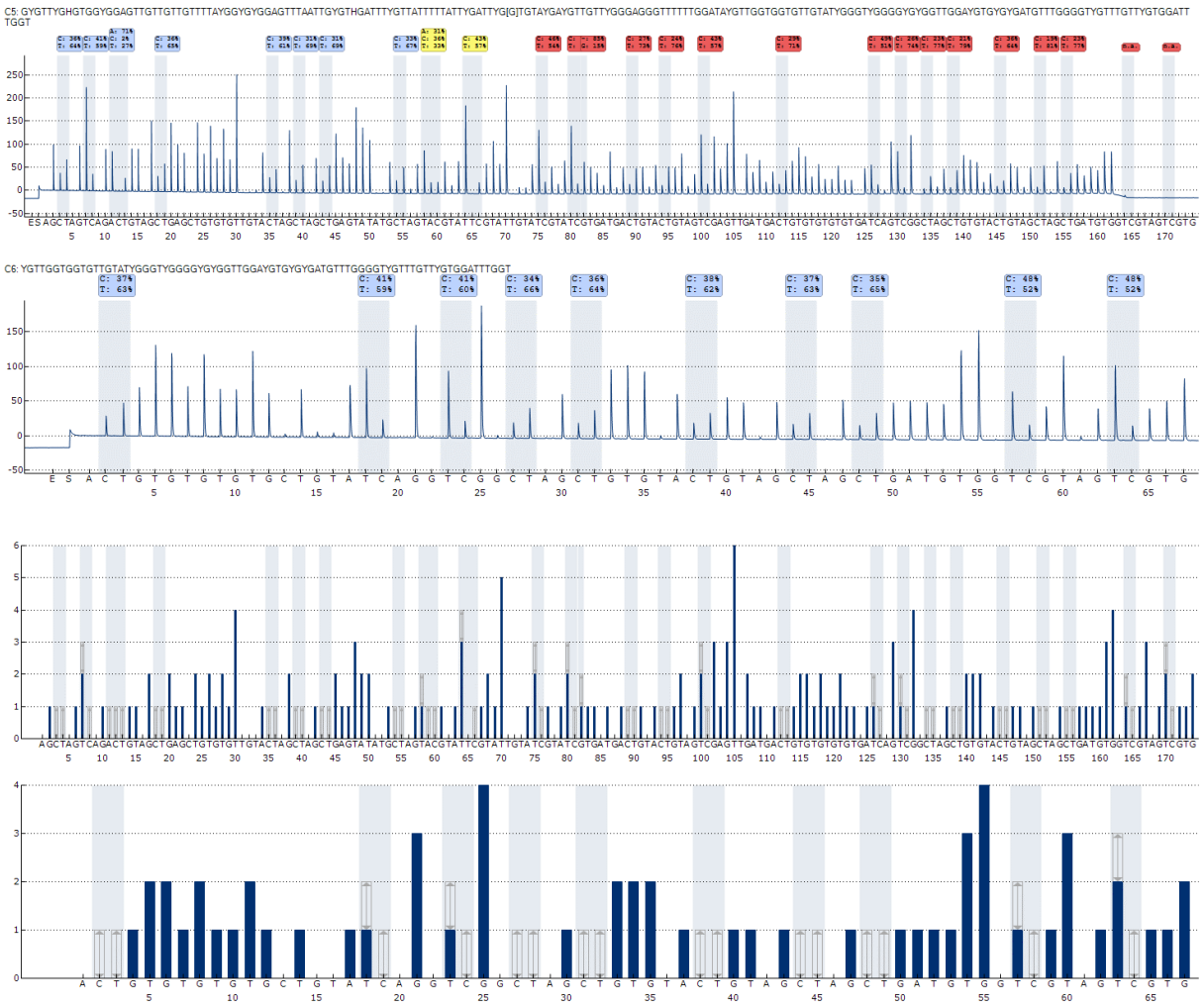

Figure 20: Representative pyrogram (top) and histogram (bottom) obtained with the two newly designed sequencing primers of assay p16 exon 2 with 50% methylated standard DNA.

4.1.4 GBX2

The design of a new PSQ assay to analyze the DNA methylation status of the GBX2 promoter was attempted within the framework of this study. The target region of GBX2 was selected based on a paper by Jeyapala *et. al.*, who defined the GBX2 promoter as the region ranging from 1500 bp upstream to 500 bp downstream of the transcription start site (chr2: 236167409-236169609 (GRCh38.p13)). This nucleotide sequence, including flanking regions of approximately 1000 bases, was taken from the *NCBI* database (Accession number: NC_000002.12), and imported to the *PyroMark Assay Design* software. As part of this thesis, two primer sets were designed for the GBX2 promoter, as seen in **Figure 21**.

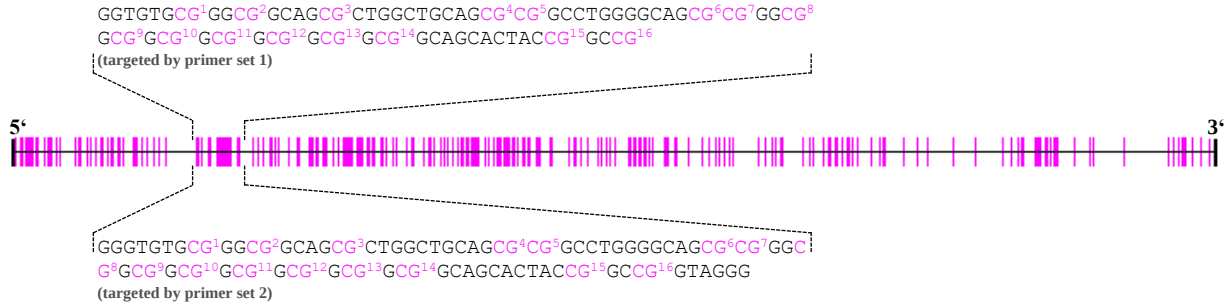

Figure 21: GBX2 assays employed in this thesis.

4.1.4.1 GBX2 primer set 1

The original upper strand sequence of the GBX2 promoter is shown in **Figure 22**, including primer set 1. The bisulfite converted upper strand was used for the design of this forward assay. The amplicon consists of 131 bp and the target region for PSQ has a length of 123 bp, covering 16 CpGs.

TCCCGCCCCCTCGTCCCGGCTGCGCGCGCCGCCGACTCACCGAGCGAAGCCTGCACCGTCTCGGCCGCGGAGAAG
GCGAGCAGCGAGCCCTCTTTGGCCAGGAAGCCTTTGCCGTCCTCCGCGTCAGCCTGCAGCGCCTCCGCCTTGTCG
AAGTTACCGCCGCCGGGCAGCGGCTGCGGCGCGAACTTGCGGGCCGCTGCCGCCTCCTGGTGCTGGGGCGACGCG
GAGAAGCCGCCGGGGAGCGTGGCCATGAGCGTAGAGGTGAGCGCCATGCCCTGCGCCAGGCTGGAGCAGAAGCCT
GTGGGCAGGCTGGGGATCTGGTGGTGAGGGTGTGCGGGCGGCAGCGCTGGCTGCAGCGCGGCCTGGGGCAGCGCG
GGCGGCGGCGGCGGCGGCGGCGGCGCAGCACTACCGGCCGGTAGGGCATGAACATGGGGTAGCCGGTGTAGACGAAA
TGGCCGGGGCTGGGCTGCGGCGGGCTGCCGATCAGCGAGTCTATGCTGAAGGCGGTGCTACTCCCCAGCGGGCGC
TGCATCATCATCAGCGACGGCGGGAACGCTGCGCTCATAGACGCGCTCGGTAGAGGCCAGCGAGAGGCGAAAAGT
CCCCGCCGCCGCCGCCGCCGGGAAGCCCGCCGGACGCCGGGAGCACCGCCGGGAGCGCCGGGCAGGGGCCGAGC
GGGACCCGGAGAGCAGACGCCTCCGCCCCTCAGTCCTGGGCCCGCTGCATGCCGGGCGGGTGCAGGGGGTGTGCG
GGGTGAGGCCGTGCGCCCCGGAGTGGAGAGGGCGCCCGGGCCCCGAGGGCTCGCCGGAGCCCCCGTCCGCCGCTT
GCCCGTCGGAGCCCGCGCGCTTCGCCGGGTTTGGCCCTCGGCCCCGGTAAGCTGCCGTCCGTCCGTCCGTCCGCC
GTCCGTCGCCTCCCGCGGGCCGCTGGGGAGCGCGCGAAGCCGGCGTACTTATCTCCGGCGGGCGCAGCCAGCACC
TTTAAATCGCGCTCCTCTTTCTCATTCACATTTTGCCTGCCGCCTGGCCCGGCTCGCCTCACGTGGGGCTGGGCG
CCTCTGGCCATTGGCTGAGCGGGGCGGGGGTGGGGCGAAAGCGGGGCCCCGCCCTTTCCACCCAAGCTGGCCTCG
AGCGGGCTGCGGGCGCCACCGTCGGAGCGCGCGGGCCGGGGAGCCGGAGCCTGCATGCCTAGCCCGTGCCGCGCA
AACTTGAGACGGGCGGATGGCACCTCCAAGGCTCGGACCTTGGGGCCCTGCAGCCTTGTCGAGGCCACCTCGAAG
GGTAGCCTCCGGGGCCCGCACCCCCACGGCTGGGCCGGGGGCGCTTTATTTCTTTTACTGTATTTGCCATGGAAC
CAACCTGCCTGCGGCTCACTCCAGCGCTGGGTGCTCCGGCTGCGCCTGGGGTCCGGGCGAGGGTCCTGGAGTTGG
GGGCAGGGTCCTGCCCCTCCGGAGCCACCCCCGGGGCGAAGGCTGGGAGCTGGCAGCGCCTGCCCGCCGCCAGAA
ACCCGCCGGGTTGCTCGCTGTAGGTCCGCGCACCGGGTGGGGCGGGGAGGCTGCTGCTTCCCCCATCCCGGGCTG

GGCCCTCCCGTGAGCGATCCCGTCTCTCATTTTTCATGACATTCTTAATCATCGCACCTATTTACACACTTTGCC
AGCGCGCACCAAAATAACAACCACGATAATTATGATAATAAAGAGAGTCCTTTATCTGCTCCATCCTCGGGGAGG
AAGGGGGGAGTTGCTGTGCCTCCAGATTGTATAACGTGAGATTATCCTGATGAAAGCTTTATGATGTTTGCTCAA
ATAAAAGCTGCGTTTTGTAAATAGGCGCTAATTAAGCACGTTGCGAACGCAAGGAGTGCTCACCCTGGCGCCGCC
GCCCGGTTTCCAGCGCGAGGACTCGAGGGCGCGCGGTTCCTCTTTGCTAACTGCAGGATGGAGCCGATCCCCTCA
GGATGTTTCCCCTGTTCTCGACAACGGTAAAGACCCCCAAATTTGAAAGTAAGGGAATTTTGGGGTGGAGGGAAA
CTAGGGACGTACTTATCCCCTCTTCCATTTTCAAACAAAAAACTTTCAGCTCTTGTCTTCCCTTTAAAAATGGAA
TCACTTCTTGACAACGGCAGACCGTGCAGAGCGCACCAGCGCGAGCGGGGCTTCCTCGAGTCTCCAAGGCCCGGG
CTTCAACTTCCCGGGTCTAGACGTCA

Figure 22: Genomic sequence of the GBX2 promotor region. Cyan highlighted and bold: binding sites of the forward and reverse primer, red and underlined: binding site of the sequencing primer, green highlighted: CpGs, pink highlighted: analyzed CpGs.

Table 6 lists the sequences, secondary structures, and melting temperatures of primer set 1. According to *OligoCalc* the salt-adjusted T_m predictions for both the forward and reverse primer were the same, namely 58.4 °C. No off-target products were found in bisulfite-converted human genomic DNA by the *BiSearch* web server, and no frequent SNPs are located in the primer binding sites. The *RNAfold* online tool predicted a low tendency to form secondary structures. However, the formation of heterodimers between the forward and reverse primer according to the *OligoAnalyzer* web tool is possible. Unfortunately, the most stable heterodimer has 5 complementary base pairs with a ΔG of -11.16 kcal/mol, making interference with PCR likely. Nonetheless, primer set 1 was ordered and an optimization of PCR parameters was attempted.

Table 6: Characteristics of primer set 1 for the GBX2 promoter.

Primer (5'→3')	Sequence	Secondary structure	T_m [°C]
Forward	TAGGTTGGGGATTTGGTGGT		58.4
Reverse	[btn]-ACTACCCCATATTCATACCCTA	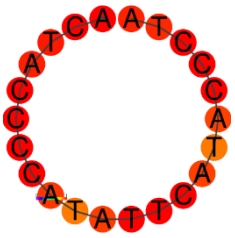	58.4
Sequencing	GGATTTGGTGGTGAG	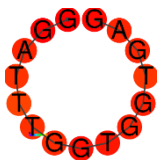	46

The functionality of the designed primers and optimal reaction parameters were investigated by testing two different primer concentrations (0.2 µM and 0.4 µM) at a T_a of 56.4 °C. Bisulfite converted DNA standards with known methylation levels were used as templates.

Unfortunately, PCR of the region of interest was not successful, as seen in **Figure 23**. DNA standards with different methylation levels (0%, 25%, 50%, 75%, and 100%) showed varying amplification curves, with Ct-values ranging from 32.2 to 41.1. Methylated standard DNA generally produced a higher PCR product yield than other standards with lower methylation levels, at least for one of their replicates. Moreover, replicates for all samples did not provide matching results, making this PCR non-repeatable. Additionally, the signal intensity of the NTC samples did rise at the end of the PCR, indicating the formation of primer dimers. The primer concentrations 0.2 µM and 0.4 µM showed similar results. The associated HRM further strengthened these observations. For all amplified samples a peak with its maximum height at a low temperature of 71 °C was found, which can be attributed to primer dimer formation. Furthermore, additional melt peaks can be seen that do not correspond to the expected peaks for the methylated and unmethylated DNA samples, suggesting the synthesis of non-specific products. Therefore, primer set 1 was not fit to successfully amplify the region of interest and for this reason a new set was designed.

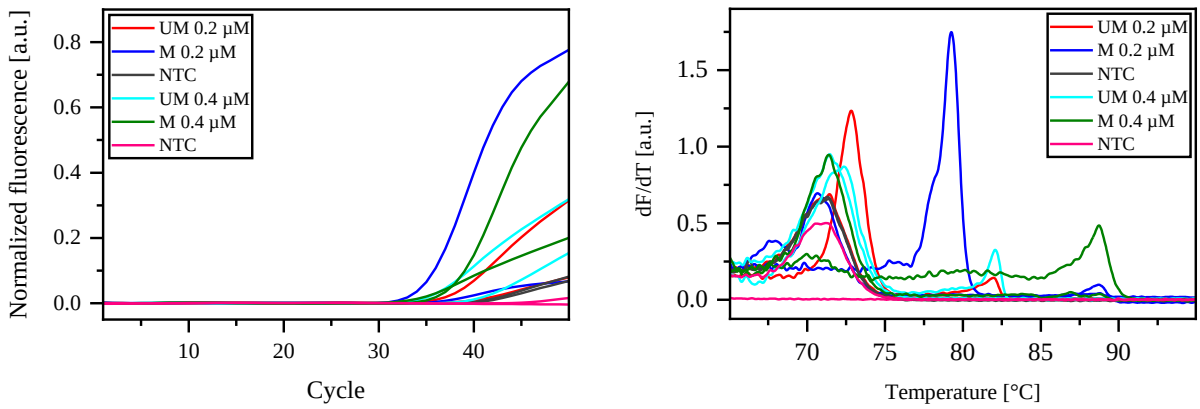

Figure 23: Amplification plot and derivative HRM plot obtained for GBX2 primer set 1. Primer concentration: 0.2 & 0.4 µM. T_a = 56.4 °C, T_e = 72 °C. UM = unmethylated standard DNA, M = methylated standard DNA, NTC = no-template control.

4.1.4.2 GBX2 primer set 2

To overcome the formation of secondary structures in the first primer set, new forward and reverse primers were designed. The accompanying sequencing primer was unchanged. However, the development of a new primer set for the GBX2 promoter region proved challenging. The region of interest contained a high density of CpG sites, leaving hardly any space for primers that do not contain a CpG themselves. Primers should generally not include

any CpG sites within their sequence because their presence could lead to biased amplification of methylated or unmethylated DNA. Moreover, a considerable amount of A and T homopolymer stretches were located in areas between individual CpGs, further complicating the design of a novel PSQ assay for the GBX2 promoter.

Regardless, new forward and reverse primers, which both include a single CpG, were designed for the bisulfite converted upper strand. This assay consists of two forward primers, containing either a C or T at the CpG site and three reverse primers that accommodate a C, A or G at their respective CpG site. The amplified PCR product is 174 bp long and the target region for PSQ has a length of 133 bp, covering the same 16 CpGs as primer set 1 (see **Figure 24**).

TCCCGCCCCCTCGTCCCGGCTGCGCGCGCCGCCGACTCACCGAGCGAAGCCTGCACCGTCTCGGCCGCGGAGAAG
GCGAGCAGCGAGCCCTCTTTGGCCAGGAAGCCTTTGCCGTCCTCCGCGTCAGCCTGCAGCGCCTCCGCCTTGTCG
AAGTTACCGCCGCCGGGCAGCGGCTGCGGCGCGAACTTGCGGGCCGCTGCCGCCTCCTGGTGCTGGGGCGACGCG
GAGAAGCCGCCGGGGAGCGTGGCCATGAGCGTAGAGGTGAGCGCCA**TGCCCTGCGCCAGGCTGGAGCAGAAG**CCT
GTGGGCAGGCTGGGGATCTGGTGGTGAGGGTGTGCGGGCGGCAGCGCTGGCTGCAGCGCGGCCTGGGGCAGCGCG
GGCGGCGGCGGCGGCGGCGGCGGCGCAGCACTACCGGCCGGTAGGG**CATGAACATGGGGTAGCCGGTGTAG**ACGAAA
TGGCCGGGGCTGGGCTGCGGCGGGCTGCCGATCAGCGAGTCTATGCTGAAGGCGGTGCTACTCCCCAGCGGGCGC
TGCATCATCATCAGCGACGGCGGGAACGCTGCGCTCATAGACGCGCTCGGTAGAGGCCAGCGAGAGGCGAAAAGT
CCCCGCCGCCGCCGCCGCCGGGAAGCCCGCCGGACGCCGGGAGCACCGCCGGGAGCGCCGGGCAGGGGCCGAGC
GGGACCCGGAGAGCAGACGCCTCCGCCCCTCAGTCCTGGGCCCGCTGCATGCCGGGCGGGTGCAGGGGGTGTGCG
GGGTGAGGCCGTGCGCCCCGGAGTGGAGAGGGCGCCCGGGCCCCGAGGGCTCGCCGGAGCCCCCGTCCGCCGCTT
GCCCGTCGGAGCCCGCGCGCTTCGCGGGTTTGGCCCTCGGCCCCGGTAAGCTGCCGTCCGTCCGTCCGTCCGCCC
GTCCGTCGCCTCCCGCGGGCCGCTGGGGAGCGCGCGAAGCCGGCGTACTTATCTCCGGCGGGCGCAGCCAGCACC
TTTAAATCGCGCTCCTCTTTCTCATTCACATTTTGCCTGCCGCCTGGCCCGGCTCGCCTCACGTGGGGCTGGGCG
CCTCTGGCCATTGGCTGAGCGGGGCGGGGGTGGGGCGAAAGCGGGGCCCCGCCCTTTCCACCCAAGCTGGCCTCG
AGCGGGCTGCGGGCGCCACCGTCGGAGCGCGCGGGCCGGGGAGCCGGAGCCTGCATGCCTAGCCCGTGCCGCGCA
AACTTGAGACGGGCGGATGGCACCTCCAAGGCTCGGACCTTGGGGCCCTGCAGCCTTGTCGAGGCCACCTCGAAG
GGTAGCCTCCGGGGCCCGCACCCCCACGGCTGGGCCGGGGGCGCTTTATTTCTTTTACTGTATTTGCCATGGAAC
CAACCTGCCTGCGGCTCACTCCAGCGCTGGGTGCTCCGGCTGCGCCTGGGGTCCGGGCGAGGGTCCTGGAGTTGG
GGGCAGGGTCCTGCCCCTCCGGAGCCACCCCCGGGGCGAAGGCTGGGAGCTGGCAGCGCCTGCCCGCCGCCAGAA
ACCCGCCGGTTGCTCGCTGTAGGTCCGCGCACCGGGTGGGGCGGGGAGGCTGCTGCTTCCCCCATCCCGGGCTG
GGCCCTCCCGTGAGCGATCCCGTCTCTCATTTTTCATGACATTCTTAATCATCGCACCTATTTACACACTTTGCC
AGCGCGCACCAAAATAACAACCACGATAATTATGATAATAAAGAGAGTCCTTTATCTGCTCCATCCTCGGGGAGG
AAGGGGGGAGTTGCTGTGCCTCCAGATTGTATAACGTGAGATTATCCTGATGAAAGCTTTATGATGTTTGCTCAA
ATAAAAGCTGCGTTTTGTAAATAGGCGCTAATTAAGCACGTTGCGAACGCAAGGAGTGCTCACCCTGGCGCCGCC
GCCCGGTTTCCAGCGCGAGGACTCGAGGGCGCGCGGTTCCTCTTTGCTAACTGCAGGATGGAGCCGATCCCCTCA
GGATGTTTCCCCTGTTCTCGACAACGGTAAAGACCCCCAAATTTGAAAGTAAGGGAATTTTGGGGTGGAGGGAAA
CTAGGGACGTACTTATCCCCTCTTCCATTTTCAAACAAAAAACTTTCAGCTCTTGTCTTCCCTTTAAAAATGGAA
TCACTTCTTGACAACGGCAGACCGTGCAGAGCGCACCAGCGCGAGCGGGGCTTCCTCGAGTCTCCAAGGCCCGGG
CTTCAACTTCCCGGGTCTAGACGTCA

Figure 24: Genomic sequence of the GBX2 promotor region. Cyan highlighted and bold: binding sites of the forward and reverse primer, red and underlined: binding site of the sequencing primer, green highlighted: CpGs, pink highlighted: analyzed CpGs.

The primer sequences, secondary structures, and melting temperatures are shown in **Table 7**. The salt-adjusted T_m predictions according to the *OligoCalc* online tool reveal a maximum T_m difference of 2.1 °C between the fw-C (64.6 °C) and the rev-A (62.5 °C) primer. Primer pairs should generally have a similar T_m to define the necessary T_a more easily. However, due to the design of multiple primers as part of this PSQ assay, higher T_m differences were unavoidable.

Table 7: Characteristics of primer set 2 for the GBX2 promoter. Green-highlighted: CpG site.

Primer (5‘→3‘)	Sequence	Secondary structure	T_m [°C]
Fw-C	TGTTTTGCGTTAGGTTGGAGTAGAAG	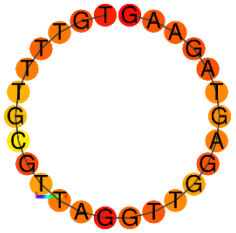	64.6
Fw-T	TGTTTTGTGTTAGGTTGGAGTAGAAG	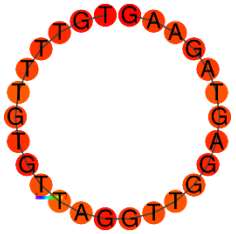	62.9
Rev-G	[btn]-TCTACACCGACTACCCCATATTCAT	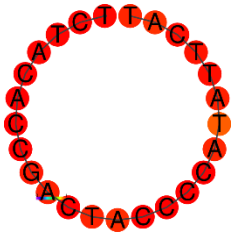	64.1
Rev-A	[btn]-TCTACACCAACTACCCCATATTCAT	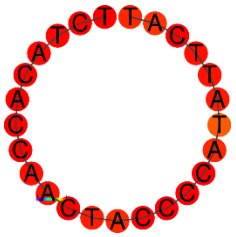	62.5
Rev-C	[btn]-CTACACCCACTACCCCATATTCATA	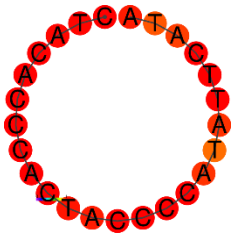	64.1
Seq	GGATTTGGTGGTGAG		46

The *BiSearch* web server predicted no off-target products and the primer binding sites do not contain any frequent SNPs. Homopolymer stretches are found in the forward primers (TTTT) as well as in the reverse primers (CCCC), but according to the *RNAfold* online tool none of them were likely to form secondary structures, such as hairpin structures. For this primer set homodimerization with a maximum of 2 (fw) and 4 (rev) complementary base pairs was found.

Heterodimers were predicted in each possible primer combination with a maximum of 5 possible base pairings and a ΔG of -8.31 kcal/mol. Two annealing temperatures (60.5 °C and 62.1 °C), multiple primer combinations, and concentrations (ranging from 0.2 µM to 0.6 µM) were applied in order to test the functionality of the designed primers. Bisulfite converted DNA standards were used as templates for the optimization of the reaction parameters. A summary of all tested PCR conditions is given in section 7.3.1.

During PCR, the NTC samples did not show any rise in their signal intensity, which indicates that no primer dimers were formed. Furthermore, their melt curves did not show any peaks during the heating interval from 65 °C to 95 °C, further verifying that the formation of primer dimers was prevented with primer set 2. A T_a of 60.5 °C generally resulted in lower Ct-values and higher signal intensities than a T_a of 62.1 °C. However, the tested PCR conditions did not bring forth satisfactory results. The DNA samples were amplified insufficiently under all tested reaction parameters. Moreover, the respective Ct-values for the three DNA standards with different methylation levels (0%, 50%, 100%) differed considerably from each other. The highest Ct-value was attained for the unmethylated DNA standard, followed by the 50% methylated and 100% methylated DNA standard. The methylation level of the DNA samples seems to influence the overall yield, indicating a possible PCR bias and making a comparison difficult (see **Figure 25**).

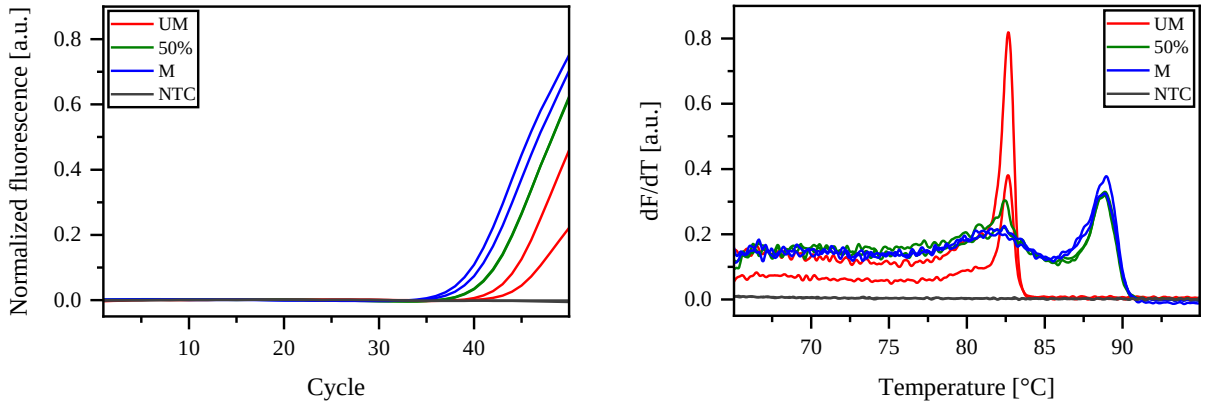

Figure 25: Amplification plot and derivative HRM plot obtained for GBX2 primer set 2. fw-C & rev-G = 0.2 µM, fw-T & rev-A = 0.4 µM. T_a = 60.5 °C, T_e = 72 °C. UM = unmethylated standard DNA, 50% = 50% methylated standard DNA, M = methylated standard DNA, NTC = no-template control.

The best results were obtained by using lower primer concentrations (0.2 µM to 0.4 µM) for fw-C and rev-G, and higher primer concentrations (0.4 µM to 0.6 µM) for fw-T and rev-A. Although primer set 2 provided only unsatisfactory results, a pyrosequencing reaction was still attempted. The PCR products obtained under the following conditions were subjected to PSQ analysis:

T_a = 60.5 °C, T_e = 72 °C, fw-C & rev-G (0.2 µM), fw-T & rev-A (0.4 µM). **Figure 26** shows the obtained pyrogram of the 50% methylated DNA standard using a 1.26-fold reaction setup (see **Table 5**). Unfortunately, only unsatisfying results were obtained (failed analyses, marked red). According to the internal quality control of the employed software, analysis of the respective CpGs failed due to high peak height deviation at the beginning of the sequence. Only considerably low peak heights were obtained in general, making potential deviations more noticeable. Additionally, the poly-G region at the beginning of the sequence is likely responsible for the low peak height intensities in the following positions.

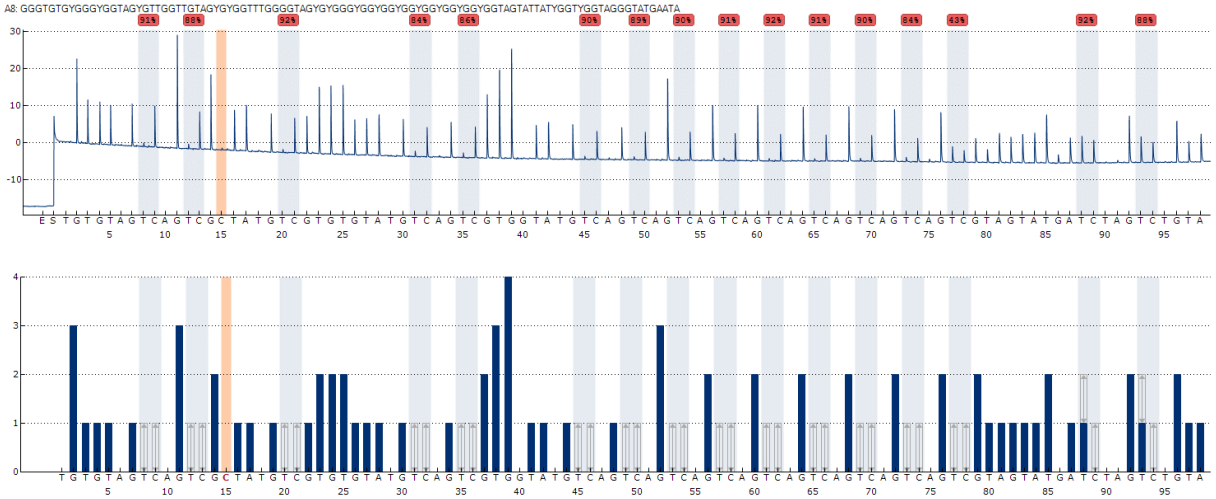

Figure 26: Representative pyrogram (top) and histogram (bottom) of GBX2 primer set 2 with 50% methylated standard DNA.

Since both primer sets did not provide satisfactory results, the methylation status in the GBX2 promoter region was not analyzed as part of this master's thesis. As previously stated, the design of a novel primer set for this gene region remains to be challenging. In order to analyze the CpG sites of the GBX2 promoter, more work needs to be done in the design and development of novel primers.

4.2 Analysis of the DNA methylation status in GBM samples

The methylation status of the genes MGMT, ABCB1, ABCG2, ABCA7, and p16 in GBM-related DNA extracts was determined in this study. Due to the limited amount of the sample set, not every assay was applied to all available samples. If possible, at least two replicates were used to provide confidence in the reliability of the employed assays. However, in a few instances some GBM samples were analyzed only once because of the short supply of said sample set. Raw data for all employed assays is shown in section 7.3.2. In the following section, a statistical analysis of the acquired data is presented. The aim of this thesis was to find correlations between the methylation status of a number of potential biomarkers and other clinical characteristics. For example, the correlation between the methylation levels of the MGMT enhancers and MGMT expression was investigated.

4.2.1 Methylation of the MGMT promoter

The MGMT promoter methylation status was determined for twelve CpGs by Katja Zappe prior to this master's thesis. The employed assay was originally developed by Switzeny *et. al.* and covers the CpGs 72-83 in the MGMT promoter region on chr10: 129467212-129467309 (GRCh38.p13).[156] The used primer set is given in section 7.3.1 (**Supplementary Table 13**). All 40 DNA extracts of the GBM sample set were analyzed, and the corresponding raw data can be found in section 7.3.2 (**Supplementary Table 39**).

As seen in **Table 8**, a statistically significant, negative correlation between mean MGMT promoter methylation and MGMT expression could be found, with a Spearman-Rho coefficient of $r_S = -0.824$ and a p-value of < 0.001.

Table 8: Two-tailed Spearman-Rho test for correlations between MGMT promoter methylation and MGMT expression. r_S = Spearman-Rho correlation coefficient, ***: $p < 0.001$.

CpG	r_S	p-value	CpG	r_S	p-value
72	-0.793^{***}	< 0.001	78	-0.760^{***}	< 0.001
73	-0.824^{***}	< 0.001	79	-0.826^{***}	< 0.001
74	-0.827^{***}	< 0.001	80	-0.824^{***}	< 0.001
75	-0.824^{***}	< 0.001	81	-0.824^{***}	< 0.001
76	-0.824^{***}	< 0.001	82	-0.824^{***}	< 0.001
77	-0.792^{***}	< 0.001	83	-0.824^{***}	< 0.001
mean	-0.824^{***}	< 0.001			

Significant correlation was observed for all twelve analyzed CpGs. Switzeny *et. al.* also discovered a relationship between the level of promoter methylation and MGMT suicide-enzyme activity (two-tailed Spearman-Rho test, $r_S = -0.69$, $p < 0.01$). These findings are in line with a number of earlier studies reporting a negative correlation between MGMT promoter methylation and expression of MGMT, as previously stated in section 1.3.3.

However, if the methylation status of the MGMT promoter region is plotted against the GBM sample set, we see that not all samples follow this trend between MGMT promoter methylation and MGMT expression (see **Figure 27**). L01 showed no detectable methylation (< LLOQ) in the investigated promoter region, even though it is a non-MGMT expressing sample. The corresponding patient would not receive GBM-treatment with TMZ, because an unmethylated MGMT promoter suggests low response to TMZ. However, the MGMT expression level indicates that said patient would in fact benefit from this treatment option. This further demonstrates the existence of inconsistencies between MGMT promoter methylation and MGMT expression. These discrepancies must be kept in mind when MGMT is used as a predictive biomarker for treatment success with TMZ.

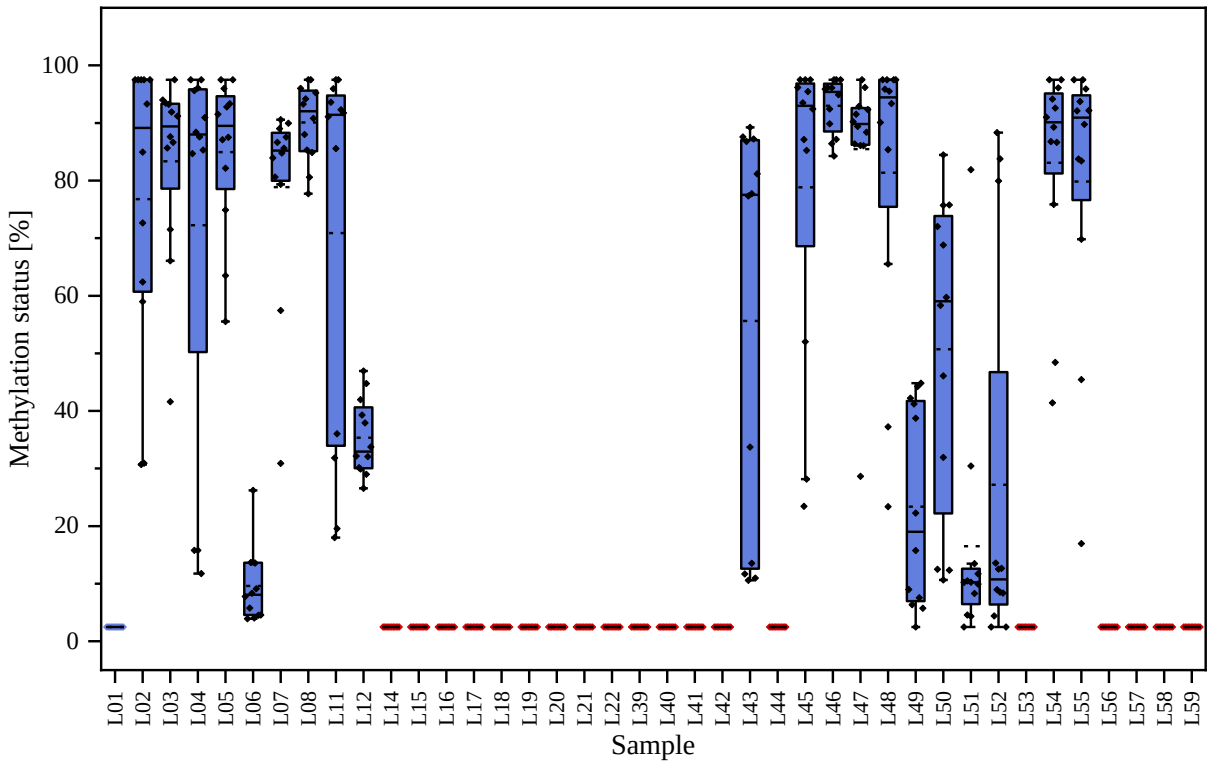

Figure 27: Methylation status of twelve CpGs in the MGMT promoter region, ordered by sample. Blue plots: non-MGMT expressing samples, red plots: MGMT expressing samples, continuous lines: median, dashed lines: mean.

Non-MGMT expressing samples (marked blue) showed a high heterogeneity in their mean methylation values, ranging from 2.5% (< LLOQ) in sample L01 to 93.0% in sample L46. In contrast, all 19 MGMT expressing samples (marked red) displayed results below LLOQ.

According to the data provided by our research partner, the DNA extracts could be grouped into 21 non-MGMT expressing and 19 MGMT expressing samples. A boxplot was generated for these two groups and ordered by CpG, as seen in **Figure 28**. A clear contrast in the methylation status of the pictured groups could be seen in all twelve investigated CpG sites. Additionally, a Mann-Whitney U test was performed, which demonstrated a highly significant difference between non-MGMT and MGMT expression for each CpG ($p < 0.001$).

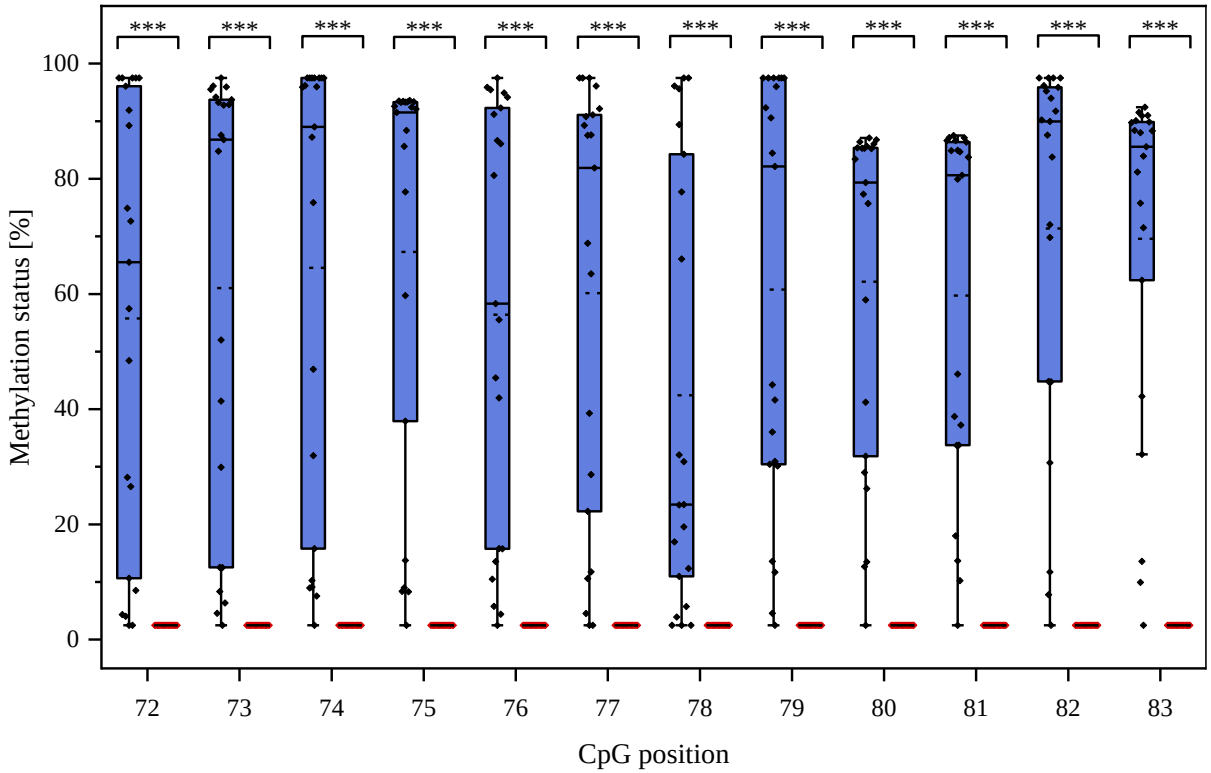

Figure 28: Methylation status of twelve CpGs in the MGMT promoter region, ordered by CpG. Blue plots: non-MGMT expressing samples, red plots: MGMT expressing samples, continuous lines: median, dashed lines: mean, ***: $p < 0.001$.

The association between MGMT promoter methylation and characteristics of GBM patients was also investigated. **Table 9** compiles the percentage of the mean methylation status upon sex and age at surgery. Using the whole GBM sample set for reference, male patients had significantly lower methylation levels than female patients. 13 out of the 15 women did not show any MGMT expression at all, in contrast to only 8 out of 25 men. However, no statistical differences in promoter methylation ($r_S = -0.151$, $p = 0.591$) or MGMT expression ($r_S = 0.509$, $p = 0.053$) were found between the two sexes. The MGMT promoter region of elderly patients

was methylated to a lesser degree than the average patient. Having said that, when only the methylated MGMT samples are examined, the results look quite different. The mean methylation levels of the investigated characteristics are homogeneous, and no statistical differences were found. Only a higher age corresponds to a lower overall methylation status of the promoter region.

Table 9: Characteristics of patients and their MGMT promoter methylation status in 40 GBM samples.

	GBM sample set		Methylated MGMT samples	
Characteristics	**n**	**Methylation status [%]**	**n**	**Methylation status [%]**
All patients	40	33.2	20	63.9
Women	15	51.0	12	63.1
Men	25	22.5	8	65.0
Age at surgery < 70	29	35.0	15	65.3
Age at surgery > 70	11	28.4	5	59.6

Additionally, the MGMT promoter methylation status did not significantly correlate with the OS of the patients ($r_S = 0.256$, $p = 0.116$). Only the age at surgery showed a significant negative correlation with the OS ($r_S = -0.478$, $p = 0.002$).

4.2.2 Methylation of the MGMT enhancers

4.2.2.1 MGMT enhancer E

The methylation status of 14 CpGs (No. 1-3, 7-13, 19-22) in MGMT enhancer E was determined by PSQ. 24 DNA extracts of the GBM sample set were already applied to the CpGs 7-13 and 19-22 by Katharina Pühringer. The corresponding raw data was taken from her master's thesis and can be found there. In this work, the methylation status of the 14 CpGs was investigated for the remaining samples. Due to the general scarcity of the GBM sample set, the CpGs 1-3, 7, and 8 were not analyzed in samples L44, L56, and L58. Moreover, the assay targeting the CpGs 19-22 was not applied to sample L56. Raw MGMT enhancer E methylation data for the employed PSQ assays is given in 7.3.2 (**Supplementary Table 40-43**).

Correlation analysis between MGMT enhancer methylation levels and MGMT expression revealed a significant positive correlation ($r_S = 0.696$, $p < 0.001$) for all 14 analyzed CpGs, as seen in **Table 10**. Consequently, the methylation status of the MGMT enhancer might help to predict MGMT expression in cases where the application of the promoter methylation alone would lead to false predictions. For instance, sample L01 did not show any detectable

methylation patterns in the investigated promoter region, although it exhibits no expression of MGMT.

Table 10: Two-tailed Spearman-Rho test for correlations between MGMT enhancer E methylation and MGMT expression. r_S = Spearman-Rho correlation coefficient, *: p < 0.05, **: p < 0.01.

CpG	rs	p-value	CpG	rs	p-value
1	0.653^{***}	< 0.001	11	0.588^{***}	< 0.001
2	0.459^{**}	0.004	12	0.554^{***}	< 0.001
3	0.792^{***}	< 0.001	13	0.622^{***}	< 0.001
7	0.602^{***}	< 0.001	19	0.568^{***}	< 0.001
8	0.556^{***}	< 0.001	20	0.558^{***}	< 0.001
9	0.712^{***}	< 0.001	21	0.491^{**}	0.002
10	0.623^{***}	< 0.001	22	0.651^{***}	< 0.001
mean	0.696^{***}	< 0.001			

Since the correlation was found to be positive, it is to be expected that L01 shows a low methylation status in the respective enhancer region. However, this was not the case. The overall mean methylation grade of the 14 analyzed CpGs for sample L01 was 61.4%, ranging from 36.7% at CpG site No. 13 to 97.5% at CpG site No. 2 (see **Figure 29**).

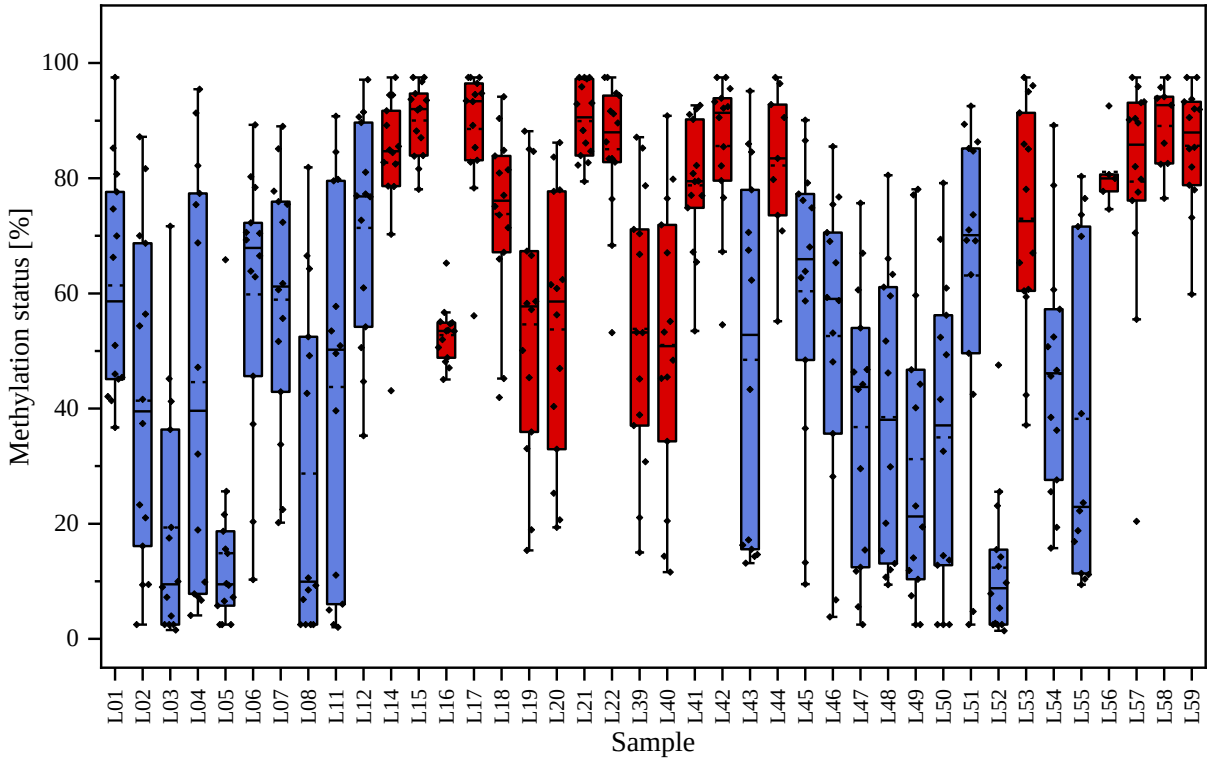

Figure 29: Methylation status of 14 CpGs in MGMT enhancer E, ordered by sample. Blue plots: non-MGMT expressing samples, red plots: MGMT expressing samples, continuous lines: median, dashed lines: mean.

Even though L01 is a non-MGMT expressing sample, the average methylation status exceeded 50% in the investigated region. Therefore, employing MGMT enhancer E would lead to the same wrong predictions as with the MGMT promoter. However, the average methylation status of MGMT enhancer E comprised only 14 CpGs that greatly varied in their overall methylation levels. Examining a higher number of CpGs might provide better results, since some CpGs could show a stronger correlation with MGMT expression than others. Additionally, examination of only one sample does not yield satisfying insights. Ideally, a large sample set with a discrepancy between MGMT promoter methylation and expression of MGMT should be investigated.

MGMT expressing samples tended to show a higher methylation status than non-expressing samples. Furthermore, a high heterogeneity between the 14 CpG sites was observed in the investigated region. **Figure 30** presents the methylation values of the investigated CpG sites divided into two groups. A significant difference was discovered graphically, as well as statistically.

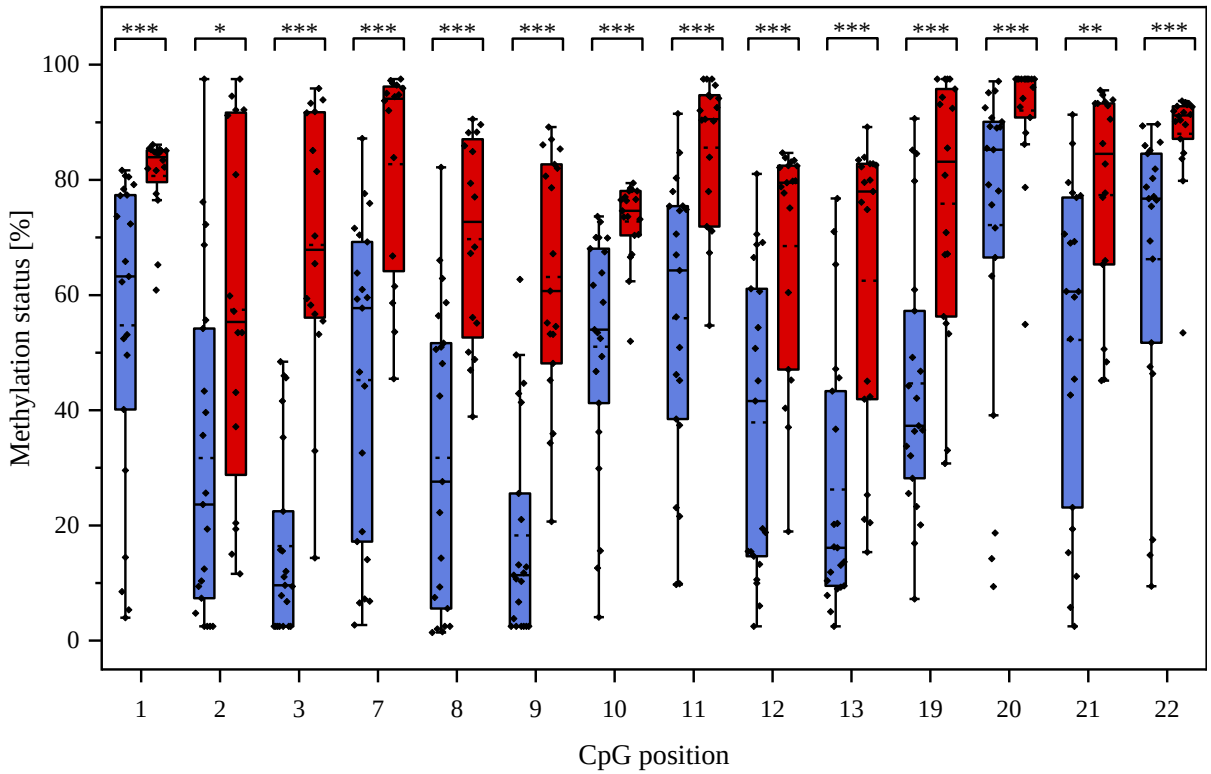

Figure 30: Methylation status of 14 CpGs in MGMT enhancer E, ordered by CpG. Blue plots: non-MGMT expressing samples, red plots: MGMT expressing samples, continuous lines: median, dashed lines: mean, *: $p < 0.05$, **: $p < 0.01$, ***: $p < 0.001$.

A Mann-Whitney U test demonstrated a highly significant difference between non-MGMT and MGMT expressing samples for each CpG. A p-value of < 0.001 was obtained for all CpGs,

except for CpG No. 2 ($p < 0.05$) and CpG No. 21 ($p < 0.01$). In non-MGMT expressing samples, the mean methylation levels of the investigated CpG sites ranged from 16.4% (CpG No. 3) to 72.2% (CpG No. 20). Mean methylation levels in MGMT expressing samples lay between 57.4% (CpG No. 2) and 92.0% (CpG No. 20). In conclusion, MGMT enhancer E methylation was associated with expression of MGMT.

4.2.2.2 MGMT enhancer K-M

MGMT enhancer K-M methylation levels were determined for 19 CpG sites (No. 5-8, 11-18, 24-27, and 37-39) by PSQ. The same 24 DNA extracts of the GBM sample set have already been applied by Simon Pflug as in the master's thesis of Katharina Pühringer. The raw data was again taken from the corresponding work and is presented there. The remaining DNA extracts were analyzed in this project, with a few exceptions. The CpGs 24-27 and 37-39 were not investigated in samples L44, L56, and L58. Additionally, CpG No. 24 was only analyzed in 22 of the 40 DNA extracts, since the associated PSQ assay had to be improved as part of this master's thesis. The PSQ results for the investigated CpG sites of the K-M enhancer are presented in section 7.3.2 (**Supplementary Table 44-47**).

A negative correlation (Spearman-Rho test) between MGMT enhancer K-M methylation and expression of MGMT was observed for most CpGs, but none of them was significant at a 5% level (see **Table 11**).

Table 11: Two-tailed Spearman-Rho test for correlations between MGMT enhancer K-M methylation and MGMT expression, applied to all 40 GBM samples. r_S = Spearman-Rho correlation coefficient.

CpG	r_S	p-value	CpG	r_S	p-value
5	-0.049	0.762	17	-0.180	0.267
6	-0.048	0.769	18	-0.185	0.254
7	-0.128	0.430	24	0.228	0.307
8	-0.083	0.611	25	-0.018	0.917
11	-0.101	0.534	26	0.234	0.164
12	-0.122	0.454	27	0.104	0.539
13	-0.011	0.946	37	-0.098	0.562
14	-0.160	0.323	38	-0.043	0.802
15	-0.047	0.773	39	0.063	0.710
16	-0.058	0.721			
mean	0.006	0.972			

Consequently, the methylation of MGMT enhancer K-M might be associated with lower MGMT expression levels, but a significant difference was not found. The GBM sample set was then reduced to the 19 MGMT expressing samples and the statistical analysis repeated. For all analyzed CpG sites, except CpGs No. 25-27, a negative correlation could be found, but once again the results were not statistically significant (see **Table 12**). Only CpG No. 17 was close to being significant (r_S = -0.437, p = 0.062).

Table 12: Two-tailed Spearman-Rho test for correlations between MGMT enhancer K-M methylation and MGMT expression, applied to the 19 MGMT expressing samples. r_S = Spearman-Rho correlation coefficient.

CpG	r_S	p-value	CpG	r_S	p-value
5	-0.052	0.833	17	-0.437	0.062
6	-0.191	0.434	18	-0.299	0.214
7	-0.114	0.642	24	-0.043	0.913
8	-0.207	0.394	25	0.249	0.353
11	-0.158	0.518	26	0.162	0.549
12	-0.244	0.314	27	0.192	0.477
13	-0.170	0.486	37	-0.361	0.169
14	-0.092	0.707	38	-0.345	0.191
15	-0.228	0.347	39	-0.514	0.072
16	-0.345	0.148			
mean	-0.360	0.130			

These findings suggest that a negative correlation might exist, but MGMT enhancer K-M methylation alone seems to be a poor predictor of MGMT expression. Since a nearly significant correlation was found for CpG No. 17, it could act as a predictive marker for MGMT expression in cases, where the promoter methylation alone would lead to wrong predictions. Of the available GBM sample set, L01 did not follow the rule of negative correlation between methylation of the MGMT promoter and expression of MGMT. Using CpG No. 17 as a predictive marker would ideally show high methylation levels for L01 in said CpG site. Indeed, a mean methylation status of 91.0% was found for CpG No. 17 in sample L01, accurately predicting its MGMT expression. However, the whole GBM sample set displayed high methylation levels, with a mean methylation value of 78.5% for non-MGMT and 82.8% for MGMT expressing samples. It has to be noted that the samples L43 (21.8%) and L54 (10.4%) are statistical outliers and consequently lower the mean methylation value for non-MGMT expression samples from 85.0% to 78.5%. **Figure 31** illustrates a boxplot comparison of the CpG 17 methylation status between the two examined groups.

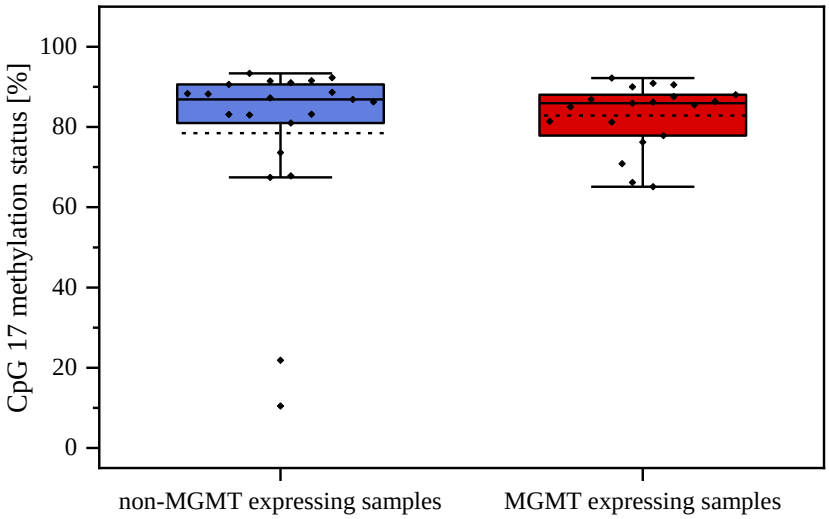

Figure 31: Boxplot comparison of CpG 17 methylation status in MGMT enhancer K-M. Blue plot: non-MGMT expressing samples, red plot: MGMT expressing samples, continuous lines: median, dashed lines: mean.

The Whitney-Mann U test reported no significant difference (p = 0.533), omitting L43 and L54 did not change the outcome (p = 0.220). All in all, MGMT enhancer K-M methylation does not seem to be a useful predictor of MGMT expression. It is highly methylated in both non-MGMT and MGMT expressing samples. Only L43 and L54 are exceptions to this rule. Having said that, only 19 of the 46 CpGs in the investigated region were analyzed as part of this study. The remaining 27 CpGs might show a stronger correlation with expression of MGMT.

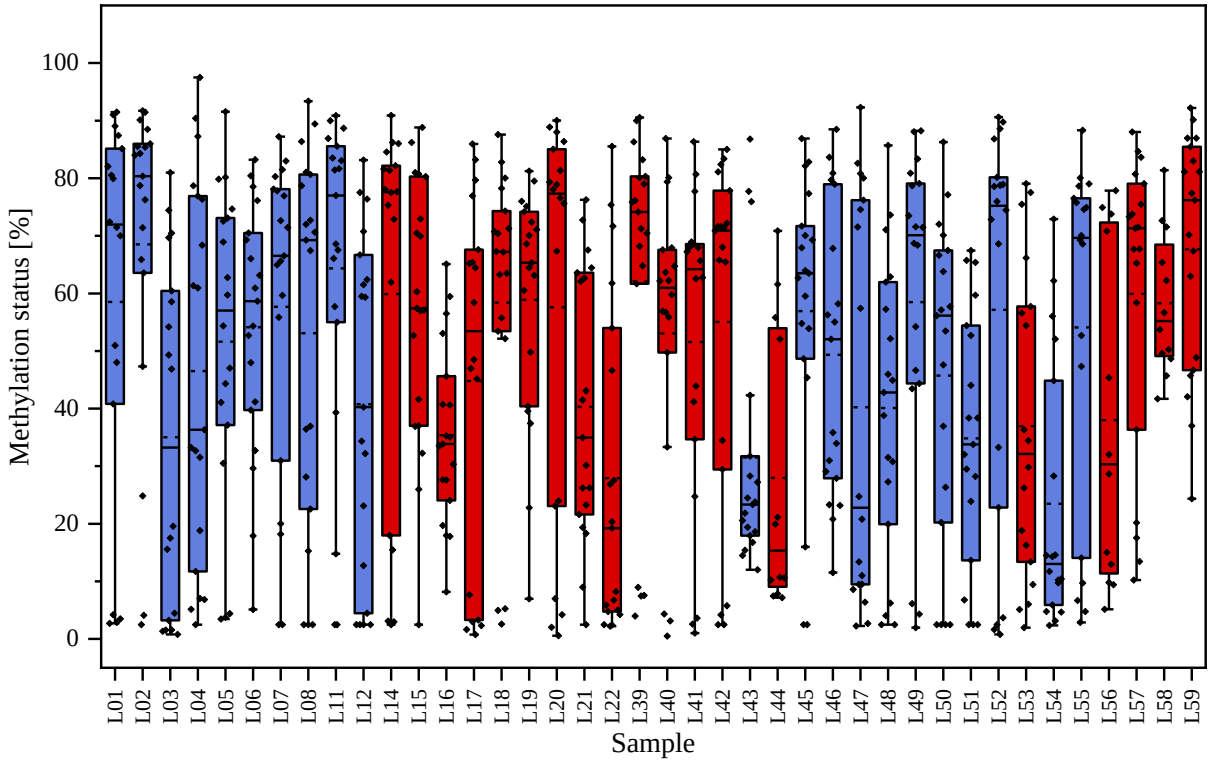

Figure 32: Methylation status of 19 CpGs in MGMT enhancer K-M, ordered by sample. Blue plots: non-MGMT expressing samples, red plots: MGMT expressing samples, continuous lines: median, dashed lines: mean.

The distribution of the MGMT enhancer K-M methylation levels of the 19 analyzed CpG sites ordered by sample is presented in **Figure 32**. No significant difference between non-MGMT and MGMT expressing samples is visible. Ordering the methylation levels by CpG does not provide any discernable differences between the two examined groups, as seen in **Figure 33**.

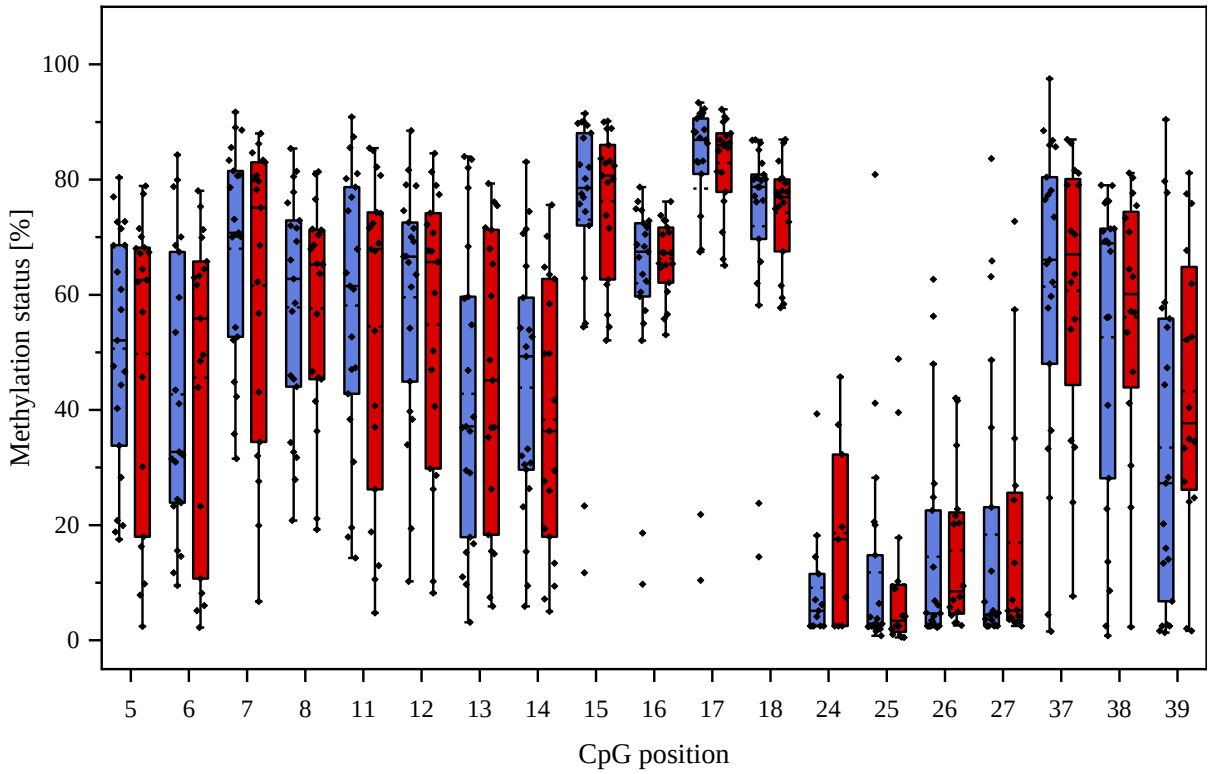

Figure 33: Methylation status of 19 CpGs in MGMT enhancer K-M, ordered by CpG. Blue plots: non-MGMT expressing samples, red plots: MGMT expressing samples, continuous lines: median, dashed lines: mean.

According to Chen *et. al.*, MGMT enhancer K-M is also responsible for expression of the proliferation marker Ki67, albeit to a lesser extent than for MGMT. Therefore, a possible correlation between K-M enhancer methylation and Ki67 expression was also investigated. Our cooperation partner provided data on Ki67 expression for 29 samples. However, only rough estimates of expression strength were available, classifying 15 samples as "low" and 14 samples as "high". Samples with high Ki67 expression generally showed lower mean methylation levels, except for the CpGs No. 12 and 37-39. The K-M enhancer methylation levels of these two groups were tested for significant difference. Out of the 19 analyzed CpG sites only CpG No. 14 showed a statistically significant difference ($p = 0.047$), as seen in **Table 13**. A boxplot comparison of the methylation status of CpG No. 14 between the two examined groups is shown in **Figure 34**. Taking the acquired data into account, it seems that high K-M enhancer methylation values coincide with low MGMT and Ki67 expression. In other words, MGMT enhancer K-M hypomethylation leads to expression of MGMT and Ki67. Nevertheless, it has

to be noted that no statistically significant differences were found for most of the available data, bringing this correlation into question.

Table 13: Comparison of MGMT enhancer K-M methylation between samples with low and high Ki67 expression. *: $p < 0.05$.

CpG	Methylation status [%]		p-value	CpG	Methylation status [%]		p-value
	Ki67 low	Ki67 high			Ki67 low	Ki67 high	
5	54.5	48.3	0.247	17	84.6	79.1	0.647
6	49.5	44.1	0.445	18	75.9	71.7	0.810
7	67.8	67.5	0.616	24	20.6	10.0	0.171
8	61.2	56.2	0.395	25	15.9	8.1	0.382
11	60.9	56.5	0.348	26	17.0	15.5	0.778
12	59.5	60.2	0.983	27	21.6	14.0	0.198
13	53.2	41.2	0.198	37	54.3	68.0	0.383
14	50.9	32.9	0.047*	38	49.8	57.8	0.538
15	79.5	72.9	0.247	39	39.2	39.2	1.000
16	65.5	63.9	0.616				
mean	52.5	49.1	0.499	MGMT expr.	0.3	0.2	0.297

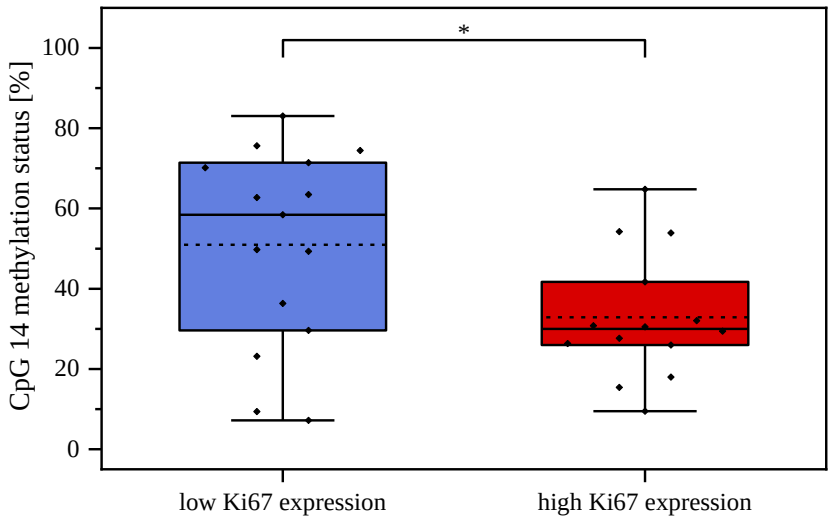

Figure 34: Boxplot comparison of CpG 14 methylation status in MGMT enhancer K-M. Blue plot: low Ki67 expressing samples, red plot: high Ki67 expressing samples, continuous lines: median, dashed lines: mean, *: $p < 0.05$.

4.2.3 Methylation of ABC-transporters

4.2.3.1 ABCB1 & ABCG2

The promoter methylation status was determined for ABCB1 and ABCG2 by PSQ. The ABCB1 assay targeted seven CpGs downstream of the transcription start site (TSS), whereas the ABCG2 assay encompassed eight CpGs upstream of the TSS. 27 DNA extracts of the GBM sample set were analyzed for both promoter regions as part of this master's thesis. The corresponding raw data is given in section 7.3.2 (**Supplementary Table 48 & 49**).

The promoter methylation values of ABCB1 (marked blue) and ABCG2 (marked red) in the 27 analyzed GBM samples are given in **Figure 35**. In general, the methylation levels in the investigated regions showed high heterogeneity, especially for the ABCG2 promoter. The average promoter methylation status of ABCB1 ranged from 3.3% (< LLOQ) for sample L54 to 91.5% for sample L12. Average promoter methylation levels of ABCG2 lay between 2.5% (< LLOQ) for samples L02, L12, and L49, and 96.5% for sample L40. The ABCB1 promoter was hypomethylated only in sample L54, whereas 4 samples (L02, L12, L16, and L49) were found to be unmethylated in the ABCG2 promoter. **Figure 36** presents the promoter methylation values of the investigated CpG sites for ABCB1 (seven CpGs) and ABCG2 (eight CpGs). The seven CpGs in the ABCB1 promoter showed an average methylation status of 45.8%, ranging from 31.0% (CpG No. 6) to 61.0% (CpG No. 1). The average methylation status of the eight CpGs targeted in the ABCG2 promoter was 43.5%, encompassing 39.7% (CpG No. 2) and 50.2% (CpG No. 6).

Sorting the promoter methylation values of ABCB1 and ABCG2 by sample, no obvious correlations could be discovered graphically. Furthermore, statistical analysis (Spearman-Rho) did not reveal any significant correlations either ($r_S = 0.113$, $p = 0.582$). This is in stark contrast to a previous in-house study, where the same two PSQ assays were used to investigate the promoter methylation status of ABCB1 and ABCG2 in tumor tissues from breast cancer patients ($r_S = 0.621$, $p = 0.010$).[157] While the two ABC-transporters have been found to be commonly co-expressed, they do act independently from each other.[107] The mean promoter methylation status for the analyzed CpG sites of ABCB1 and ABCG2 was neither associated with the OS time ($r_S = -0.244$, $p= 0.229$ and $r_S = 0.228$, $p = 0.262$), nor with the age at surgery ($r_S = 0.202$, $p = 0.312$ and $r_S = 0.257$, $p = 0.195$).

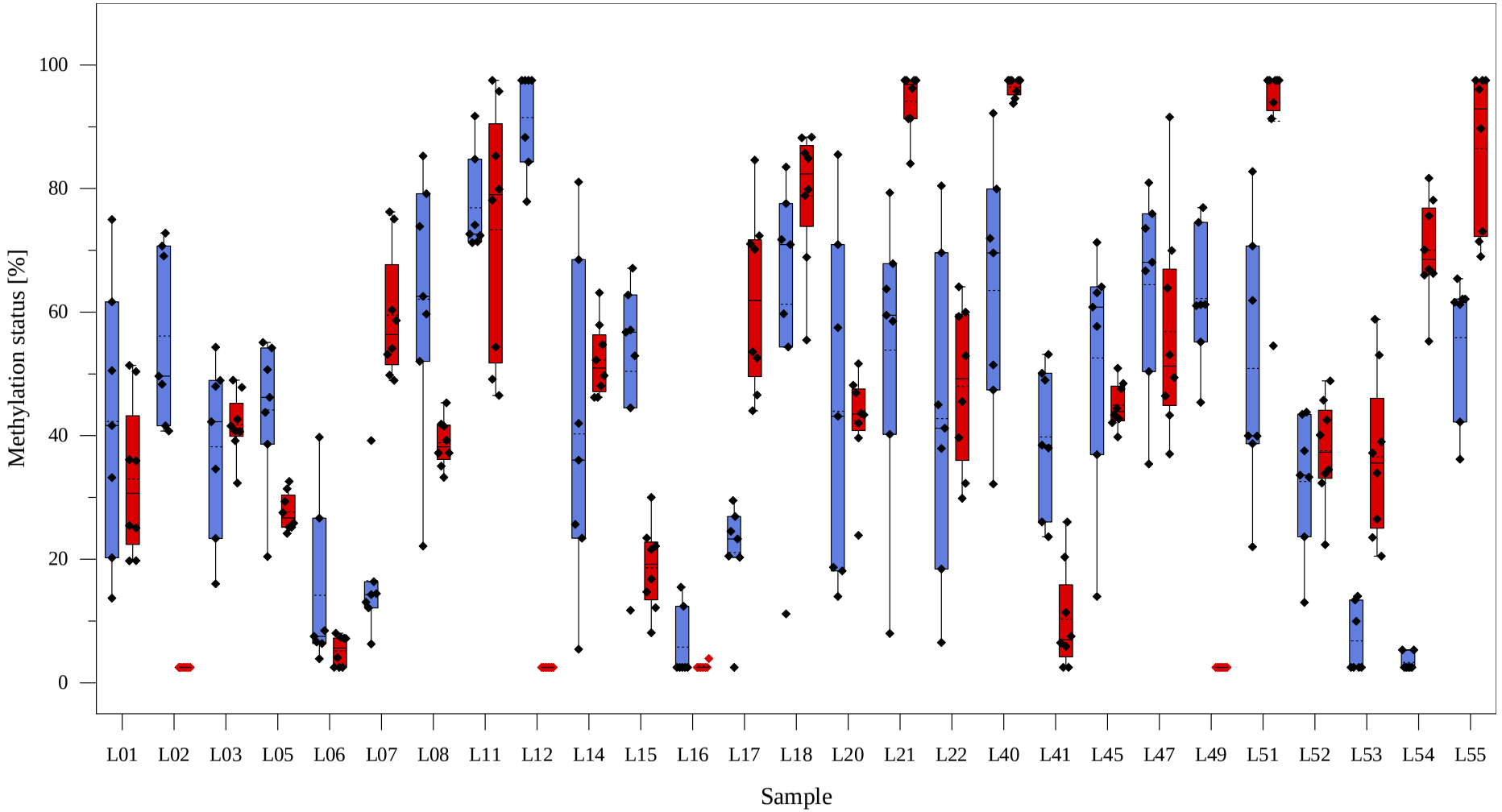

Figure 35: Boxplot comparison of promoter methylation status of ABCB1 (marked blue) and ABCG2 (marked red) in 27 GBM samples, ordered by sample. Continuous lines: median, dashed lines: mean.

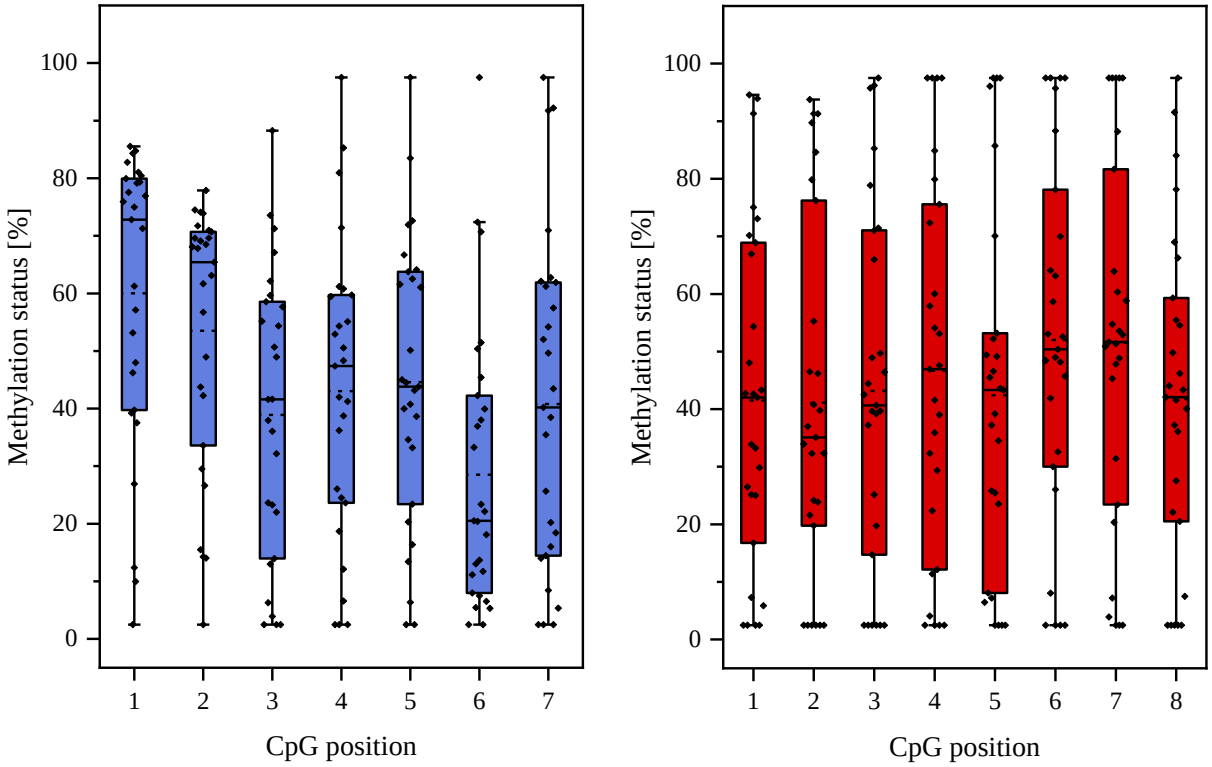

Figure 36: Promoter methylation status of ABCB1 (marked blue) and ABCG (marked red) in 27 GBM samples, ordered by CpG. Continuous lines: median, dashed lines: mean.

4.2.3.2 ABCA7 exon 5 / intron 5

The methylation status of seven CpGs in the ABCA7 exon 5 / intron 5 region was determined by PSQ. In this work, 27 DNA extracts of the 40 available GBM samples were used for the analysis of the investigated region. Raw data for the employed PSQ assay is presented in section 7.3.2 (**Supplementary Table 50**).

In order to apply statistics to the available raw data, mean values of two technical replicates for each sample were employed, if possible. Replicates with mean methylation values within 10 % were considered acceptable. Unfortunately, 19 out of the 27 analyzed samples exceeded the threshold in this PSQ assay, bringing the validity of the available data into question. It has to be said that previous in-house studies did not report any issues with the technical repeatability of their samples using this assay.[153,154] One possible explanation could be that individual DNA strands were methylated to different degrees. As a result, different results were obtained depending on which aliquot was analyzed. The employed PSQ assay has not been applied to GBM samples before, preventing a thorough comparison of raw data. The large differences between technical replicates were not limited to a single CpG, instead all seven CpGs showed occasional significant deviations. Since EvaGreen dye was added to the PCR master mix, the amplification and melt curves could be analyzed to search for any inconsistencies. As seen in **Figure 37**, the unmethylated DNA standard was amplified to a higher degree than the

methylated DNA standard. Preferential amplification of either standard – also known as PCR-bias – leads to inaccurate results that do not correctly reflect the real situation. After bisulfite conversion, the sequences of unmethylated and methylated standards look different, which might result in a bias during PCR amplification leading to an inaccurate estimate of the methylation status.[158,159] Still, the high deviations between individual replicates could not be explained by this phenomenon. Since the GBM sample set was successfully applied to a number of PSQ assays as part of this master's thesis, the DNA extracts did not seem to be responsible for this disparity. A possible cause for the low technical repeatability was not discovered and needs to be kept in mind for further studies of the ABCA7 exon 5 / intron 5 region.

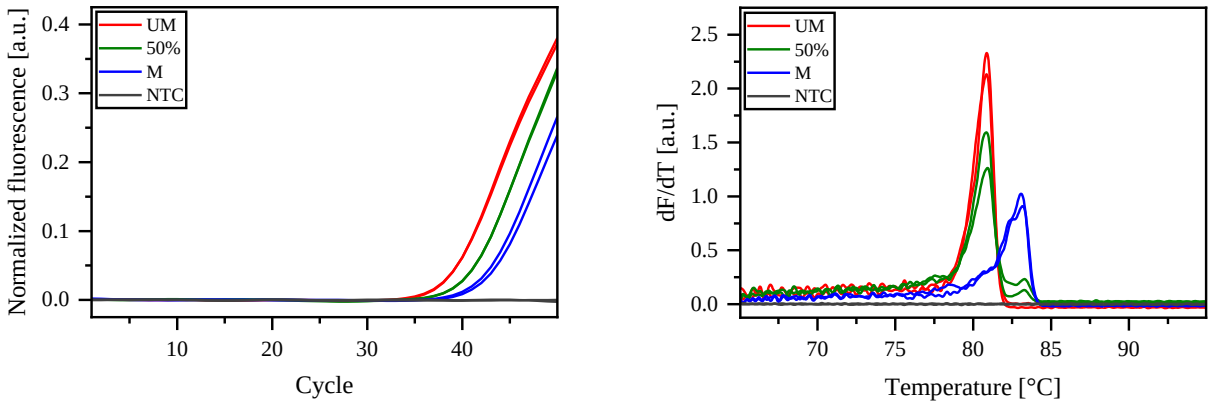

Figure 37: Amplification plot and derivative HRM plot obtained for the PSQ assay of ABCA 7 exon 5 / intron 5. Primer concentration = 0.2 µM, T_a = 58.3 °C, T_e = 72.0 °C. UM = unmethylated standard DNA, 50% = 50% methylated standard DNA, M = methylated standard DNA, NTC = no-template control.

Out of the 27 utilized DNA extracts, the mean methylation values of the replicates deviated only slightly in eight samples. Since the obtained data precluded a meaningful statistical analysis, it was omitted in this study. The mean methylation values of the eight samples showed high heterogeneity, ranging from 11.4% for sample L14 and 87.9% for sample L47, as seen in **Figure 38**.

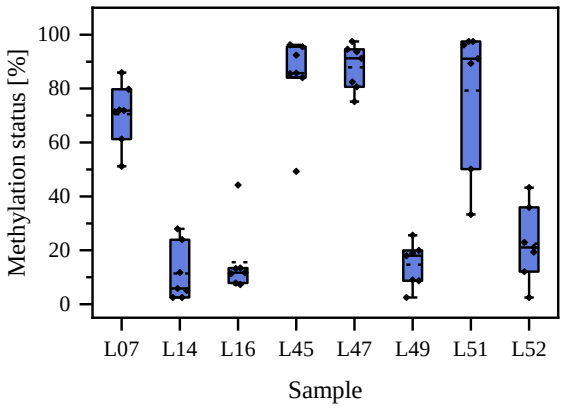

Figure 38: Methylation status of seven CpGs in the ABCA7 exon 5 / intron 5 region in eight samples, ordered by sample. Continuous lines: median, dashed lines: mean.

4.2.3.3 ABCA7 exon 6 / intron 6

The methylation status of nine CpGs in the ABCA7 exon 6 / intron 6 region was determined by PSQ. With this assay, 27 DNA extracts of the GBM sample set were analyzed. The corresponding raw data is presented in section 7.3.2 (**Supplementary Table 51**).

The analyzed GBM samples showed a relatively high homogeneity in their methylation values. Apart from sample L49 (49.5%), all samples exhibited a mean methylation status above 50% and 19 out of the 27 DNA extracts exceeded 70% (see **Figure 39**). Mean methylation values ranged from 49.5% for sample L49 to 83.7% for sample L15.

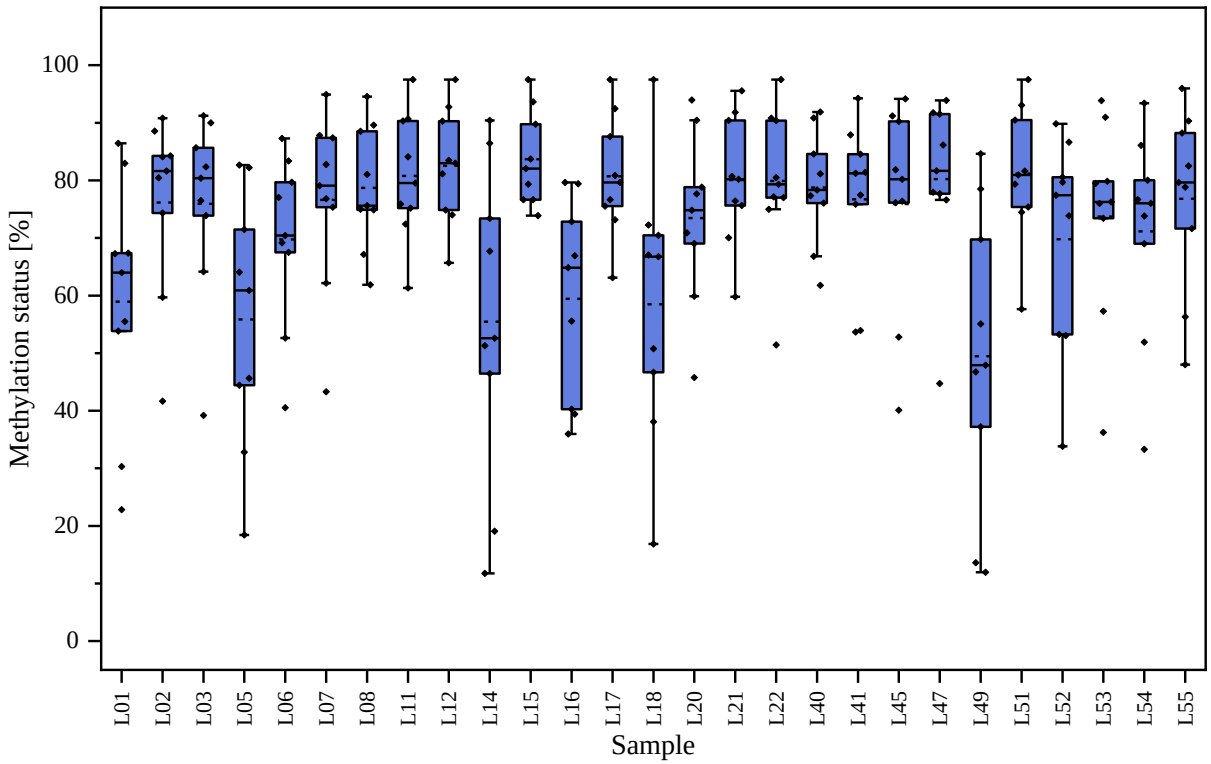

Figure 39: Methylation status of nine CpGs in the ABCA7 exon 6 / intron 6 region in 27 GBM samples, ordered by sample. Continuous lines: median, dashed lines: mean.

A high homogeneity was also found for the individual CpG sites, in contrast to other PSQ assays employed in this master's thesis, as seen in **Figure 40**. Only CpG No. 5 showed a mean methylation status (47.2%) below 50%. Mean methylation values lay between 47.2% for CpG No. 5 and 92.1% for CpG No. 8. Compared to the investigated promoter regions in ABCB1 and ABCG2, the average methylation levels in the ABCA7 exon 6 / intron 6 region were much higher. The analyzed CpG sites of the ABCB1 and ABCG2 promoter showed a mean methylation status of 45.8% and 43.5% respectively, whereas 72.6% was found for the ABCA7 exon 6 / intron 6 region.

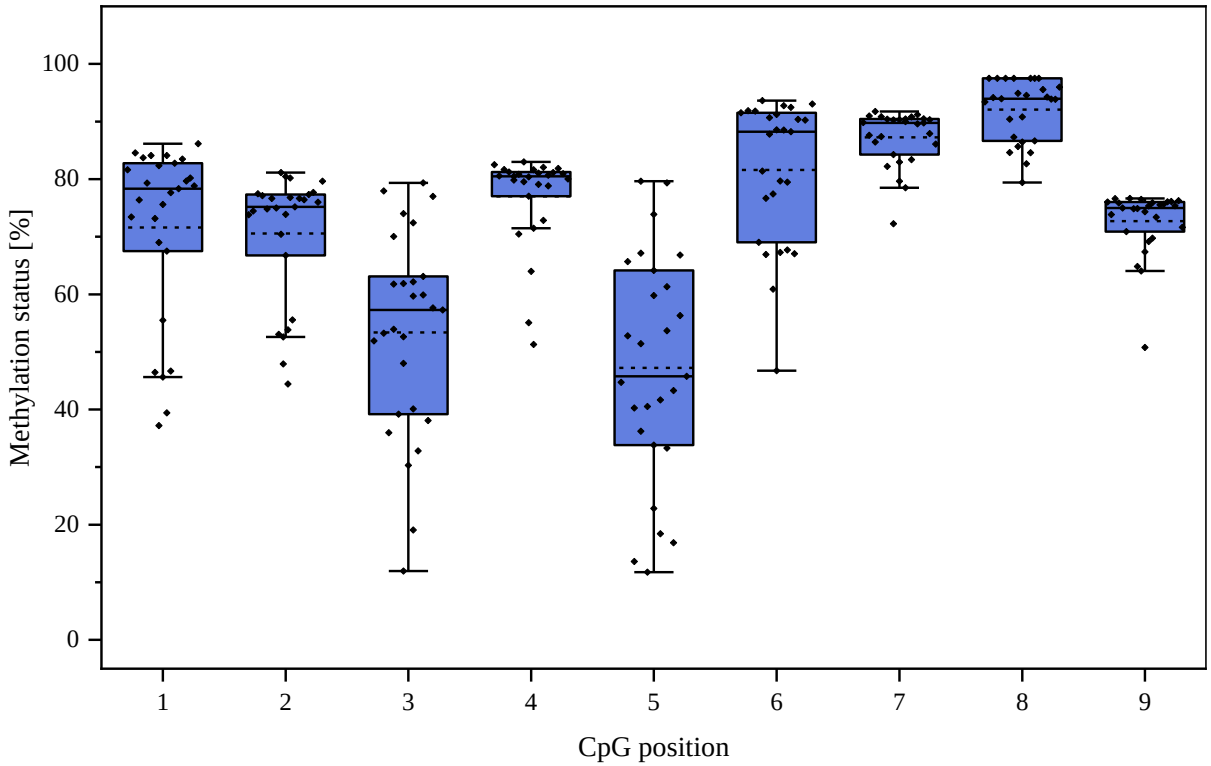

Figure 40: Methylation status of nine CpGs in the ABCA7 exon 6 / intron 6 region in 27 GBM samples, ordered by CpG. Continuous lines: median, dashed lines: mean.

Since there was a visible difference between the methylation values of the ABCA7 exon 6 / intron 6 region and the ABCB1 and ABCG2 promoter, a statistical analysis of the available data was carried out. However, the mean methylation status of the ABCA7 exon 6 / intron 6 region did neither significantly correlate with ABCB1 (r_S = 0.378, p = 0.052), nor with ABCG2 (r_S = 0.307, p = 0.120). Furthermore, no significant correlations were found with the age at surgery (r_S = -0.108, p = 0.591) or the OS time (r_S = 0.034, p = 0.871).

4.2.4 Methylation of p16

4.2.4.1 p16 promoter

The PSQ analysis of the methylation status of seven CpGs in the p16 promoter region was attempted. 35 out of the 40 GBM samples were employed for this task. Raw data for the investigated CpG sites is given in section 7.3.2 (**Supplementary Table 52 & 53**).

Before the methylation values of the 36 samples could be determined by PSQ, the samples had to be amplified by PCR first. Unfortunately, 19 out of the 35 DNA extracts showed high Ct values and low fluorescence signal intensities, indicating low yields. Deletion of the p16 encoding region has been investigated in a number of studies and is linked to various types of tumors. [113–115] This deletion mechanism is the most likely cause of the reduced amplification during PCR. Moreover, a PCR bias was observed for the employed standards, favoring the

unmethylated DNA standard over the methylated one. Additionally, this bias was also noted in the HRM peaks (see **Figure 41**). The peak corresponding to the methylated DNA standard had a significantly lower intensity than the peak of the unmethylated one. Nevertheless, determination of the methylation status by PSQ was attempted for the successfully amplified GBM samples.

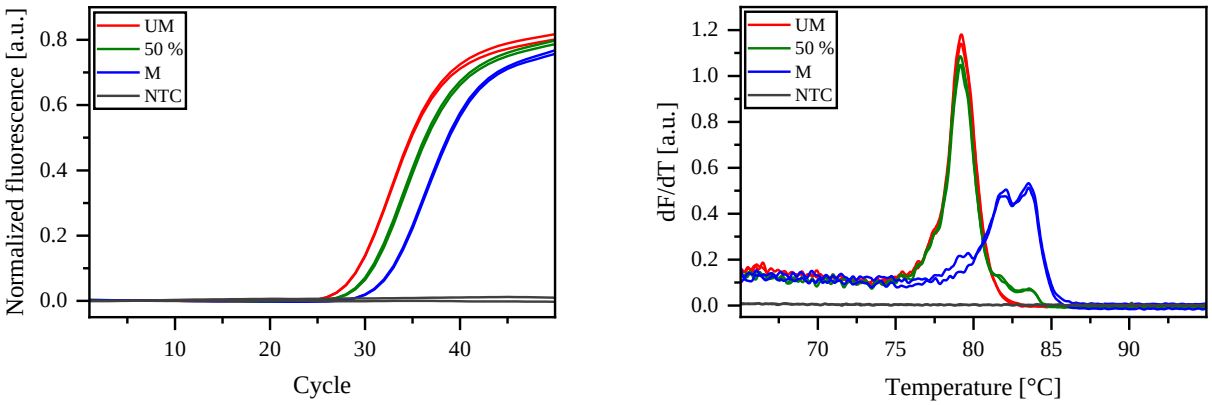

Figure 41: Amplification plot and derivative HRM plot obtained for the PSQ assay of the p16 promoter. Primer concentration = 0.4 µM, Ta = 59.5 °C, Te = 72.0 °C. UM = unmethylated standard DNA, 50% = 50% methylated standard DNA, M = methylated standard DNA, NTC = no-template control.

Unfortunately, this bias was also noticeable in the acquired PSQ data. For instance, the methylation values of the investigated CpG sites only ranged from 1.3% to 19.5% for the 0%, 25%, 50%, and 75% methylated DNA standards. **Figure 42** presents the acquired PSQ results of the 75% methylated DNA standard. Only the fully methylated DNA standard showed the expected methylation range in the seven analyzed CpGs (see **Supplementary Table 52**). This bias was not mentioned in the original literature, where the methylation values of breast cancer cell lines were investigated.[155]

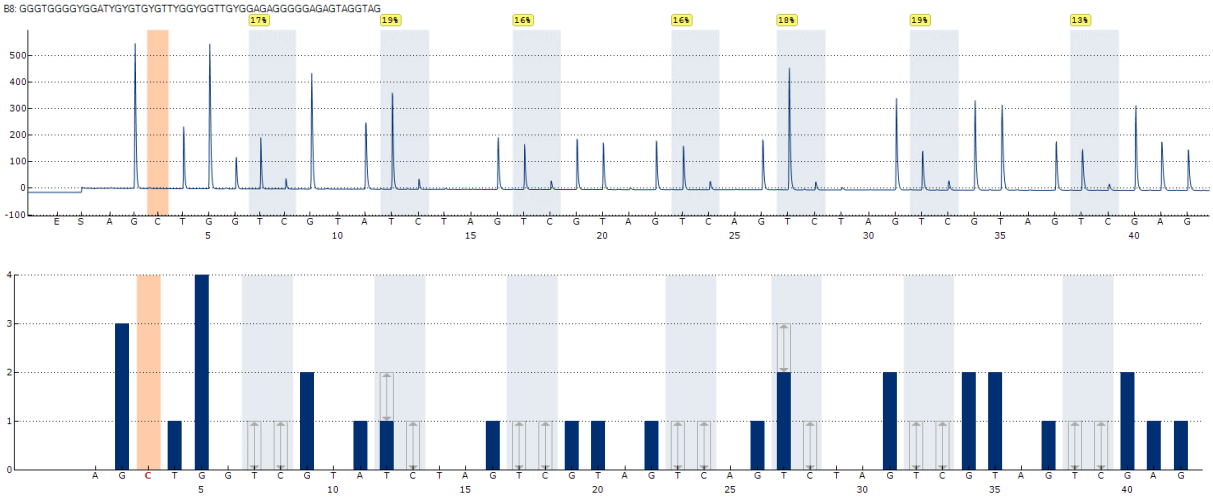

Figure 42: Representative pyrogram (top) and histogram (bottom) of seven CpGs in the p16 promoter region with 75% methylated standard DNA.

Since the employed primer set has been applied to GBM samples for the first time as part of this master's thesis, the results could not be compared to previous data. Instead, the methylation values of 16 GBM samples were determined by HRM, in order to generate useable data. Detailed information on HRM analysis and data evaluation is given in section 3.3.4. After the fluorescence signals were standardized, the calibration curve was plotted without the 100% methylated standard (see **Figure 43**).

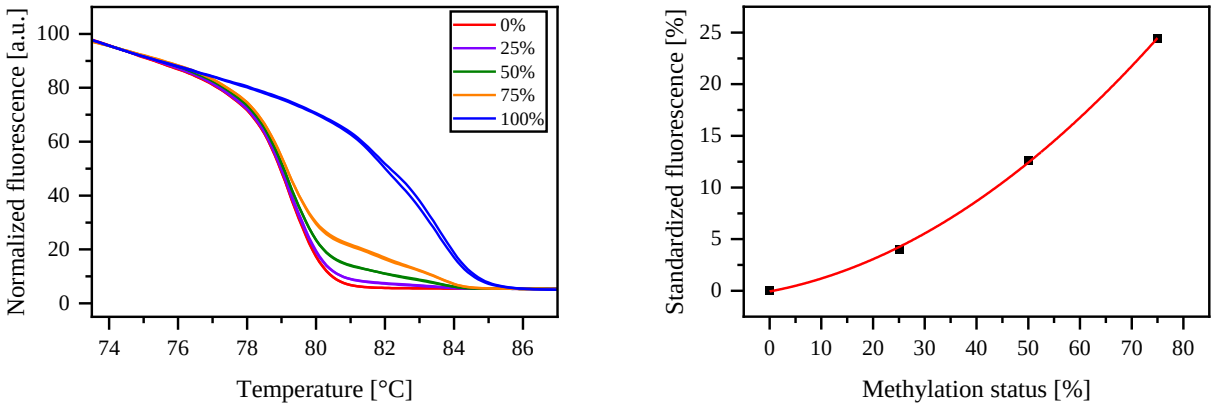

Figure 43: Normalized melt curves of the employed DNA standards (0%, 25%, 50%, 75%, and 100%) and polynomial calibration curve (0%, 25%, 50%, and 75%) for the p16 promoter region.

If possible, the 16 GBM samples were analyzed in two replicates in order to calculate the mean methylation status (see **Supplementary Table 53**). However, five of the analyzed samples displayed replicates with mean methylation values outside of the acceptable deviation range (10% threshold). Due to the PCR bias and the high deviations between replicates in some samples, a statistical analysis was not attempted. Instead, the average methylation values of the 16 GBM samples were compared with each other in a bar graph, as seen in **Figure 44**. None of the investigated DNA extracts exhibited a mean methylation status above 35%, ranging from 6.3% for sample L16 to 22.9% for sample L52 instead. The low methylation levels of the analyzed GBM samples might be explained by the observed PCR bias. All in all, the acquired data for the p16 promoter region does not seem trustworthy and should be treated as such. Ideally, a new assay should be designed for this gene region, since the available assay was not able to reliably determine the methylation status of the p16 promoter region in GBM samples.

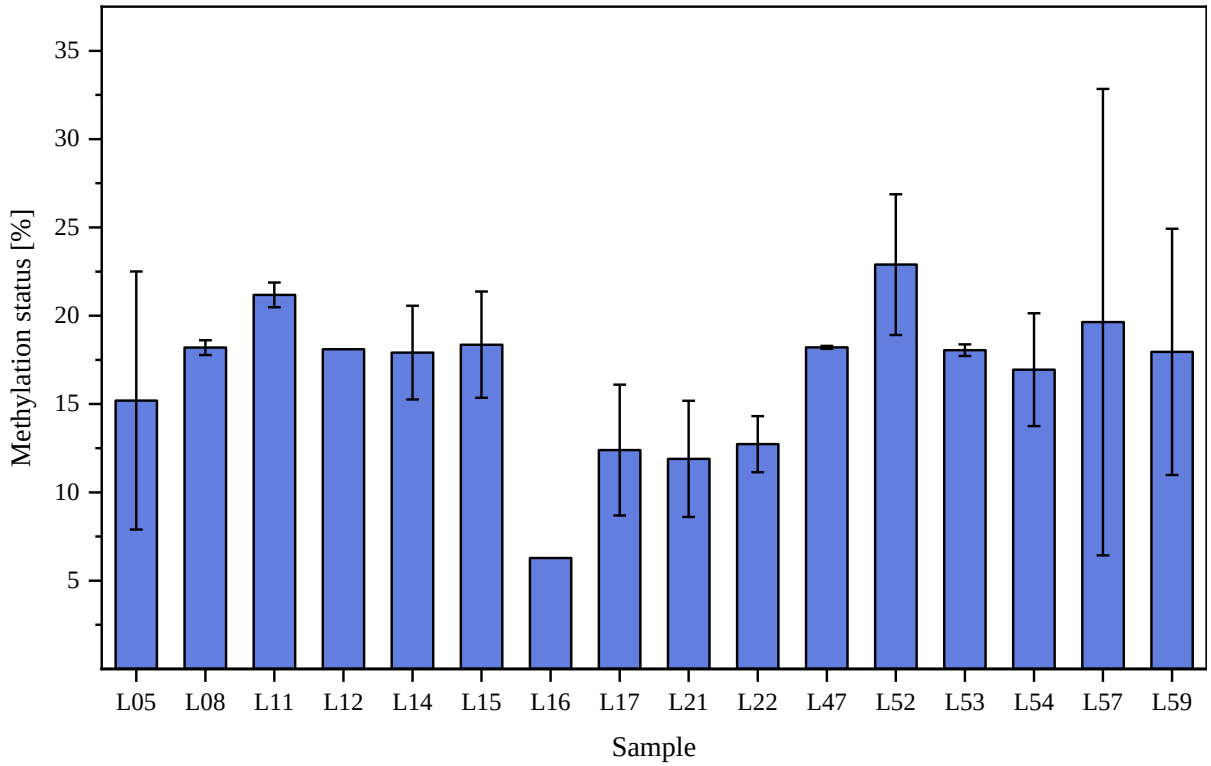

Figure 44: Average methylation status of seven CpGs in the p16 promoter region, determined by HRM. Mean values of two technical replicates (except for L12 and L16) and standard deviation.

4.2.4.2 p16 exon 2

The methylation values of 24 CpGs in the p16 exon 2 region were determined by PSQ. As part of this master's thesis, 35 DNA extracts of the GBM sample set were used and two new sequencing primers, designed by Katja Zappe, were tested. The corresponding raw data is given in section 7.3.2 (**Supplementary Table 54**).

Once again, only a small number of the applied samples exhibited acceptable Ct values and fluorescence intensity signals relative to the employed DNA standards (see **Figure 45**). As previously mentioned, the deletion of the p16 gene region has been reported as a common genetic alteration in a number of different tumor types and might be the cause for the low amplification yields. The following samples were successfully amplified in both the p16 promoter and exon 2 assay: L05, L08, L11, L12, L14, L15, L16, L17, L21, L22, L47, L52, L53, L57, and L59. Comparing the available data of the corresponding GBM patients did not bring any insight into the question why these 16 DNA samples were successfully amplified. Mutations have been associated with p16 deletion in the literature, but this was not verified as part of this master's thesis. Since deletion of the p16 gene region influences the analysis outcome, the affected GBM samples should be examined more closely in further in-house studies.

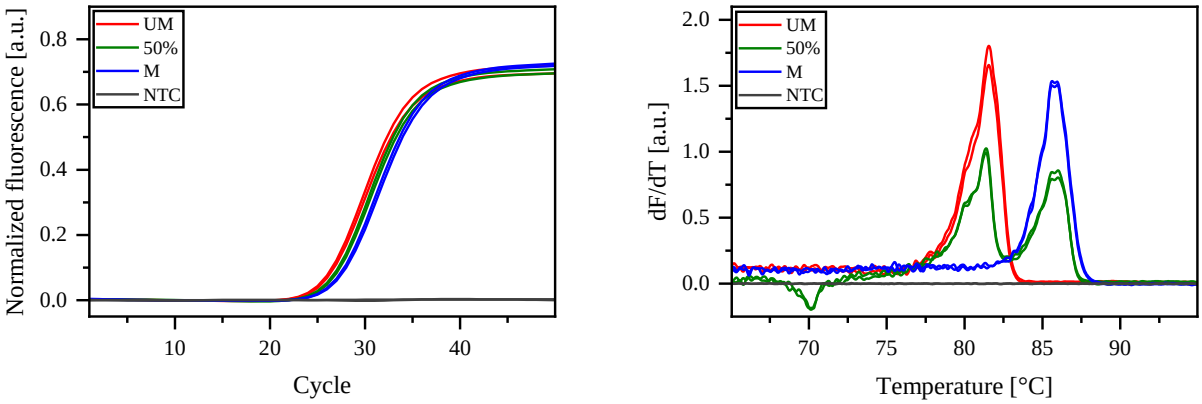

Figure 45: Amplification plot and derivative HRM plot obtained for the PSQ assay of p16 exon 2. Primer concentration = 0.4 µM, Ta = 62.1 °C, Te = 72.0 °C. NTC = no-template control, UM = unmethylated standard DNA, 50% = 50% methylated standard DNA, M = methylated standard DNA.

Moreover, thorough investigation of the employed primer set revealed that another sequence could potentially be amplified during PCR. More precisely, the *Bisearch* web server indicated the amplification of a 230 bp long stretch in the p15 gene region on chr9: 22006032-22006261 (GRCh38.p13). Further information and explanations of the p16 exon 2 PSQ assay will be found in the dissertation of Katja Zappe, which is in progress as of writing this master's thesis. Following PCR, a PSQ analysis was attempted for the 26 somewhat adequately amplified GBM samples. Using two sequencing primers for the same amplified region, 24 CpGs could be analyzed. The first 14 CpGs were targeted by the first sequencing primer and the last ten CpGs by the second sequencing primer.

Unfortunately, the mean methylation values of the replicates were outside the acceptable range (10% threshold) for ten samples. Moreover, ten out of the 16 DNA extracts with similar replicates displayed mean methylation differences within 5-10%. Due to the uncertainty of the acquired results, a statistical analysis was omitted in this study. Alternatively, the distribution of methylation levels of the 24 determined CpG sites and of the 16 successfully analyzed GBM samples were investigated. Mean methylation values ranged from 10.4% for sample L02 to 90.2% for sample L05, as seen in **Figure 46**. 12 out of the 16 examined samples showed a mean methylation status above 50%. Comparing the distribution of methylation levels of all 24 analyzed CpGs revealed a high homogeneity, with a few notable exceptions (see **Figure 47**). CpG No. 3 showed methylation values of 2.5% (< LLOQ) for all GBM samples, except for sample L12 (94.0%). Samples L12 (18.3%) and L47 (66.3%) did not exhibit a mean methylation status above 80% for CpG No. 13, like the rest of the samples.

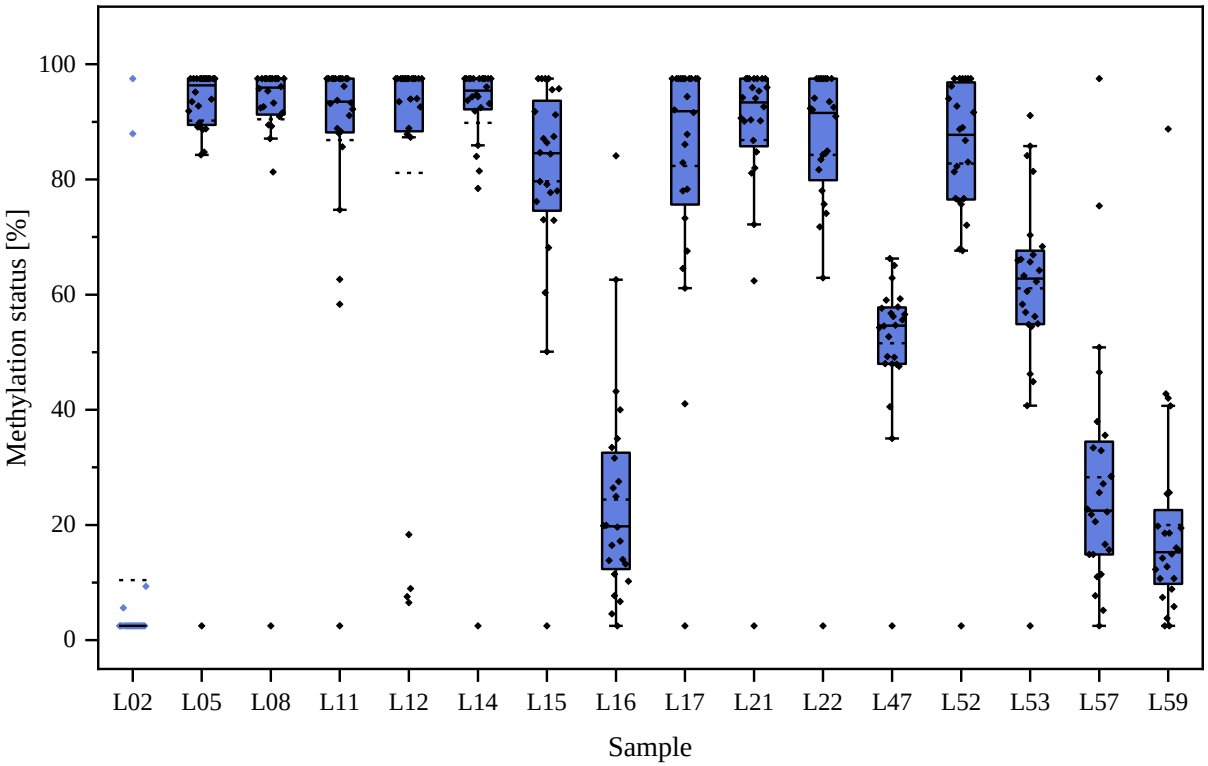

Figure 46: Methylation status of 24 CpGs in p16 exon 2 of 16 samples, ordered by sample. Continuous lines: median, dashed lines: mean.

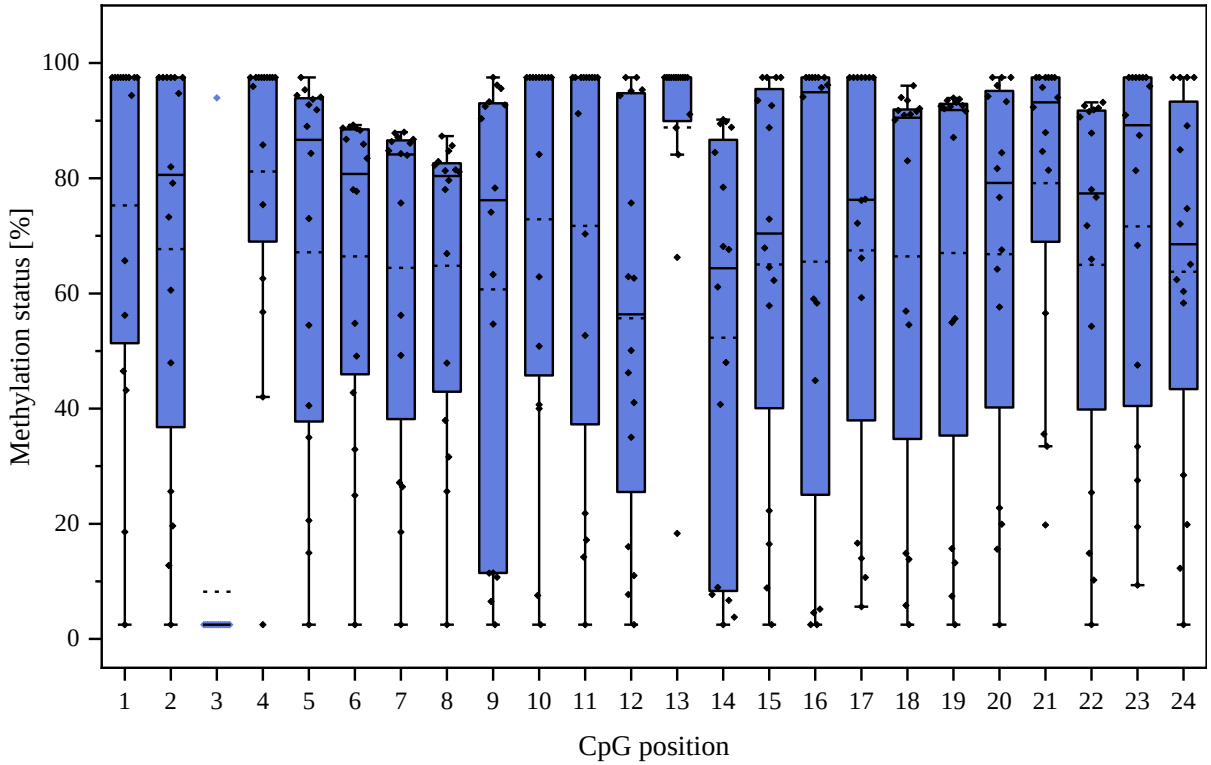

Figure 47: Methylation status of 24 CpGs in p16 exon 2 of 16 samples, ordered by CpG. Continuous lines: median, dashed lines: mean.

Investigating the methylation status of the GBM samples for the p16 gene region proved to be difficult. First, a number of samples could not be sufficiently amplified during PCR, which could be explained by the deletion of the region of interest in various tumor types. Furthermore, for both assays the replicates displayed high variations between each other, making the calculation of the average methylation status and a statistical analysis difficult. Since these occurrences were only observed for GBM samples, the underlying reasons should be discovered before continuing to use these assays for the rest of the GBM sample set. Additionally, new primer sets could be designed for the p16 gene region to further investigate these issues.

5 Conclusion

In this project, the methylation values of individual CpGs were determined for MGMT, ABCB1, ABCG2, ABCA7, and p16. For these regions, PSQ assays have already been developed in-house. They were applied to a set of samples from primary cell lines, which were isolated from GBM tumor tissue by our cooperation partner Sabine Spiegl-Kreinecker and coworkers. The PSQ assays for ABCB1, ABCG2, ABCA7, and p16 were employed for the first time to GBM samples as part of this master's thesis.

The CpG sites of two separate MGMT enhancers, namely enhancer E and K-M, were analyzed in this study. The goal was to elucidate any correlation between the methylation status of the enhancers and expression of MGMT. There have been reported cases where the tumors of patients express MGMT despite having a hypermethylated promoter or *vice versa*. A possible explanation could be that a MGMT enhancer overrules this effect. For the analyzed CpGs, a statistically significant correlation between these events could be found for MGMT enhancer E, but not for enhancer K-M ($r_S = 0.696$, $p < 0.001$ and $r_S = 0.006$, $p = 0.972$, respectively). The methylation status of the MGMT promoter had the main impact on MGMT expression. However, MGMT expression of one (L01) out of the 40 GBM samples was not correctly predicted by promoter methylation. Unfortunately, both enhancers were not able to explain this behavior and would have led to the same error as a prediction based on promoter methylation. All in all, MGMT enhancer E seems to be a better predictor for MGMT expression than enhancer K-M. Still, only 19 out of the 46 CpGs located on the K-M enhancer were analyzed as part of this study. Analyzing the remaining ones might lead to better predictions of MGMT expression.

The methylation status of four gene regions encoding for the ABC-transporters, namely ABCB1, ABCG2, ABCA7 exon 5 / intron 5, and ABCA7 exon 6 / intron 6, was determined. The average methylation values for ABCB1 (45.8%) and ABCG2 (43.5%) were quite similar, whereas 72.6% was found for the ABCA7 exon 6 / intron 6 region. No statistically significant correlations were discovered between the investigated ABC-transporters, which is in contrast to previous in-house studies. The methylation status of the analyzed CpG sites was not associated with any of the clinical data, including OS time and age at surgery. Despite previous successful applications of the PSQ assay for the ABCA7 exon 5 / intron 5 region, its application to the GBM sample set failed. A PCR-bias was discovered, displaying a preferential amplification of the unmethylated DNA standard. Moreover, the technical replicates of more

than half of the investigated samples showed a high variability of > 10%. Consequently, the respective PSQ assay needs to be improved for the GBM sample set.

Analyzing the methylation status of the p16 promoter and exon 2 proved to be difficult. The associated PSQ assays were developed in-house and successfully applied to breast cancer cell lines before the start of this master's thesis. However, the analysis of the GBM samples was not as straightforward. Firstly, a high number of the examined samples was insufficiently amplified during PCR. A probable cause could be the deletion of the p16 gene region, which leads to an accelerated cell cycle and an increased risk of a number of cancers, such as gliomas, mesotheliomas, and bladder cancer, among others. Additionally, a PCR-bias was observed for the p16 promoter, favoring the amplification of the unmethylated DNA standard. This bias was also noticeable during PSQ where the methylated standards displayed much lower methylation values than expected. Calculating the overall methylation status via HRM instead resulted in more realistic results, but a high variability between the technical replicates was observed. The observed PCR-bias was not as pronounced in p16 exon 2, however, other disruptive factors were noticed. Another sequence, namely a 230 bp long stretch in the p15 gene region, was probably amplified during PCR. These findings show that more work needs to be done in the design and optimization of PSQ assays for the p16 gene region.

Finally, the design of a novel PSQ assay for the GBX2 promoter proved to be a challenging process. The promoter region contained a high density of CpG sites and many homopolymeric stretches of A and T, making it difficult to find positioning sites for the primers. Nevertheless, two primer sets were designed as part of this master's thesis, but they did not reach our high quality standards. Optimization experiments were employed for PCR, but did not significantly improve the results. In order to successfully determine the methylation status of the GBX2 promoter, new primer sets need to be designed and optimized.

6 References

(1) Sung, H.; Ferlay, J.; Siegel, R. L.; Laversanne, M.; Soerjomataram, I.; Jemal, A. *et. al.* Global Cancer Statistics 2020: GLOBOCAN Estimates of Incidence and Mortality Worldwide for 36 Cancers in 185 Countries. *CA-Cancer J Clin* **2021**, *71* (3), 209–249. https://doi.org/10.3322/caac.21660.

(2) Mattiuzzi, C.; Lippi, G. Current Cancer Epidemiology *JEGH* **2019**, *9* (4), 217-222. https://doi.org/10.2991/jegh.k.191008.001.

(3) *What Is Cancer? - NCI*. https://www.cancer.gov/about-cancer/understanding/what-is-cancer (accessed 2022-09-16).

(4) *Understanding Cancer - NIH Curriculum Supplement Series - NCBI Bookshelf*. https://www.ncbi.nlm.nih.gov/books/NBK20362/ (accessed 2022-09-16).

(5) Bertram, J. S. The Molecular Biology of Cancer. *Mol Aspects Med* **2001**, *21* (6), 167-223. https://doi.org/10.1016/S0098-2997(00)00007-8 .

(6) Rock, K.; Mcardle, O.; Forde, P.; Dunne, M.; Fitzpatrick, D.; O'Neill, B. *et. al.* Clinical Review of Treatment Outcomes in Glioblastoma Multiforme—the Validation in a Non-Trial Population of the Results of a Randomised Phase III Clinical Trial: Has a More Radical Approach Improved Survival? *BJR* **2012**, *85* (1017), e729–e733. https://doi.org/10.1259/bjr/83796755.

(7) Oronsky, B.; Reid, T. R.; Oronsky, A.; Sandhu, N.; Knox, S. J. A Review of Newly Diagnosed Glioblastoma. *Front Oncol* **2021**, *10*, 574012. https://doi.org/10.3389/fonc.2020.574012.

(8) Alifieris, C.; Trafalis, D. T. Glioblastoma Multiforme: Pathogenesis and Treatment. *Pharmacology Ther* **2015**, *152*, 63–82. https://doi.org/10.1016/j.pharmthera.2015.05.005.

(9) Ostrom, Q. T.; Gittleman, H.; Truitt, G.; Boscia, A.; Kruchko, C.; Barnholtz-Sloan, J. S. CBTRUS Statistical Report: Primary Brain and Other Central Nervous System Tumors Diagnosed in the United States in 2011–2015. *Neuro Oncol* **2018**, *20* (suppl_4), iv1–iv86. https://doi.org/10.1093/neuonc/noy131.

(10) Shergalis, A.; Bankhead, A.; Luesakul, U.; Muangsin, N.; Neamati, N. Current Challenges and Opportunities in Treating Glioblastoma. *Pharmacol Rev* **2018**, *70* (3), 412–445. https://doi.org/10.1124/pr.117.014944.

(11) Ohgaki, H.; Kleihues, P. The Definition of Primary and Secondary Glioblastoma. *Clin Cancer Res* **2013**, *19* (4), 764–772. https://doi.org/10.1158/1078-0432.CCR-12-3002.

(12) Sarkar, C.; Sinha, S.; Sharma, M. C.; Kumar, R.; Mehta, V. S. Supratentorial Glioblastoma in Adults: Identification of Subsets and Their Clinical Correlation. *Brain Tumor Pathol* **2004**, *21* (1), 7–12. https://doi.org/10.1007/BF02482170.

(13) Wilson, T.; Karajannis, M.; Harter, D. Glioblastoma Multiforme: State of the Art and Future Therapeutics. *Surg Neurol Int* **2014**, *5* (1), 64. https://doi.org/10.4103/2152-7806.132138.

(14) Verhaak, R. G. W.; Hoadley, K. A.; Purdom, E.; Wang, V.; Qi, Y.; Wilkerson, M. D. *et. al.* Integrated Genomic Analysis Identifies Clinically Relevant Subtypes of Glioblastoma Characterized by Abnormalities in PDGFRA, IDH1, EGFR, and NF1. *Cancer Cell* **2010**, *17* (1), 98–110. https://doi.org/10.1016/j.ccr.2009.12.020.

(15) Nicolaidis, S. Biomarkers of Glioblastoma Multiforme. *Metabolism* **2015**, *64* (3), S22–S27. https://doi.org/10.1016/j.metabol.2014.10.031.

(16) Sonoda, Y.; Yokosawa, M.; Saito, R.; Kanamori, M.; Yamashita, Y.; Kumabe, T. *et. al.* O 6-Methylguanine DNA Methyltransferase Determined by Promoter Hypermethylation and Immunohistochemical Expression Is Correlated with Progression-Free Survival in Patients with Glioblastoma. *Int J Clin Oncol* **2010**, *15* (4), 352–358. https://doi.org/10.1007/s10147-010-0065-6.

(17) Etcheverry, A.; Aubry, M.; de Tayrac, M.; Vauleon, E.; Boniface, R.; Guenot, F. *et. al.* DNA Methylation in Glioblastoma: Impact on Gene Expression and Clinical Outcome. *BMC Genomics* **2010**, *11* (1), 701. https://doi.org/10.1186/1471-2164-11-701.

(18) Weller, M.; Le Rhun, E.; Preusser, M.; Tonn, J.-C.; Roth, P. How We Treat Glioblastoma. *ESMO Open* **2019**, *4*, e000520. https://doi.org/10.1136/esmoopen-2019-000520.

(19) Hegi, M. E.; Hamou, M.-F.; de Tribolet, N.; Kros, J. M.; Mariani, L.; Mirimanoff, R. O.; Stupp, R. MGMT Gene Silencing and Benefit from Temozolomide in Glioblastoma. *The N Eng J Med* **2005**, *352* (10), 997-1003. https://doi.org/10.1056/NEJMoa043331.

(20) Newlands, E.; Blackledge, G.; Slack, J.; Rustin, G.; Smith, D.; Stuart, N. *et. al.* Phase I Trial of Temozolomide (CCRG 81045: M&B 39831: NSC 362856). *Br J Cancer* **1992**, *65* (2), 287–291. https://doi.org/10.1038/bjc.1992.57.

(21) Louis, D. N.; Perry, A.; Reifenberger, G.; von Deimling, A.; Figarella-Branger, D.; Cavenee, W. K. *et. al.* The 2016 World Health Organization Classification of Tumors of the Central Nervous System: A Summary. *Acta Neuropathol* **2016**, *131* (6), 803–820. https://doi.org/10.1007/s00401-016-1545-1.

(22) Denny, B. J.; Wheelhouse, R. T.; Stevens, M. F. G.; Tsang, L. L. H.; Slack, J. A. NMR and Molecular Modeling Investigation of the Mechanism of Activation of the Antitumor Drug Temozolomide and Its Interaction with DNA. *Biochemistry* **1994**, *33* (31), 9045–9051. https://doi.org/10.1021/bi00197a003.

(23) Moody, C.; Wheelhouse, R. The Medicinal Chemistry of Imidazotetrazine Prodrugs. *Pharmaceuticals* **2014**, *7* (7), 797–838. https://doi.org/10.3390/ph7070797.

(24) Agarwala, S. S.; Kirkwood, J. M. Temozolomide, a Novel Alkylating Agent with Activity in the Central Nervous System, May Improve the Treatment of Advanced Metastatic Melanoma. *Oncologist* **2000**, *5* (2), 144–151. https://doi.org/10.1634/theoncologist.5-2-144.

(25) Newlands, E. S.; Stevens, M. F. G.; Wedge, S. R.; Wheelhouse, R. T.; Brock, C. Temozolomide: A Review of Its Discovery, Chemical Properties, Pre-Clinical Development and Clinical Trials. *Cancer Treat Rev* **1997**, *23* (1), 35–61. https://doi.org/10.1016/s0305-7372(97)90019-0.

(26) Delello Di Filippo, L.; Hofstätter Azambuja, J.; Paes Dutra, J. A.; Tavares Luiz, M.; Lobato Duarte, J.; Nicoleti, L. R. *et. al.* Improving Temozolomide Biopharmaceutical Properties in Glioblastoma Multiforme (GBM) Treatment Using GBM-Targeting Nanocarriers. *Eur J Pharm Biopharm* **2021**, *168*, 76–89. https://doi.org/10.1016/j.ejpb.2021.08.011.

(27) Mojas, N.; Lopes, M.; Jiricny, J. Mismatch Repair-Dependent Processing of Methylation Damage Gives Rise to Persistent Single-Stranded Gaps in Newly Replicated DNA. *Genes Dev* **2007**, *21* (24), 3342–3355. https://doi.org/10.1101/gad.455407.

(28) Ramirez, Y.; Weatherbee, J.; Wheelhouse, R.; Ross, A. Glioblastoma Multiforme Therapy and Mechanisms of Resistance. *Pharmaceuticals* **2013**, *6* (12), 1475–1506. https://doi.org/10.3390/ph6121475.

(29) Zhang, J.; Stevens, M. F. G.; Bradshaw, T. D. Temozolomide: Mechanisms of Action, Repair and Resistance. *Curr Mol Pharmacol* **2012**, *5* (1), 102-114. https://doi.org/10.2174/1874467211205010102.

(30) Silber, J. R.; Bobola, M. S.; Blank, A.; Chamberlain, M. C. O6-Methylguanine-DNA Methyltransferase in Glioma Therapy: Promise and Problems. *Biochim Biophys Acta* **2012**, *1826* (1), 71–82. https://doi.org/10.1016/j.bbcan.2011.12.004.

(31) Tubbs, J. L.; Pegg, A. E.; Tainer, J. A. DNA Binding, Nucleotide Flipping, and the Helix-Turn-Helix Motif in Base Repair by O6-Alkylguanine-DNA Alkyltransferase and Its Implications for Cancer Chemotherapy. *DNA Repair* **2007**, *6* (8), 1100–1115. https://doi.org/10.1016/j.dnarep.2007.03.011.

(32) Stojic, L.; Brun, R.; Jiricny, J. Mismatch Repair and DNA Damage Signalling. *DNA Repair* **2004**, *3* (8–9), 1091–1101. https://doi.org/10.1016/j.dnarep.2004.06.006.

(33) Arora, A.; Somasundaram, K. Glioblastoma vs Temozolomide: Can the Red Queen Race Be Won? *Cancer Biol Ther* **2019**, *20* (8), 1083–1090. https://doi.org/10.1080/15384047.2019.1599662.

(34) Hunter, C.; Smith, R.; Cahill, D. P.; Stephens, P.; Stevens, C.; Teague, J. *et. al.* A Hypermutation Phenotype and Somatic *MSH6* Mutations in Recurrent Human Malignant Gliomas after Alkylator Chemotherapy. *Cancer Res* **2006**, *66* (8), 3987–3991. https://doi.org/10.1158/0008-5472.CAN-06-0127.

(35) Ronen, A.; Glickman, B. W. Human DNA Repair Genes. *Environ Mol Mutagen* **2001**, *37* (3), 241–283. https://doi.org/10.1002/em.1033.

(36) Krokan, H. E.; Bjoras, M. Base Excision Repair. *Cold Spring Harb Perspect Biol* **2013**, *5* (4), a012583–a012583. https://doi.org/10.1101/cshperspect.a012583.

(37) Binabaj, M. M.; Bahrami, A.; ShahidSales, S.; Joodi, M.; Joudi Mashhad, M.; Hassanian, S. M. *et. al.* The Prognostic Value of MGMT Promoter Methylation in Glioblastoma: A Meta-analysis of Clinical Trials. *J Cell Physiol* **2018**, *233* (1), 378–386. https://doi.org/10.1002/jcp.25896.

(38) Kaina, B.; Christmann, M.; Naumann, S.; Roos, W. P. MGMT: Key Node in the Battle against Genotoxicity, Carcinogenicity and Apoptosis Induced by Alkylating Agents. *DNA Repair* **2007**, *6* (8), 1079–1099. https://doi.org/10.1016/j.dnarep.2007.03.008.

(39) Watts, G. S.; Pieper, R. O.; Costello, J. F.; Peng, Y. M.; Dalton, W. S.; Futscher, B. W. Methylation of Discrete Regions of the O6-Methylguanine DNA Methyltransferase (MGMT) CpG Island Is Associated with Heterochromatinization of the MGMT Transcription Start Site and Silencing of the Gene. *Mol Cell Biol* **1997**, *17* (9), 5612–5619. https://doi.org/10.1128/MCB.17.9.5612.

(40) Komine, C.; Watanabe, T.; Katayama, Y.; Yoshino, A.; Yokoyama, T.; Fukushima, T. Promoter Hypermethylation of the DNA Repair Gene O6-Methylguanine-DNA Methyltransferase Is an Independent Predictor of Shortened Progression Free Survival in Patients with Low-Grade Diffuse Astrocytomas. *Brain Pathol* **2006**, *13* (2), 176–184. https://doi.org/10.1111/j.1750-3639.2003.tb00017.x.

(41) Jacinto, F. V.; Esteller, M. MGMT Hypermethylation: A Prognostic Foe, a Predictive Friend. *DNA Repair* **2007**, *6* (8), 1155–1160. https://doi.org/10.1016/j.dnarep.2007.03.013.

(42) Nagarajan, R. P.; Costello, J. F. Epigenetic Mechanisms in Glioblastoma Multiforme. *Semin Cancer Biol* **2009**, *19* (3), 188–197. https://doi.org/10.1016/j.semcancer.2009.02.005.

(43) Preusser, M.; Charles Janzer, R.; Felsberg, J.; Reifenberger, G.; Hamou, M.-F.; Diserens, A.-C. *et. al.* Anti-O6-Methylguanine-Methyltransferase (MGMT) Immunohistochemistry in Glioblastoma Multiforme: Observer Variability and Lack of Association with Patient Survival Impede Its Use as Clinical Biomarker. *Brain Pathol* **2008**, 18 (4), 520-532 https://doi.org/10.1111/j.1750-3639.2008.00153.x.

(44) Mason, S.; McDonald, K. MGMT Testing for Glioma in Clinical Laboratories: Discordance with Methylation Analyses Prevents the Implementation of Routine Immunohistochemistry. *J Cancer Res Clin Oncol* **2012**, *138* (11), 1789–1797. https://doi.org/10.1007/s00432-012-1312-1.

(45) Shah, N.; Lin, B.; Sibenaller, Z.; Ryken, T.; Lee, H.; Yoon, J.-G.; Rostad, S. *et. al.* Comprehensive Analysis of MGMT Promoter Methylation: Correlation with MGMT Expression and Clinical Response in GBM. *PLoS ONE* **2011**, *6* (1), e16146. https://doi.org/10.1371/journal.pone.0016146.

(46) Bell, E. H.; Pugh, S. L.; McElroy, J. P.; Gilbert, M. R.; Mehta, M.; Klimowicz, A. C. *et. al.* Molecular-Based Recursive Partitioning Analysis Model for Glioblastoma in the Temozolomide Era: A Correlative Analysis Based on NRG Oncology RTOG 0525. *JAMA Oncol* **2017**, *3* (6), 784-792. https://doi.org/10.1001/jamaoncol.2016.6020.

(47) Butler, M.; Pongor, L.; Su, Y.-T.; Xi, L.; Raffeld, M.; Quezado, M. *et. al.* MGMT Status as a Clinical Biomarker in Glioblastoma. *Trends Cancer* **2020**, *6* (5), 380–391. https://doi.org/10.1016/j.trecan.2020.02.010.

(48) Hegi, M. E.; Liu, L.; Herman, J. G.; Stupp, R.; Wick, W.; Weller, M. *et. al.* Correlation of O ^{6} -Methylguanine Methyltransferase (MGMT) Promoter Methylation With Clinical Outcomes in Glioblastoma and Clinical Strategies to Modulate MGMT Activity. *JCO* **2008**, *26* (25), 4189–4199. https://doi.org/10.1200/JCO.2007.11.5964.

(49) Spiegl-Kreinecker, S.; Pirker, C.; Filipits, M.; Lotsch, D.; Buchroithner, J.; Pichler, J. *et. al.* O6-Methylguanine DNA Methyltransferase Protein Expression in Tumor Cells Predicts Outcome of Temozolomide Therapy in Glioblastoma Patients. *Neuro-Oncol* **2010**, *12* (1), 28–36. https://doi.org/10.1093/neuonc/nop003.

(50) Mansouri, A.; Hachem, L. D.; Mansouri, S.; Nassiri, F.; Laperriere, N. J.; Xia, D. *et. al.* MGMT Promoter Methylation Status Testing to Guide Therapy for Glioblastoma: Refining the Approach Based on Emerging Evidence and Current Challenges. *Neuro-Oncol* **2019**, *21* (2), 167–178. https://doi.org/10.1093/neuonc/noy132.

(51) Waddington, C. H. The Epigenotype. *Int J Epidemiol* **2012**, *41* (1), 10–13. https://doi.org/10.1093/ije/dyr184.

(52) Holliday, R. Epigenetics: A Historical Overview. *Epigenetics* **2006**, *1* (2), 76–80. https://doi.org/10.4161/epi.1.2.2762.

(53) Reyngold, M.; Chan, T. A. DNA Methylation. In: *Molecular Oncology*; Gelmann, E. P., Sawyers, C. L., Rauscher, III, F. J., Eds.; Cambridge University Press, **2013**; pp 37–45. https://doi.org/10.1017/CBO9781139046947.006.

(54) Bernstein, E.; Allis, C. D. RNA Meets Chromatin. *Genes Dev* **2005**, *19* (14), 1635–1655. https://doi.org/10.1101/gad.1324305.

(55) Ng, H.-H.; Adrian, B. DNA Methylation and Chromatin Modification. *Curr Opin Genet Dev* **1999**, *9* (2), 158–163. https://doi.org/10.1016/S0959-437X(99)80024-0.

(56) Moore, L. D.; Le, T.; Fan, G. DNA Methylation and Its Basic Function. *Neuropsychopharmacol* **2013**, *38* (1), 23–38. https://doi.org/10.1038/npp.2012.112.

(57) Ehrlich, M.; Gama-Sosa, M. A.; Huang, L.-H.; Midgett, R. M.; Kuo, K. C.; McCune, R. A. *et. al.* Amount and Distribution of 5-Methylcytosine in Human DNA from Different Types of Tissues or Cells. *Nucl Acids Res* **1982**, *10* (8), 2709–2721. https://doi.org/10.1093/nar/10.8.2709.

(58) Saxonov, S.; Berg, P.; Brutlag, D. L. A Genome-Wide Analysis of CpG Dinucleotides in the Human Genome Distinguishes Two Distinct Classes of Promoters. *Proc Natl Acad Sci U.S.A.* **2006**, *103* (5), 1412–1417. https://doi.org/10.1073/pnas.0510310103.

(59) Antequera, F.; Bird, A. Number of CpG Islands and Genes in Human and Mouse. *Proc Natl Acad Sci U.S.A.* **1993**, *90* (24), 11995–11999. https://doi.org/10.1073/pnas.90.24.11995.

(60) Illingworth, R. S.; Gruenewald-Schneider, U.; Webb, S.; Kerr, A. R. W.; James, K. D.; Turner, D. J. *et. al.* Orphan CpG Islands Identify Numerous Conserved Promoters in the Mammalian Genome. *PLoS Genet* **2010**, *6* (9), e1001134. https://doi.org/10.1371/journal.pgen.1001134.

(61) Mohn, F.; Weber, M.; Rebhan, M.; Roloff, T. C.; Richter, J.; Stadler, M. B. *et. al.* Lineage-Specific Polycomb Targets and De Novo DNA Methylation Define Restriction and Potential of Neuronal Progenitors. *Mol Cell* **2008**, *30* (6), 755–766. https://doi.org/10.1016/j.molcel.2008.05.007.

(62) Straussman, R.; Nejman, D.; Roberts, D.; Steinfeld, I.; Blum, B.; Benvenisty, N. *et. al.* Developmental Programming of CpG Island Methylation Profiles in the Human Genome. *Nat Struct Mol Biol* **2009**, *16* (5), 564–571. https://doi.org/10.1038/nsmb.1594.

(63) Esteller, M. DNA Methylation Patterns in Hereditary Human Cancers Mimic Sporadic Tumorigenesis. *Hum Mol Genet* **2001**, *10* (26), 3001–3007. https://doi.org/10.1093/hmg/10.26.3001.

(64) Esteller, M.; Goodman, S. N.; Herman, J. G. Inactivation of the DNA-Repair Gene MGMT and the Clinical Response of Gliomas to Alkylating Agents. *N Engl J Med* **2000**, *343* (19), 1350-1354. https://doi.org/10.1056/NEJM200011093431901.

(65) Esteller, M. Promoter Hypermethylation and BRCA1 Inactivation in Sporadic Breast and Ovarian Tumors. *J Natl Cancer Inst* **2000**, *92* (7), 564–569. https://doi.org/10.1093/jnci/92.7.564.

(66) Gu, M.; Kim, D. S.; Bae, Y. K.; Choi, J. H.; Kim, S. W.; Song, S. K. Analysis of Microsatellite Instability, Protein Expression and Methylation Status of HMLH1 and HMSH2 Genes in Gastric Carcinomas. *Hepatogastroenterology* **2009**, *56* (91–92), 899–904. PMID: 19621725.

(67) Merlo, A.; Herman, J. G.; Mao, L.; Lee, D. J.; Gabrielson, E.; Burger, P. C. *et. al.* 5' CpG Island Methylation Is Associated with Transcriptional Silencing of the Tumour Suppressor P16/CDKN2/MTS1 in Human Cancers. *Nat Med* **1995**, *1* (7), 686–692. https://doi.org/10.1038/nm0795-686.

(68) Sakai, T.; Toguchida, J.; Ohtani, N.; Yandell, D. W.; Rapaport, J. M.; Dryja, T. P. Allele-Specific Hypermethylation of the Retinoblastoma Tumor-Suppressor Gene. *Am J Hum Genet* **1991**, *48* (5), 880-888. PMID: 1673287; PMCID: PMC1683063.

(69) Herman, J. G.; Latif, F.; Weng, Y.; Lerman, M. I.; Zbar, B.; Liu, S. *et. al.* Silencing of the VHL Tumor-Suppressor Gene by DNA Methylation in Renal Carcinoma. *Proc Natl Acad Sci U.S.A.* **1994**, *91* (21), 9700–9704. https://doi.org/10.1073/pnas.91.21.9700.

(70) Toyota, M.; Ahuja, N.; Ohe-Toyota, M.; Herman, J. G.; Baylin, S. B.; Issa, J.-P. J. CpG Island Methylator Phenotype in Colorectal Cancer. *Proc Natl Acad Sci USA* **1999**, *96* (15), 8681-8686. https://doi.org/10.1073/pnas.96.15.8681.

(71) Wilson, A. S.; Power, B. E.; Molloy, P. L. DNA Hypomethylation and Human Diseases. *Biochim Biophys Acta* **2007**, *1775* (1), 138–162. https://doi.org/10.1016/j.bbcan.2006.08.007.

(72) Frigola, J.; Solé, X.; Paz, M. F.; Moreno, V.; Esteller, M.; Capellà, G. *et. al.* Differential DNA Hypermethylation and Hypomethylation Signatures in Colorectal Cancer. *Hum Mol Genet* **2005**, *14* (2), 319–326. https://doi.org/10.1093/hmg/ddi028.

(73) Sato, N.; Maitra, A.; Fukushima, N.; van Heek, N. T.; Matsubayashi, H.; Iacobuzio-Donahue, C. A. *et. al.* Frequent Hypomethylation of Multiple Genes Overexpressed in Pancreatic Ductal Adenocarcinoma. *Cancer Res* **2003**, *63* (14), 4158-4166. PMID: 12874021.

(74) Sasmita, A. O.; Wong, Y. P.; Ling, A. P. K. Biomarkers and Therapeutic Advances in Glioblastoma Multiforme. *Asia-Pac J Clin Oncol* **2018**, *14* (1), 40–51. https://doi.org/10.1111/ajco.12756.

(75) Szopa, W.; Burley, T. A.; Kramer-Marek, G.; Kaspera, W. Diagnostic and Therapeutic Biomarkers in Glioblastoma: Current Status and Future Perspectives. *Biomed Res Int* **2017**, *2017*, 1–13. https://doi.org/10.1155/2017/8013575.

(76) Lalezari, S.; Chou, A. P.; Tran, A.; Solis, O. E.; Khanlou, N.; Chen, W. *et. al.* Combined Analysis of O6-Methylguanine-DNA Methyltransferase Protein Expression and Promoter Methylation Provides Optimized Prognostication of Glioblastoma Outcome. *Neuro Oncol* **2013**, *15* (3), 370–381. https://doi.org/10.1093/neuonc/nos308.

(77) Sangar, V.; Funk, C. C.; Kusebauch, U.; Campbell, D. S.; Moritz, R. L.; Price, N. D. Quantitative Proteomic Analysis Reveals Effects of Epidermal Growth Factor Receptor (EGFR) on Invasion-Promoting Proteins Secreted by Glioblastoma Cells. *Mol Cell Proteomics* **2014**, *13* (10), 2618-2631. https://doi.org/10.1074/mcp.M114.040428.

(78) Wang, Y.; Li, S.; Zhang, Z.; Chen, X.; You, G.; Yang, P. *et. al.* Surgical Extent Impacts the Value of the Established Prognosticators in Glioblastoma Patients: A Prospective Translational Study in Asia. *Head Neck Oncol* **2012**, *4* (4), 80. PMID: 23250152.

(79) Park, C.-K.; Kim, J. E.; Kim, J. Y.; Song, S. W.; Kim, J. W.; Choi, S. H. *et. al.* The Changes in MGMT Promoter Methylation Status in Initial and Recurrent Glioblastomas. *Transl Oncol* **2012**, *5* (5), 393-397. https://doi.org/10.1593/tlo.12253.

(80) Kitange, G. J.; Mladek, A. C.; Carlson, B. L.; Schroeder, M. A.; Pokorny, J. L.; Cen, L. *et. al.* Inhibition of Histone Deacetylation Potentiates the Evolution of Acquired Temozolomide Resistance Linked to MGMT Upregulation in Glioblastoma Xenografts. *Clin Cancer Res* **2012**, *18* (15), 4070–4079. https://doi.org/10.1158/1078-0432.CCR-12-0560.

(81) Kreth, S.; Thon, N.; Eigenbrod, S.; Lutz, J.; Ledderose, C.; Egensperger, R. *et. al.* O6-Methylguanine-DNA Methyltransferase (MGMT) MRNA Expression Predicts Outcome in

Malignant Glioma Independent of MGMT Promoter Methylation. *PLoS ONE* **2011**, *6* (2), e17156. https://doi.org/10.1371/journal.pone.0017156.

(82) Karlow, J. A.; Miao, B.; Xing, X.; Wang, T.; Zhang, B. Common DNA Methylation Dynamics in Endometriod Adenocarcinoma and Glioblastoma Suggest Universal Epigenomic Alterations in Tumorigenesis. *Commun Biol* **2021**, *4* (1), 607. https://doi.org/10.1038/s42003-021-02094-1.

(83) Chong, A.; Teo, J. X.; Ban, K. H. K. Distinct Epigenetic Signatures Elucidate Enhancer-Gene Relationships That Delineate CIMP and Non-CIMP Colorectal Cancers. *Oncotarget* **2016**, *7* (19), 28027–28039. https://doi.org/10.18632/oncotarget.8473.

(84) Kurdistani, S. K. Enhancer Dysfunction: How the Main Regulators of Gene Expression Contribute to Cancer. *Genome Biol* **2012**, *13* (5), 156. https://doi.org/10.1186/gb-2012-13-5-156.

(85) Wickström, M.; Dyberg, C.; Milosevic, J.; Einvik, C.; Calero, R.; Sveinbjörnsson, B. *et. al.* Wnt/β-Catenin Pathway Regulates MGMT Gene Expression in Cancer and Inhibition of Wnt Signalling Prevents Chemoresistance. *Nat Commun* **2015**, *6* (1), 8904. https://doi.org/10.1038/ncomms9904.

(86) Bulger, M.; Groudine, M. Enhancers: The Abundance and Function of Regulatory Sequences beyond Promoters. *Dev Biol* **2010**, *339* (2), 250–257. https://doi.org/10.1016/j.ydbio.2009.11.035.

(87) He, A.; Chen, B.; Bi, J.; Wang, W.; Chen, J.; Qian, Y. *et. al.* Long-Range Gene Regulation Network of the MGMT Enhancer in Modulating Glioma Cell Sensitivity to Temozolomide. *J Genet Genomics* **2020**, *48* (10), 946-949. https://doi.org/10.1101/2020.11.03.367268.

(88) Rees, D. C.; Johnson, E.; Lewinson, O. ABC Transporters: The Power to Change. *Nat Rev Mol Cell Biol* **2009**, *10* (3), 218–227. https://doi.org/10.1038/nrm2646.

(89) Linton, K. J. Structure and Function of ABC Transporters. *Physiology* **2007**, *22* (2), 122–130. https://doi.org/10.1152/physiol.00046.2006.

(90) Dean, M.; Rzhetsky, A.; Allikmets, R. The Human ATP-Binding Cassette (ABC) Transporter Superfamily. *Genome Res* **2001**, *11* (7), 1156-1166. https://doi.org/10.1101/gr.184901.

(91) Li, W.; Zhang, H.; Assaraf, Y. G.; Zhao, K.; Xu, X.; Xie, J. *et. al.* Overcoming ABC Transporter-Mediated Multidrug Resistance: Molecular Mechanisms and Novel Therapeutic Drug Strategies. *Drug Resist Updat* **2016**, *27*, 14–29. https://doi.org/10.1016/j.drup.2016.05.001.

(92) Kaminski, W. E.; Orsó, E.; Diederich, W.; Klucken, J.; Drobnik, W.; Schmitz, G. Identification of a Novel Human Sterol-Sensitive ATP-Binding Cassette Transporter (ABCA7). *Biochem Biophys Res Commun* **2000**, *273* (2), 532–538. https://doi.org/10.1006/bbrc.2000.2954.

(93) Domenichini, A.; Adamska, A.; Falasca, M. ABC Transporters as Cancer Drivers: Potential Functions in Cancer Development. *Biochim Biophys Acta* **2019**, *1863* (1), 52–60. https://doi.org/10.1016/j.bbagen.2018.09.019.

(94) Adamska, A.; Falasca, M. ATP-Binding Cassette Transporters in Progression and Clinical Outcome of Pancreatic Cancer: What Is the Way Forward? *WJG* **2018**, *24* (29), 3222–3238. https://doi.org/10.3748/wjg.v24.i29.3222.

(95) Elsnerova, K.; Mohelnikova-Duchonova, B.; Cerovska, E.; Ehrlichova, M.; Gut, I.; Rob, L. *et. al.* Gene Expression of Membrane Transporters: Importance for Prognosis and Progression of Ovarian Carcinoma. *Oncol Rep* **2016**, *35* (4), 2159–2170. https://doi.org/10.3892/or.2016.4599.

(96) Liu, X.; Li, Q.; Zhou, J.; Zhang, S. ATP-binding Cassette Transporter A7 Accelerates Epithelial-to-mesenchymal Transition in Ovarian Cancer Cells by Upregulating the Transforming Growth Factor-β Signaling Pathway. *Oncol Lett* **2018**, *16* (5), 5868-5874. https://doi.org/10.3892/ol.2018.9366.

(97) De Roeck, A.; Van Broeckhoven, C.; Sleegers, K. The Role of ABCA7 in Alzheimer's Disease: Evidence from Genomics, Transcriptomics and Methylomics. *Acta Neuropathol* **2019**, *138* (2), 201–220. https://doi.org/10.1007/s00401-019-01994-1.

(98) Bodor, M.; Kelley, E. J.; Ho, R. J. Characterization of the Human MDR1 Gene. *AAPS J* **2005**, *7* (1), E1–E5. https://doi.org/10.1208/aapsj070101.

(99) Chen, C. J.; Clark, D.; Ueda, K.; Pastan, I.; Gottesman, M. M.; Roninson, I. B. Genomic Organization of the Human Multidrug Resistance (MDR1) Gene and Origin of P-Glycoproteins. *J Biol Chem* **1990**, *265* (1), 506–514. https://doi.org/10.1016/S0021-9258(19)40260-3.

(100) Zappe, K.; Cichna-Markl, M. Aberrant DNA Methylation of ABC Transporters in Cancer. *Cells* **2020**, *9* (10), 2281. https://doi.org/10.3390/cells9102281.

(101) Pan, S.-T.; Li, Z.-L.; He, Z.-X.; Qiu, J.-X.; Zhou, S.-F. Molecular Mechanisms for Tumour Resistance to Chemotherapy. *Clin Exp Pharmacol Physiol* **2016**, *43* (8), 723–737. https://doi.org/10.1111/1440-1681.12581.

(102) Bhatia, A.; Schäfer, H.-J.; Hrycyna, C. A. Oligomerization of the Human ABC Transporter ABCG2: Evaluation of the Native Protein and Chimeric Dimers. *Biochemistry* **2005**, *44* (32), 10893–10904. https://doi.org/10.1021/bi0503807.

(103) Bailey-Dell, K. J.; Hassel, B.; Doyle, L. A.; Ross, D. D. Promoter Characterization and Genomic Organization of the Human Breast Cancer Resistance Protein (ATP-Binding Cassette Transporter G2) Gene. *Biochim Biophys Acta* **2001**, *1520* (3), 234–241. https://doi.org/10.1016/S0167-4781(01)00270-6.

(104) Nakanishi, T.; Ross, D. D. Breast Cancer Resistance Protein (BCRP/ABCG2): Its Role in Multidrug Resistance and Regulation of its Gene Expression. *Chin J Cancer* **2012**, *31* (2), 73-99. https://doi.org/10.5732/cjc.011.10320

(105) Yang, W.-J.; Song, M.-J.; Park, E. Y.; Lee, J.-J.; Park, J.-H.; Park, K. *et. al.* Transcription Factors Sp1 and Sp3 Regulate Expression of Human ABCG2 Gene and Chemoresistance Phenotype. *Mol Cells* **2013**, *36* (4), 368–375. https://doi.org/10.1007/s10059-013-0191-x.

(106) Mo, W.; Zhang, J.-T. Human ABCG2: Structure, Function, and Its Role in Multidrug Resistance. *Int J Biochem Mol Biol* **2012**, *3* (1), 1-27. PMID: 22509477; PMCID: PMC3325772.

(107) Robinson, A. N.; Tebase, B. G.; Francone, S. C.; Huff, L. M.; Kozlowski, H.; Cossari, D. *et. al.* Coexpression of ABCB1 and ABCG2 in a Cell Line Model Reveals Both Independent and Additive Transporter Function. *Drug Metab Dispos* **2019**, *47* (7), 715–723. https://doi.org/10.1124/dmd.118.086181.

(108) Sherr, C. J.; Weber, J. D. The ARF/P53 Pathway. *Curr Opin Genet Dev* **2000**, *10* (1), 94–99. https://doi.org/10.1016/S0959-437X(99)00038-6.

(109) Diehl, J. A.; Zindy, F.; Sherr, C. J. Inhibition of Cyclin D1 Phosphorylation on Threonine-286 Prevents Its Rapid Degradation via the Ubiquitin-Proteasome Pathway. *Genes Dev* **1997**, *11* (8), 957–972. https://doi.org/10.1101/gad.11.8.957.

(110) Zhang, H. S.; Postigo, A. A.; Dean, D. C. Active Transcriptional Repression by the Rb–E2F Complex Mediates G1 Arrest Triggered by P16INK4a, TGFbeta, and Contact Inhibition. *Cell* **1999**, *97* (1), 53-61. https://doi.org/10.1016/s0092-8674(00)80714-x.

(111) Agarwal, P.; Lutful Kabir, F. M.; DeInnocentes, P.; Curtis, R. Tumor Suppressor Gene P16/INK4A/CDKN2A and Its Role in Cell Cycle Exit, Differentiation, and Determination of Cell Fate. *Tumor Suppressor Genes* **2012**. https://doi.org/10.5772/27882.

(112) Rocco, J. W.; Sidransky, D. P16(MTS-1/CDKN2/INK4a) in Cancer Progression. *Exp Cell Res* **2001**, *264* (1), 42–55. https://doi.org/10.1006/excr.2000.5149.

(113) Ladanyi, M. Implications of P16/CDKN2A Deletion in Pleural Mesotheliomas. *Lung Cancer* **2005**, *49*, S95–S98. https://doi.org/10.1016/j.lungcan.2005.03.017.

(114) Brandau, S.; Böhle, A. Bladder Cancer. *Eur Urol* **2001**, *39*, 491–497. https://doi.org/10.1159/000052494.

(115) Izumoto, S.; Arita, N.; Ohnishi, T.; Hiraga, S.; Taki, T.; Hayakawa, T. Homozygous Deletions of p161NK4/MTS1 and p151NK4B/MTS2 genes in Glioma Cells and Primary Glioma Tissues. *Cancer Lett* **1995**, *97* (2), 241-247. https://doi.org/10.1016/0304-3835(95)03981-2.

(116) Xu, X.; Gammon, M. D.; Zhang, Y.; Cho, Y. H.; Wetmur, J. G.; Bradshaw, P. T. *et. al.* Gene Promoter Methylation Is Associated with Increased Mortality among Women with Breast Cancer. *Breast Cancer Res Treat* **2010**, *121* (3), 685–692. https://doi.org/10.1007/s10549-009-0628-2.

(117) Asokan, G. S. Promoter Hypermethylation Profile of Tumour Suppressor Genes in Oral Leukoplakia and Oral Squamous Cell Carcinoma. *J Clin Diagn Res* **2014**, *8* (10), ZC09-12. https://doi.org/10.7860/JCDR/2014/9251.4949.

(118) Kim, J. C.; Choi, J. S.; Roh, S. A.; Cho, D. H.; Kim, T. W.; Kim, Y. S. Promoter Methylation of Specific Genes Is Associated with the Phenotype and Progression of Colorectal Adenocarcinomas. *Ann Surg Oncol* **2010**, *17* (7), 1767–1776. https://doi.org/10.1245/s10434-009-0901-y.

(119) Kempster, S.; Phillips, W. A.; Baindur-Hudson, S.; Thomas, R. J. S.; Dow, C.; Rockman, S. P. Methylation of Exon 2 of P16 Is Associated with Late Stage Oesophageal Cancer. *Cancer Letters* **2000**, *150* (1), 57–62. https://doi.org/10.1016/S0304-3835(99)00372-9.

(120) Spitzwieser, M.; Entfellner, E.; Werner, B.; Pulverer, W.; Pfeiler, G.; Hacker, S.; Cichna-Markl, M. Hypermethylation of CDKN2A Exon 2 in Tumor, Tumor-Adjacent and Tumor-Distant Tissues from Breast Cancer Patients. *BMC Cancer* **2017**, *17* (1), 260. https://doi.org/10.1186/s12885-017-3244-2.

(121) Ye, X.; Mo, M.; Xu, S.; Yang, Q.; Wu, M.; Zhang, J. *et. al.* The Hypermethylation of P16 Gene Exon 1 and Exon 2: Potential Biomarkers for Colorectal Cancer and Are Associated with Cancer Pathological Staging. *BMC Cancer* **2018**, *18* (1), 1023. https://doi.org/10.1186/s12885-018-4921-5.

(122) Hrycaj, S. M.; Wellik, D. M. Hox Genes and Evolution. *F1000Res* **2016**, *5*, 859. https://doi.org/10.12688/f1000research.7663.1.

(123) Wang, Z.; Nakayama, Y.; Tsuda, S.; Yamasu, K. The Role of Gastrulation Brain Homeobox 2 (Gbx2) in the Development of the Ventral Telencephalon in Zebrafish Embryos. *Differentiation* **2018**, *99*, 28–40. https://doi.org/10.1016/j.diff.2017.12.005.

(124) Thomson A. W.; Lotze M. T. The Cytokine Handbook. *Academic Press* **2003**, *4*.

(125) Gao, A. C.; Lou, W.; Isaacs, J. T. Enhanced GBX2 Expression Stimulates Growth of Human Prostate Cancer Cells via Transcriptional Up-Regulation of the Interleukin 6 Gene. *Clin Cancer Res* **2000**, *6* (2), 493-497. PMID: 10690529.

(126) Xiong, Y.; Song, X.; Kudusi; Zu, X.; Chen, M.; He, W.; Qi, L. Oncogenic GBX2 Promotes the Malignant Behaviors of Bladder Cancer Cells by Binding to the ITGA5 Promoter and Activating Its Transcription. *Funct Integr Genomics* **2022**, *22* (5), 937-950. https://doi.org/10.1007/s10142-022-00870-8.

(127) Wang, Y.; Hui, J.; Li, R.; Fu, Q.; Yang, P.; Xiao, Y.; Hui, J. GBX2, as a Tumor Promoter in Lung Adenocarcinoma, Enhances Cells Viability, Invasion and Migration by Regulating the AKT/ERK Signaling Pathway. *J Gene Med* **2020**, *22* (2). https://doi.org/10.1002/jgm.3147.

(128) Jeyapala, R.; Savio, A. J.; Olkhov-Mitsel, E.; Kamdar, S.; Zhao, F.; Cuizon, C. *et. al.* GBX2 Methylation Is a Novel Prognostic Biomarker and Improves Prediction of Biochemical Recurrence Among Patients with Prostate Cancer Negative for Intraductal Carcinoma and Cribriform Architecture. *Eur Urol Oncol* **2019**, *2* (3), 231–238. https://doi.org/10.1016/j.euo.2018.08.003.

(129) Demokan, S.; Chuang, A. Y.; Pattani, K. M.; Sidransky, D.; Koch, W.; Califano, J. A. Validation of Nucleolar Protein 4 as a Novel Methylated Tumor Suppressor Gene in Head and Neck Cancer. *Oncol Rep* **2014**, *31* (2), 1014–1020. https://doi.org/10.3892/or.2013.2927.

(130) Yu, K.-D.; Zhu, R.; Zhan, M.; Rodriguez, A. A.; Yang, W.; Wong, S. *et. al.* Identification of Prognosis-Relevant Subgroups in Patients with Chemoresistant Triple-Negative Breast Cancer. *Clin Cancer Res* **2013**, *19* (10), 2723–2733. https://doi.org/10.1158/1078-0432.CCR-12-2986.

(131) Tolkach, Y.; Merseburger, A.; Herrmann, T.; Kuczyk, M.; Serth, J.; Imkamp, F. Signatures of Adverse Pathological Features, Androgen Insensitivity and Metastatic Potential in Prostate Cancer. *Anticancer Res* **2015**, *35* (10), 5443-5451. PMID: 26408707.

(132) Frommer, M.; McDonald, L. E.; Millar, D. S.; Collis, C. M.; Watt, F.; Grigg, G. W. *et. al.* A Genomic Sequencing Protocol That Yields a Positive Display of 5-Methylcytosine Residues in Individual DNA Strands. *Proc Natl Acad Sci U.S.A.* **1992**, *89* (5), 1827–1831. https://doi.org/10.1073/pnas.89.5.1827.

(133) Susan, J. Ci.; Harrison, J.; Paul, C. L.; Frommer, M. High Sensitivity Mapping of Methylated Cytosines. *Nucl Acids Res* **1994**, *22* (15), 2990–2997. https://doi.org/10.1093/nar/22.15.2990.

(134) Mullis, K. B. The Polymerase Chain Reaction. *Angew Chem In Ed Engl* **1994**, *33*, 1209-1213. https:// doi.org/10.1002/anie.199412091

(135) Garibyan, L.; Avashia, N. Polymerase Chain Reaction. *J Invest Dermatol* **2013**, *133* (3), 1–4. https://doi.org/10.1038/jid.2013.1.

(136) Sambrook, J.; Russell, D. W. The Basic Polymerase Chain Reaction. *Cold Spring Harb Protoc* **2006**, *2006* (1), pdb.prot3824. https://doi.org/10.1101/pdb.prot3824.

(137) *File:Polymerase chain reaction.svg - Wikimedia Commons*. https://commons.wikimedia.org/wiki/File:Polymerase_chain_reaction.svg?_ga=2.17319225.1085727701.1666165195-1019821847.1666165195 (accessed 2022-10-19).

(138) Wittwer, C. T.; Herrmann, M. G.; Moss, A. A.; Rasmussen, R. P. Continuous Fluorescence Monitoring of Rapid Cycle DNA Amplification. *BioTechniques 30th Anniversary GEM* **2013**, *54* (6), 314-320. https://doi.org/10.2144/000114043.

(139) Erali, M.; Wittwer, C. T. High Resolution Melting Analysis for Gene Scanning. *Methods* **2010**, *50* (4), 250–261. https://doi.org/10.1016/j.ymeth.2010.01.013.

(140) Ronaghi, M.; Uhlén, M.; Nyrén, P. A Sequencing Method Based on Real-Time Pyrophosphate. *Science* **1998**, *281* (5375), 363–365. https://doi.org/10.1126/science.281.5375.363.

(141) Ahmadian, A.; Ehn, M.; Hober, S. Pyrosequencing: History, Biochemistry and Future. *Clin Chim Acta* **2006**, *363* (1–2), 83–94. https://doi.org/10.1016/j.cccn.2005.04.038.

(142) Harrington, C. T.; Lin, E. I.; Olson, M. T.; Eshleman, J. R. Fundamentals of Pyrosequencing. *Arch Pathol Lab Med* **2013**, *137* (9), 1296–1303. https://doi.org/10.5858/arpa.2012-0463-RA.

(143) van der Torre, M. H.; Novak-Frazer, L.; Rautemaa-Richardson, R. Detecting Azole-Antifungal Resistance in Aspergillus Fumigatus by Pyrosequencing. *JoF* **2020**, *6* (1), 12. https://doi.org/10.3390/jof6010012.

(144) Mikeska, T.; Felsberg, J.; Hewitt, C. A.; Dobrovic, A. Analysing DNA Methylation Using Bisulphite Pyrosequencing. *Methods Mol Biol* **2011**, *791*, 33-53. https://doi.org/10.1007/978-1-61779-316-5_4.

(145) Delaney, C.; Garg, S. K.; Yung, R. Analysis of DNA Methylation by Pyrosequencing. *Methods Mol Biol* **2015**, *1343*, 249-264. https://doi.org/10.1007/978-1-4939-2963-4_19.

(146) McPherson, M. J.; Moller, S. G. PCR: Second Edition. Taylor & Francis, London, **2006**.

(147) EpiTect® HRM™ PCR Handbook; Qiagen, **2009**.

(148) PyroMark® Q24 User Manual; Qiagen, **2016**.

(149) Pühringer, K. DNA Methylation Analysis of MGMT Enhancers in Glioblastoma. Master's Thesis, University of Vienna, Vienna, **2022**.

(150) Pflug, S. The Methylation Status of a Novel MGMT Enhancer as Marker for MGMT Expression. Master's Thesis, University of Vienna, Vienna, **2022**.

(151) Chen, X.; Zhang, M.; Gan, H.; Wang, H.; Lee, J.-H.; Fang, D. *et. al.* A Novel Enhancer Regulates MGMT Expression and Promotes Temozolomide Resistance in Glioblastoma. *Nat Commun* **2018**, *9* (1), 2949. https://doi.org/10.1038/s41467-018-05373-4.

(152) Spitzwieser, M. Development and Application of Analytical Methods for the Determination of the DNA Methylation Status in Biopsy Samples and Cultured Cells. Doctoral thesis, University of Vienna, Vienna, **2016**.

(153) Scheichel, A. Search for a DNA Methylation Based Biomarker for Early Diagnosis of Late-Onset Alzheimer's Disease. Diploma thesis, University of Vienna, Vienna, **2016**.

(154) Schier, A.-K. DNA Methylation Analysis of ABCA7 in Cancer Cell Lines. Master's thesis, University of Vienna, Vienna, **2021**.

(155) Jenik, A. Entwicklung von Pyrosequenziermethoden zur Untersuchung des Methylierungsstatus des Promotors und des zweiten Exons von p16. Diploma thesis, University of Vienna, Vienna, **2021**.

(156) Switzeny, O. J.; Christmann, M.; Renovanz, M.; Giese, A.; Sommer, C.; Kaina, B. MGMT Promoter Methylation Determined by HRM in Comparison to MSP and Pyrosequencing for Predicting High-Grade Glioma Response. *Clin Epigenet* **2016**, *8* (1), 49. https://doi.org/10.1186/s13148-016-0204-7.

(157) Spitzwieser, M.; Pirker, C.; Koblmüller, B.; Pfeiler, G.; Hacker, S.; Berger, W.; Heffeter, P.; Cichna-Markl, M. Promoter Methylation Patterns of *ABCB1*, *ABCC1* and *ABCG2* in Human Cancer Cell Lines, Multidrug-Resistant Cell Models and Tumor, Tumor-Adjacent and Tumor-Distant Tissues from Breast Cancer Patients. *Oncotarget* **2016**, *7* (45), 73347–73369. https://doi.org/10.18632/oncotarget.12332.

(158) Warnecke, P. M.; Stirzaker, C.; Melki, J. R.; Millar, D. S.; Paul, C. L.; Clark, S. J. Detection and Measurement of PCR Bias in Quantitative Methylation Analysis of Bisulphite-Treated DNA. *Nucleic Acids Res* **1997**, *25* (21), 4422–4426. https://doi.org/10.1093/nar/25.21.4422.

(159) Moskalev, E. A.; Zavgorodnij, M. G.; Majorova, S. P.; Vorobjev, I. A.; Jandaghi, P.; Bure, I. V. *et. al.* Correction of PCR-Bias in Quantitative DNA Methylation Studies by Means of Cubic Polynomial Regression. *Nucleic Acids Res* **2011**, *39* (11), e77–e77. https://doi.org/10.1093/nar/gkr213.

7 Appendix

7.1 Abstract

Glioblastoma multiforme (GBM), the most common and aggressive primary brain tumor, makes up more than 60% of all brain tumors in adults and has a 5-year survival rate of 5%. No curative treatment options exist, and the median overall survival (OS) is less than 2 years. Promoter methylation and as a result epigenetic silencing of the O^6-methylguanine-DNA methyltransferase (MGMT) gene have been associated with an increase in OS of patients, who received the alkylating chemotherapeutic agent temozolomide (TMZ) during treatment. Consequently, promoter methylation and expression of MGMT have emerged as major biomarkers for the success of TMZ treatment. However, inconsistencies between MGMT promoter methylation status, MGMT expression, and patient outcome have been reported in the literature. Other regulatory mechanisms might influence this correlation. This thesis aimed at investigating the methylation status of several regions and regulatory elements of genes that have been associated with GBM.

Since MGMT enhancer methylation has been brought up as a possible alternative to predict MGMT expression and treatment success, two enhancer regions were investigated as part of this thesis. In order to determine the methylation status of the enhancer regions, in-house designed assays based on pyrosequencing were applied to a set of 40 DNA samples. A significant correlation between enhancer methylation status and MGMT expression was observed for one of the investigated enhancer regions. These findings suggest that MGMT enhancer methylation contributes to MGMT regulation. The methylation status of several other regions was also investigated, including of CpGs of the ABCB1 and ABCG2 promoter, the ABCA7 exon 5 / intron 5 and ABCA7 exon 6 / intron 6 regions, and of the p16 promoter and exon 2. No correlation was found between the methylation status of these regions and MGMT expression.

7.2 Zusammenfassung

Glioblastoma multiforme (GBM) ist der häufigste und aggressivste primäre Tumor des Gehirns, der mehr als 60% aller Gehirntumore bei Erwachsenen ausmacht und eine 5-Jahres-Überlebensrate von nur 5% aufweist. Eine endgültige Heilung kann derzeit nicht erreicht werden und die mittlere Überlebenszeit liegt bei weniger als 2 Jahren. Die Promotor-Methylierung und die daraus folgende Stilllegung des O^6-Methylguanin-DNA-Methyltransferase (MGMT) Gens wurden mit einer höheren mittleren Überlebenszeit von PatientInnen, die mit dem alkylierenden Chemotherapeutikum Temozolomid (TMZ) behandelt wurden, in Verbindung gebracht. Folglich werden die Promotor-Methylierung und die Expression von MGMT als Biomarker für den Erfolg der Behandlung mit TMZ eingesetzt. In der Literatur wurde jedoch bereits über Unstimmigkeiten zwischen der MGMT-Promotor-Methylierung, der Expression und dem Ansprechen von GBM-PatientInnen auf TMZ berichtet. Andere Regulationsmechanismen könnten diese Korrelation beeinflussen. Ziel dieser Arbeit war es, den Methylierungsgrad mehrerer Regionen und regulatorischer Elemente von Genen zu untersuchen, die mit GBM in Verbindung gebracht wurden.

Da in der Literatur die MGMT-Enhancer-Methylierung als mögliche Alternative zur Vorhersage der Expression und des Behandlungserfolges genannt wurde, wurden zwei MGMT-Enhancer Regionen im Rahmen dieser Arbeit untersucht. Dafür wurden intern entwickelte, auf Pyrosequenzierung basierende Assays auf ein GBM-Set von 40 DNA-Proben angewendet. Für eine der untersuchten Enhancer-Regionen korrelierten die MGMT-Enhancer-Methylierungswerte signifikant mit der MGMT-Expression. Die Ergebnisse legen nahe, dass der Methylierungsstatus der CpGs des in dieser Arbeit untersuchten MGMT-Enhancers zur MGMT-Regulierung beiträgt. Der Methylierungsstatus mehrerer anderer Regionen wurde ebenfalls in dieser Arbeit untersucht, darunter von CpGs der Promotoren von ABC1 und ABCG2, der ABCA7 Exon 5 / Intron 5 Region, der ABCA7 Exon 6 / Intron 6 Region, des p16-Promotors und des p16 Exons 2. Für diese Regionen wurde keine Korrelation des Methylierungsgrades der untersuchten CpGs mit der MGMT-Expression gefunden.

7.3 Supplementary information

7.3.1 Overview of methods

Supplementary Table 1: Characteristics of primer set 1D for the MGMT enhancer E.

MGMT Enh E (primer set 1D)	Sequence (5‘→3‘)	Amplicon length [bp]	No. of CpGs analyzed	Reference
Fw	[btn]-GGAATGTGTTATTTAATTGGTATGT			
Rev	CAAATCCCACAACAAATCCTTAT	204	3	[149]
Seq	TCAAAAAAAAAAAATCACC			

Supplementary Table 2: Characteristics of primer set 3C for the MGMT enhancer E.

MGMT Enh E (primer set 3C)	Sequence (5‘→3‘)	Amplicon length [bp]	No. of CpGs analyzed	Reference
Fw	GAGGTTTGATATAAGTAATGATGG			
Rev	[btn]-CCTCCTAATCCCACAATACAA	128	2	[149]
Seq	TAAGTAATGATGGTATG			

Supplementary Table 3: Characteristics of primer set 4F for the MGMT enhancer E.

MGMT Enh E (primer set 4F)	Sequence (5‘→3‘)	Amplicon length [bp]	No. of CpGs analyzed	Reference
Fw	AGGTTTGATATAAGTAATGATGGTAT			
Rev-G	[btn]-CGTATTCTCTCCCACTTCAATA	257	5	[149]
Rev-A	[btn]-CATATTCTCTCCCACTTCAATA			
Seq	GTATTGTGGGATTAGGA			

Supplementary Table 4: Characteristics of primer set 5E for the MGMT enhancer E.

MGMT Enh E (primer set 5E)	Sequence (5‘→3‘)	Amplicon length [bp]	No. of CpGs analyzed	Reference
Fw	[btn]-GTGTATTGAAGTGGGAGAGAATA			
Rev	CAATAACAATTTTACAAACACAAATAACTT	241	9	[149]
Seq	ATAACTTTTCATTCA			

Supplementary Table 5: PCR reaction setup for primer set 1D, 3C, 4F, and 5E for the MGMT enhancer E. The primer concentration was 0.2 µM for 1D, 3C, and 4F, and 0.4 µM for 5E. Two reverse primers were used in the 4F assay, and the volume of the RNase-free water adjusted accordingly.

	Final primer concentration	
	0.2 µM	**0.4 µM**
Component	**Volume per reaction [µL]**	
2x HRM PCR Master Mix	10.0	10.0
RNase-free water	7.2	6.4
Fw primer [10 µM]	0.4	0.8
Rev primer [10 µM]	0.4	0.8
Volume [µL]	18	18
DNA [2.5 ng/µL]	2	2
Total volume [µL]	20	20

Supplementary Table 6: PCR conditions for primer set 1D, 3C, 4F, and 5E for the MGMT enhancer E. Annealing temperature was 53.6 °C for 1D, 56.5 °C for 3C, 54.4 °C for 4F, and 54.2 °C for 5E. Elongation temperature was set at 68 °C for 3C and 4F, and 72 °C for 1D and 5E.

	Step	**Time**	**Temperature**
	Activation	5 min	95 °C
50x	Denaturation	10 sec	94 °C
	Annealing	20 sec	variable
	Elongation	20 sec	variable
	Final elongation	10 min	variable
	Denaturation	1 min	95 °C
	Hybridization	1 min	40 °C
	HRM	-	65-95 °C

Supplementary Table 7: Characteristics of primer set 1 for the MGMT enhancer K-M.

MGMT Enh K-M (primer set 1)	Sequence (5‘→3‘)	Amplicon length [bp]	No. of CpGs analyzed	Reference
Fw	AGTTAGGAAATTAGAAATGGAATGTTT			
Rev	[btn]-CAAATCACACTCTAAATTCCCAATT	255	4	[150]
Seq	TGGTATTAGAGGTTA			

Supplementary Table 8: Characteristics of primer set 2 for the MGMT enhancer K-M.

MGMT Enh K-M (primer set 2)	Sequence (5‘→3‘)	Amplicon length [bp]	No. of CpGs analyzed	Reference
Fw	[btn]-TTAAATAAGTGGTTTAGGTAGAGG			
Rev	TACTAAACATTCCATTTCTAATTTCC	137	8	[150]
Seq	CCATTTCTAATTTCCTAACTC			

Supplementary Table 9: Characteristics of primer set 3 for the MGMT enhancer K-M.

MGMT Enh K-M (primer set 3)	Sequence (5‘→3‘)	Amplicon length [bp]	No. of CpGs analyzed	Reference
Fw	GTTGTAGGGTATATGAGTTTAGAT			
Rev	[btn]-TTCATAACTCAAATTAACACACACT	271	4	[150]
Seq	TTTTGTGTTGAATGG			

Supplementary Table 10: Characteristics of primer set 4 for the MGMT enhancer K-M.

MGMT Enh K-M (primer set 4)	Sequence (5‘→3‘)	Amplicon length [bp]	No. of CpGs analyzed	Reference
Fw	GAGGTTATTTGGAAAGTTGAGAT			
Rev	[btn]-CTAATAATCCAAACCCTCTATTC	286	3	[150]
Seq	TTTAGTGTTATGGGAG			

Supplementary Table 11: PCR reaction setup for primer set 1-4 for the MGMT enhancer K-M. The primer concentration was 0.4 µM, the concentration of each dNTP 0.2 mM, the HotStarTaq concentration 2.5 U/µL, and the DNA amount 5 ng/reaction.

Component	Volume per reaction [µL]
RNase-free water	12.5
10x QIAGEN PCR buffer	2.0
20x EvaGreen dye	1.0
dNTP mix (10 mM of each)	0.4
Fw primer [10 µM]	0.8
Rev primer [10 µM]	0.8
HotStarTaq 5 U/µL	0.5
Volume [µL]	18
DNA [2.5 ng/µL]	2
Total volume [µL]	20

Supplementary Table 12: PCR conditions for primer set 1-4 for the MGMT enhancer K-M. Annealing temperature was set at 58 °C, except for primer set 1, for which T_a was set at 59 °C instead.

	Step	Time	Temperature
	Activation	5 min	95 °C
50x	Denaturation	10 sec	94 °C
50x	Annealing	20 sec	variable
50x	Elongation	20 sec	68 °C
	Final elongation	10 min	68 °C
	Denaturation	1 min	95 °C
	Hybridization	1 min	40 °C
	HRM	-	65-95 °C

Supplementary Table 13: Characteristics of the employed primer set for the MGMT promoter.

MGMT promoter	Sequence (5‘→3‘)	Amplicon length [bp]	No. of CpGs analyzed	Reference
Fw	GGATATGTTGGGATAGTT			
Rev	[btn]-CCCAAACACTCACCAAAT	98	12	[156]
Seq	GGATATGTTGGGATAGTT			

Supplementary Table 14: Characteristics of the employed primer set for the ABCB1 promoter region.

ABCB1 promoter	Sequence (5‘→3‘)	Amplicon length [bp]	No. of CpGs analyzed	Reference
Fw	GTTGGAGGTGAGATTAATTTT			
Rev	[btn]-AAACCCCCAACTCTACCT	162	7	[152]
Seq	GAGAGTAGTAAAGGGA			

Supplementary Table 15: PCR reaction setup for the employed primer set for the ABCB1 promoter region. The primer concentration was 0.2 µM.

Component	Volume per reaction [µL]
2x PyroMark PCR Master Mix	10.0
RNase-free water	4.2
10x CoralLoad PCR buffer	2.0
20x EvaGreen dye	1.0
Fw primer [10 µM]	0.4
Rev primer [10 µM]	0.4
Volume [µL]	18
DNA [2.5 ng/µL]	2
Total volume [µL]	20

Supplementary Table 16: PCR conditions for the employed primer set for the ABCB1 promoter region.

	Step	Time	Temperature
	Activation	15 min	95 °C
50x	Denaturation	30 sec	94 °C
50x	Annealing	30 sec	58.3 °C
50x	Elongation	30 sec	72 °C
	Final elongation	10 min	72 °C
	Denaturation	1 min	95 °C
	Hybridization	1 min	40 °C
	HRM	-	65-95 °C

Supplementary Table 17: Characteristics of the employed primer set for the ABCG2 promoter region.

ABCG2 promoter	Sequence (5‘→3‘)	Amplicon length [bp]	No. of CpGs analyzed	Reference
Fw	GTTTGATTTAGTTGGGTTTGG			
Rev	[btn]-AACCACCCATTTAACTTACTCT	122	8	[152]
Seq	ATTTAGTTGGGTTTGGT			

Supplementary Table 18: PCR reaction setup for the employed primer set for the ABCG2 promoter region. The primer concentration was 0.4 µM.

Component	Volume per reaction [µL]
2x PyroMark PCR Master Mix	10.0
RNase-free water	3.4
10x CoralLoad PCR buffer	2.0
20x EvaGreen dye	1.0
Fw primer [10 µM]	0.8
Rev primer [10 µM]	0.8
Volume [µL]	18
DNA [2.5 ng/µL]	2
Total volume [µL]	20

Supplementary Table 19: PCR conditions for the employed primer set for the ABCG2 promoter region.

	Step	Time	Temperature
	Activation	15 min	95 °C
50x	Denaturation	30 sec	94 °C
50x	Annealing	30 sec	54.8 °C
50x	Elongation	30 sec	72 °C
	Final elongation	10 min	72 °C
	Denaturation	1 min	95 °C
	Hybridization	1 min	40 °C
	HRM	-	65-95 °C

Supplementary Table 20: Characteristics of the employed primer set for the ABCA7 exon 5 / intron 5 boundary region.

ABCA7 ex 5 / in 5	Sequence (5‘→3‘)	Amplicon length [bp]	No. of CpGs analyzed	Reference
Fw	TTGGTTGGTTTAGGGAAGTTG			
Rev	[btn]-CCCACCCTATACCCATTTC	131	7	[153]
Seq	GGTTTAGGGAAGTTGAT			

Supplementary Table 21: PCR reaction setup for the employed primer set for the ABCA7 exon 5 / intron 5 boundary region. The primer concentration was 0.2 µM.

Component	Volume per reaction [µL]
2x PyroMark PCR Master Mix	10.0
RNase-free water	4.2
10x CoralLoad PCR buffer	2.0
20x EvaGreen dye	1.0
Fw primer [10 µM]	0.4
Rev primer [10 µM]	0.4
Volume [µL]	18
DNA [2.5 ng/µL]	2
Total volume [µL]	20

Supplementary Table 22: PCR conditions for the employed primer set for the ABCA7 exon 5 / intron 5 boundary region.

	Step	Time	Temperature
	Activation	15 min	95 °C
50x	Denaturation	30 sec	94 °C
50x	Annealing	30 sec	58.3 °C
50x	Elongation	30 sec	72 °C
	Final elongation	10 min	72 °C
	Denaturation	1 min	95 °C
	Hybridization	1 min	40 °C
	HRM	-	65-95 °C

Supplementary Table 23: Characteristics of the employed primer set for the ABCA7 exon 6 / intron 6 boundary region.

ABCA7 ex 6 / in 6	Sequence (5‘→3‘)	Amplicon length [bp]	No. of CpGs analyzed	Reference
Fw	TTAATTAAGTAGTTTTTATTGGAATTAT			
Rev	[btn]-AAAACATCCCCAATACAATATC	130	9	[154]
Seq	TTTATTGGAATTATTTATGT			

Supplementary Table 24: PCR reaction setup for the employed primer set for the ABCA7 exon 6 / intron 6 boundary region. The primer concentration was 0.4 µM.

Component	Volume per reaction [µL]
2x PyroMark PCR Master Mix	10.0
RNase-free water	3.0
10x CoralLoad PCR buffer	2.0
20x EvaGreen dye	1.0
$MgCl_2$ [25 mM]	0.4
Fw primer [10 µM]	0.8
Rev primer [10 µM]	0.8
Volume [µL]	18
DNA [2.5 ng/µL]	2
Total volume [µL]	20

Supplementary Table 25: PCR conditions for the employed primer set for the ABCA7 exon 6 / intron 6 boundary region.

	Step	Time	Temperature
	Activation	15 min	95 °C
50x	Denaturation	30 sec	94 °C
50x	Annealing	30 sec	51 °C
50x	Elongation	30 sec	72 °C
	Final elongation	10 min	72 °C
	Denaturation	1 min	95 °C
	Hybridization	1 min	40 °C
	HRM	-	65-95 °C

Supplementary Table 26: Characteristics of the employed primer set for the p16 promoter region.

p16 promotor	Sequence (5‘→3‘)	Amplicon length [bp]	No. of CpGs analyzed	Reference
Fw	GAGGGGTTGGTTGGTTATTAG			
Rev	[btn]-TACCTACTCTCCCCCTCTC	75	7	[155]
Seq	GGTTGGTTGGTTATTAGA			

Supplementary Table 27: PCR reaction setup for the employed primer set for the p16 promoter region. The primer concentration is 0.4 µM.

Component	Volume per reaction [µL]
2x EpiTect HRM PCR MM	10.0
RNase-free water	6.4
Fw primer [10 µM]	0.8
Rev primer [10 µM]	0.8
Volume [µL]	18
DNA [2.5 ng/µL]	2
Total volume [µL]	20

Supplementary Table 28: PCR conditions for the employed primer set for the p16 promoter region.

	Step	Time	Temperature
	Activation	5 min	95 °C
50x	Denaturation	30 sec	94 °C
50x	Annealing	30 sec	59.5 °C
50x	Elongation	30 sec	72 °C
	Final elongation	10 min	72 °C
	Denaturation	1 min	95 °C
	Hybridization	1 min	40 °C
	HRM	-	65-95 °C

Supplementary Table 29: Characteristics of the employed primer set for p16 exon 2. The first sequencing primer was designed by Andreas Jenik as part of his diploma thesis. Seq-2 and 3 were designed by Katja Zappe.

p16 exon 2	Sequence (5‘→3‘)	Amplicon length [bp]	No. of CpGs analyzed	Reference
Fw	GTTTTTTTTGGTAGGTTATGATGATGG			
Rev	[btn]-ACCCAACTCCTCAACCAAATCC			
(Seq)	(GGAGTTGTTGTTGTTTTA)	230	(21) 24	[155]
Seq-2	AGGTTATGATGATGGGTA			
Seq-3	GGGAGGGTTTTTTGGATA			

Supplementary Table 30: PCR reaction setup for the employed primer set for p16 exon 2.

Component	Volume per reaction [µL]
2x PyroMark PCR Master Mix	10.0
RNase-free water	3.4
10x CoralLoad PCR buffer	2.0
20x EvaGreen dye	1.0
Fw primer [10 µM]	0.8
Rev primer [10 µM]	0.8
Volume [µL]	18
DNA [2.5 ng/µL]	2
Total volume [µL]	20

Supplementary Table 31: PCR conditions for the employed primer set for p16 exon 2.

	Step	Time	Temperature
	Activation	15 min	95 °C
50x	Denaturation	30 sec	94 °C
50x	Annealing	30 sec	62.1 °C
50x	Elongation	30 sec	72 °C
	Final elongation	10 min	72 °C
	Denaturation	1 min	95 °C
	Hybridization	1 min	40 °C
	HRM	-	65-95 °C

Supplementary Table 32: Characteristics of primer set 1 for the GBX2 promoter.

GBX2 (primer set 1)	Sequence (5‘→3‘)	Nt	GC [%]	Tm [°C]
Fw	TAGGTTGGGGATTTGGTGGT	20	50	58.4
Rev	[btn]-ACTACCCCATATTCATACCCTA	22	41	58.4
Seq	GGATTTGGTGGTGAG	15	53	46

Supplementary Table 33: PCR reaction setup for primer set 1 for the GBX2 promoter. The annealing temperature was set at 56.4 °C.

	Final primer concentration	
	0.2 µM	0.4 µM
Component	Volume per reaction [µL]	
2x EpiTect HRM PCR MM	10.0	10.0
RNase-free water	7.2	6.4
Fw primer [10 µM]	0.4	0.8
Rev primer [10 µM]	0.4	0.8
Volume [µL]	18	18
DNA [2.5 ng/µL]	2	2
Total volume [µL]	20	20

Supplementary Table 34: Characteristics for primer set 2 for the GBX2 promoter.

GBX2 (primer set 2)	Sequence (5‘→3‘)	Nt	GC [%]	Tm [°C]
Fw-C	TGTTTTGCGTTAGGTTGGAGTAGAAG	26	42	64.6
Fw-T	TGTTTTGTGTTAGGTTGGAGTAGAAG	26	38	62.9
Rev-G	[btn]-TCTACACCGACTACCCCATATTCAT	23	44	64.1
Rev-A	[btn]-TCTACACCAACTACCCCATATTCAT	23	40	62.5
Rev-C	[btn]-CTACACCCACTACCCCATATTCATA	23	44	64.1
Seq	GGATTTGGTGGTGAG	15	53	46

Supplementary Table 35: First PCR reaction setup for primer set 2 for the GBX2 promoter. The annealing temperature was set at 60.5 °C.

	MM1	MM2	MM3	MM4
	Final primer concentration			
	0.2 µM	0.2 µM	0.4 µM	0.4 µM
Component	Volume per reaction [µL]			
2x EpiTect HRM PCR MM	10.0	10.0	10.0	10.0
RNase-free water	6.4	6.8	4.8	5.6
Fw-C primer [10 µM]	0.4	0.4	0.8	0.8
Fw-T primer [10 µM]	0.4	0.4	0.8	0.8
Rev-G primer [10 µM]	0.4	0	0.8	0
Rev-A primer [10 µM]	0.4	0	0.8	0
Rev-C primer [10 µM]	0	0.4	0	0.8
Volume [µL]	18	18	18	18
DNA [2.5 ng/µL]	2	2	2	2
Total volume [µL]	20	20	20	20

Supplementary Table 36: Second PCR reaction setup for primer set 2 for the GBX2 promoter. The annealing temperature was set at 62.5 °C.

	MM1	MM2	MM3	MM4
	Final primer concentration			
	0.2 µM	0.2 µM	0.4 µM	0.4 µM
Component	Volume per reaction [µL]			
2x EpiTect HRM PCR MM	10.0	10.0	10.0	10.0
RNase-free water	6.4	6.4	4.8	4.8
Fw-C primer [10 µM]	0.4	0.4	0.8	0.8
Fw-T primer [10 µM]	0.4	0.4	0.8	0.8
Rev-G primer [10 µM]	0.4	0.4	0.8	0.8
Rev-A primer [10 µM]	0.4	0	0.8	0
Rev-C primer [10 µM]	0	0.4	0	0.8
Volume [µL]	18	18	18	18
DNA [2.5 ng/µL]	2	2	2	2
Total volume [µL]	20	20	20	20

Supplementary Table 37: Third PCR reaction setup for primer set 2 for the GBX2 promoter. The annealing temperature was set at 60.5 °C.

	MM1	MM2	MM3	MM4	MM5	MM6	MM7	MM8
Component	**Volume per reaction [µL]**							
2x EpiTect HRM PCR MM	10.0	10.0	10.0	10.0	10.0	10.0	10.0	10.0
RNase-free water	5.6	4.8	4.8	5.6	4.4	5.3	4.0	5.0
Fw-C primer [10 µM]	0.4 [0.2 µM]	0.6 [0.3 µM]	0.4 [0.2 µM]	0.4 [0.2 µM]	0.6 [0.3 µM]	0.6 [0.3 µM]	0.8 [0.4 µM]	0.8 [0.4 µM]
Fw-T primer [10 µM]	0.8 [0.4 µM]	1.0 [0.5 µM]	1.2 [0.6 µM]	1.2 [0.6 µM]	1.2 [0.6 µM]	1.2 [0.6 µM]	1.2 [0.6 µM]	1.2 [0.6 µM]
Rev-G primer [10 µM]	0.4 [0.2 µM]	0.6 [0.3 µM]	0.4 [0.2 µM]	0	0.6 [0.3 µM]	0	0.8 [0.4 µM]	0
Rev-A primer [10 µM]	0.8 [0.4 µM]	1.0 [0.5 µM]	1.2 [0.6 µM]	0	1.2 [0.6 µM]	0	1.2 [0.6 µM]	0
Rev-C primer [10 µM]	0	0	0	0.8 [0.4 µM]	0	0.9 [0.45 µM]	0	1.0 [0.5 µM]
Volume [µL]	18	18	18	18	18	18	18	18
DNA [2.5 ng/µL]	2	2	2	2	2	2	2	2
Total volume [µL]	20	20	20	20	20	20	20	20

Supplementary Table 38: PCR conditions for primer set 1 and 2 for the GBX2 promoter.

	Step	Time	Temperature
	Activation	5 min	95 °C
50x	Denaturation	10 sec	94 °C
	Annealing	20 sec	variable
	Elongation	20 sec	72 °C
	Final elongation	10 min	72 °C
	Denaturation	1 min	95 °C
	Hybridization	1 min	40 °C
	HRM	-	65-95 °C

Supplementary Table 39: MGMT promoter methylation status [%] of 12 CpGs, determined by PSQ (Data provided by Katja Zappe). All presented methylation grades are arithmetic means of two replicates. Values below 5% are marked <LLOQ and values over 95% are marked >ULOQ.

Sample	CpG 72	CpG 73	CpG 74	CpG 75	CpG 76	CpG 77	CpG 78	CpG 79	CpG 80	CpG 81	CpG 82	CpG 83
L01	<LLOQ	<LLOQ	<LLOQ	<LLOQ	<LLOQ	<LLOQ	<LLOQ	<LLOQ	<LLOQ	<LLOQ	<LLOQ	<LLOQ
L02	72.6	>ULOQ	>ULOQ	93.3	>ULOQ	>ULOQ	>ULOQ	30.9	59.0	84.9	30.7	62.4
L03	91.9	93.3	>ULOQ	93.4	91.2	87.6	66.1	41.6	85.7	86.6	94.0	71.5
L04	>ULOQ	87.6	15.8	88.4	15.8	11.8	>ULOQ	>ULOQ	85.3	84.7	>ULOQ	90.9
L05	74.9	92.8	>ULOQ	93.3	55.5	63.5	9>ULOQ	82.2	87.1	87.5	9>ULOQ	91.5
L06	<LLOQ	8.4	9.1	13.7	5.8	<LLOQ	<LLOQ	<LLOQ	26.2	13.7	7.8	13.6
L07	57.4	84.8	89.0	85.6	86.6	87.6	30.9	90.6	79.4	80.6	90.0	84.0
L08	>ULOQ	94.2	>ULOQ	93.3	80.6	90.8	77.7	>ULOQ	85.3	84.9	>ULOQ	88.0
L11	9>ULOQ	>ULOQ	>ULOQ	93.6	92.3	91.1	19.6	36.1	31.8	18.0	91.7	85.6
L12	26.6	29.9	46.9	37.9	42.0	39.3	32.1	30.2	29.0	33.8	44.7	32.2
L14	<LLOQ	<LLOQ	<LLOQ	<LLOQ	<LLOQ	<LLOQ	<LLOQ	<LLOQ	<LLOQ	<LLOQ	<LLOQ	<LLOQ
L15	<LLOQ	<LLOQ	<LLOQ	<LLOQ	<LLOQ	<LLOQ	<LLOQ	<LLOQ	<LLOQ	<LLOQ	<LLOQ	<LLOQ
L16	<LLOQ	<LLOQ	<LLOQ	<LLOQ	<LLOQ	<LLOQ	<LLOQ	<LLOQ	<LLOQ	<LLOQ	<LLOQ	<LLOQ
L17	<LLOQ	<LLOQ	<LLOQ	<LLOQ	<LLOQ	<LLOQ	<LLOQ	<LLOQ	<LLOQ	<LLOQ	<LLOQ	<LLOQ
L18	<LLOQ	<LLOQ	<LLOQ	<LLOQ	<LLOQ	<LLOQ	<LLOQ	<LLOQ	<LLOQ	<LLOQ	<LLOQ	<LLOQ
L19	<LLOQ	<LLOQ	<LLOQ	<LLOQ	<LLOQ	<LLOQ	<LLOQ	<LLOQ	<LLOQ	<LLOQ	<LLOQ	<LLOQ
L20	<LLOQ	<LLOQ	<LLOQ	<LLOQ	<LLOQ	<LLOQ	<LLOQ	<LLOQ	<LLOQ	<LLOQ	<LLOQ	<LLOQ

Sample	CpG 72	CpG 73	CpG 74	XpG 75	CpG 76	CpG 77	CpG 78	CpG 79	CpG 80	CpG 81	CpG 82	CpG 83
L39	<LLOQ	<LLOQ	<LLOQ	<LLOQ	<LLOQ	<LLOQ	<LLOQ	<LLOQ	<LLOQ	<LLOQ	<LLOQ	<LLOQ
L40	<LLOQ	<LLOQ	<LLOQ	<LLOQ	<LLOQ	<LLOQ	<LLOQ	<LLOQ	<LLOQ	<LLOQ	<LLOQ	<LLOQ
L41	<LLOQ	<LLOQ	<LLOQ	<LLOQ	<LLOQ	<LLOQ	<LLOQ	<LLOQ	<LLOQ	<LLOQ	<LLOQ	<LLOQ
L42	<LLOQ	<LLOQ	<LLOQ	<LLOQ	<LLOQ	<LLOQ	<LLOQ	<LLOQ	<LLOQ	<LLOQ	<LLOQ	<LLOQ
L43	89.3	86.8	87.2	77.7	13.5	10.6	11.0	11.7	77.3	33.7	87.6	81.2
L44	<LLOQ	<LLOQ	<LLOQ	<LLOQ	<LLOQ	<LLOQ	<LLOQ	<LLOQ	<LLOQ	<LLOQ	<LLOQ	<LLOQ
L45	28.2	52.0	>ULOQ	93.5	>ULOQ	>ULOQ	23.4	>ULOQ	85.2	87.1	>ULOQ	92.4
L46	>ULOQ	>ULOQ	>ULOQ	92.4	94.9	>ULOQ	84.3	>ULOQ	86.4	87.2	>ULOQ	89.9
L47	>ULOQ	92.9	>ULOQ	91.5	86.1	28.7	89.4	92.3	86.1	86.4	90.2	88.4
L48	65.5	>ULOQ	>ULOQ	93.4	>ULOQ	>ULOQ	23.4	>ULOQ	85.4	37.2	>ULOQ	90.1
L49	<LLOQ	6.4	7.6	9.0	15.8	22.3	5.7	44.2	41.2	38.7	44.8	42.2
L50	10.7	12.5	31.9	59.7	58.3	68.8	12.4	84.5	75.7	46.1	72.0	75.8
L51	<LLOQ	<LLOQ	10.3	8.3	10.5	81.9	<LLOQ	30.4	13.5	10.2	11.7	9.9
L52	8.6	12.5	9.0	8.4	<LLOQ	<LLOQ	<LLOQ	13.6	12.7	79.9	83.8	88.3
L53	<LLOQ	<LLOQ	<LLOQ	<LLOQ	<LLOQ	<LLOQ	<LLOQ	<LLOQ	<LLOQ	<LLOQ	<LLOQ	<LLOQ
L54	48.4	41.4	75.9	92.6	94.1	89.3	96.1	97.5	86.8	86.6	97.5	91.0
L55	97.5	93.7	95.9	92.1	45.4	92.2	17.0	97.5	83.4	83.8	69.8	89.8
L56	<LLOQ	<LLOQ	<LLOQ	<LLOQ	<LLOQ	<LLOQ	<LLOQ	<LLOQ	<LLOQ	<LLOQ	<LLOQ	<LLOQ

Sample	CpG 72	CpG 73	CpG 74	CpG 75	CpG 76	CpG 77	CpG 78	CpG 79	CpG 80	CpG 81	CpG 82	CpG 83
L57	<LLOQ	<LLOQ	<LLOQ	<LLOQ	<LLOQ	<LLOQ	<LLOQ	<LLOQ	<LLOQ	<LLOQ	<LLOQ	<LLOQ
L58	<LLOQ	<LLOQ	<LLOQ	<LLOQ	<LLOQ	<LLOQ	<LLOQ	<LLOQ	<LLOQ	<LLOQ	<LLOQ	<LLOQ
L59	<LLOQ	<LLOQ	<LLOQ	<LLOQ	<LLOQ	<LLOQ	<LLOQ	<LLOQ	<LLOQ	<LLOQ	<LLOQ	<LLOQ

Supplementary Table 40: MGMT enhancer E methylation status [%] of 3 CpGs, determined by PSQ (assay 1D). If possible, two replicates were used for calculation of arithmetic means. Values marked red not included in data evaluation. Values below 5% are marked <LLOQ and values over 95% are marked >ULOQ. n.a. = not available.

Sample	CpG 1	CpG 2	CpG 3	Sample	CpG 1	CpG 2	CpG 3	Sample	CpG 1	CpG 2	CpG 3
L01	81.60	>ULOQ	44.58		47.98	38.40	10.12	L20	59.51	15.44	33.15
	79.84	>ULOQ	47.38	L12	79.19	62.98	31.19		62.21	23.32	32.75
L02	81.19	68.26	41.42		78.98	53.15	35.26	L21	84.61	>ULOQ	>ULOQ
	82.12	69.13	41.81		75.53	55.21	35.29		87.59	>ULOQ	94.27
L03	5.47	<LLOQ	<LLOQ	L14	84.46	42.36	73.46	L22	83.16	90.50	90.12
	<LLOQ	<LLOQ	<LLOQ		84.46	43.82	67.06		83.64	91.90	93.16
L04	74.11	6.76	7.96	L15	80.30	90.84	91.41	L39	86.15	14.57	52.72
	80.63	7.96	7.66		82.95	93.46	92.29		84.34	15.46	53.67
L05	66.66	23.53	7.35	L16	67.20	55.92	57.02	L40	75.18	12.08	15.28
	65.02	27.73	11.90		63.34	51.03	56.35		77.81	11.13	13.46
L06	79.11	70.80	46.91		73.07	54.93	62.06	L41	80.21	54.02	64.37
	77.69	73.68	44.38	L17	85.30	94.86	92.22		84.18	52.94	66.56
L07	69.79	57.32	20.46		85.35	94.20	94.38	L42	85.45	92.18	93.88
	74.94	53.97	24.45	L18	82.99	80.01	81.71	L43	61.06	41.98	17.64
L08	7.37	<LLOQ	<LLOQ		86.71	81.78	81.22		63.52	44.66	13.50
	9.66	<LLOQ	<LLOQ	L19	84.11	55.34	59.58	L44	n.a.	n.a.	n.a.
L11	51.14	40.83	12.00		85.95	59.06	56.97	L45	78.07	75.80	48.37

Sample	CpG 1	CpG 2	CpG 3	Sample	CpG 1	CpG 2	CpG 3
	80.31	76.49	48.47	L54	52.76	20.27	17.27
L46	52.59	34.46	6.44		52.08	18.47	14.24
	53.67	36.83	7.10	L55	73.32	24.28	8.27
L47	26.29	12.15	<LLOQ		73.97	22.96	10.58
	32.84	12.72	<LLOQ	L56	n.a.	n.a.	n.a.
L48	79.59	9.33	10.14	L57	76.68	21.51	52.82
	81.44	9.50	13.93		78.48	19.35	58.15
L49	39.01	10.09	<LLOQ	L58	n.a.	n.a.	n.a.
	41.25	10.64	<LLOQ	L59	82.09	60.02	84.45
L50	15.24	<LLOQ	<LLOQ		81.81	59.68	85.75
	13.67	<LLOQ	<LLOQ				
L51	61.44	<LLOQ	<LLOQ				
	65.06	7.04	<LLOQ				
L52	5.71	<LLOQ	<LLOQ				
	<LLOQ	<LLOQ	<LLOQ				
L53	83.60	34.25	57.33				
	86.52	40.01	61.44				

Supplementary Table 41: MGMT enhancer E methylation status [%] of 2 CpGs, determined by PSQ (assay 3C). If possible, two replicates were used for calculation of arithmetic means. Values marked red not included in data evaluation. Values below 5% are marked <LLOQ and values over 95% are marked >ULOQ. n.a. = not available.

Sample	CpG 7	CpG 8
L02	88.30	55.99
	86.09	56.82
L04	16.78	82.22
	21.08	82.15
L07	75.35	51.35
	76.49	51.99
L08	6.72	<LLOQ
	6.97	<LLOQ
L12	61.55	49.49
	60.36	51.70
L19	58.92	49.67
	58.32	50.53
L39	64.35	38.45
	69.22	39.34
L42	>ULOQ	67.79
	>ULOQ	66.72
L43	16.87	14.23
	17.52	14.44
L44	n.a.	n.a.
L46	59.56	47.56
	59.03	48.66
L48	59.99	67.16
	59.11	64.89
L50	30.81	<LLOQ
	34.33	<LLOQ
L56	n.a.	n.a.
L57	>ULOQ	92.12
	94.32	87.10
L58	n.a.	n.a.
L59	93.92	90.35
	93.54	90.71

Supplementary Table 42: MGMT enhancer E methylation status [%] of 5 CpGs, determined by PSQ (assay 4F). If possible, two replicates were used for calculation of arithmetic means. Values marked red not included in data evaluation. Values below 5% are marked <LLOQ and values over 95% are marked >ULOQ. n.a. = not available.

Sample	CpG 9	CpG 10	CpG 11	CpG 12	CpG 13	Sample	CpG 9	CpG 10	CpG 11	CpG 12	CpG 13
L02	21.76	69.79	37.71	50.07	14.15		63.04	74.78	91.53	83.85	76.73
	20.32	70.20	37.06	58.65	18.11		55.48	79.08	89.68	81.91	81.57
L04	7.62	5.44	9.52	39.44	45.47		64.03	75.58	89.33	77.43	76.49
	5.26	<LLOQ	12.89	70.69	47.47	L43	12.03	66.23	63.28	15.35	11.56
	8.15	5.64	6.84	66.85	46.86		13.27	63.72	77.10	16.66	17.32
L07	43.13	60.38	73.45	62.48	21.86		13.02	71.28	78.88	12.68	15.22
	42.66	63.04	77.50	58.81	18.49	L44	55.16	73.57	>ULOQ	79.76	83.45
L08	<LLOQ	53.30	63.20	9.77	9.53	L46	<LLOQ	56.16	72.70	70.35	66.02
	<LLOQ	51.62	65.33	11.43	9.07		5.15	61.35	78.21	70.78	64.59
L12	46.09	72.70	91.35	80.66	79.51	L48	10.77	27.68	44.04	62.45	12.62
	43.29	72.74	91.62	81.42	74.04		10.68	32.10	48.36	59.74	13.55
L14	82.41	75.50	90.50	79.50	77.73	L50	13.13	47.49	52.29	41.66	13.49
L19	37.88	68.09	70.41	20.31	19.23		12.49	51.22	60.13	41.51	13.89
	34.01	65.07	64.26	17.57	11.51	L56	80.66	74.62	92.55	77.71	79.95
L39	51.89	69.70	73.11	38.09	20.17	L57	81.01	67.62	88.33	79.64	75.69
	54.61	71.03	69.10	35.98	21.96		83.00	73.34	92.45	80.02	76.58
L42	53.63	74.13	91.41	82.37	77.58	L58	85.32	74.76	>ULOQ	82.30	54.66

Sample	CpG 9	CpG 10	CpG 11	CpG 12	CpG 13
	84.61	75.97	94.85	84.18	83.31
	87.55	77.08	93.43	80.67	81.81
L59	85.91	73.39	90.67	77.43	77.60
	84.84	72.92	93.38	80.17	78.36

Supplementary Table 43: MGMT enhancer E methylation status [%] of 4 CpGs, determined by PSQ (assay 5E). If possible, two replicates were used for calculation of arithmetic means. Values marked red not included in data evaluation. Values below 5% are marked <LLOQ and values over 95% are marked >ULOQ. n.a. = not available.

Sample	CpG 19	CpG 20	CpG 21	CpG 22	Sample	CpG 19	CpG 20	CpG 21	CpG 22
L02	23.33	10.39	<LLOQ	8.87	L43	84.58	>ULOQ	70.94	88.15
	23.24	8.36	<LLOQ	10.02		84.50	92.79	70.26	83.74
L04	32.78	>ULOQ	92.09	75.15	L44	70.84	>ULOQ	90.53	92.79
	31.39	93.42	90.58	75.64	L46	26.65	85.85	72.27	77.53
L07	33.05	88.51	81.60	85.67		29.75	85.16	65.78	75.95
	34.47	89.48	73.93	84.53	L48	19.96	62.44	13.69	51.29
L08	50.42	64.16	43.73	81.87		20.21	64.17	16.85	52.13
	47.93	68.90	41.52	81.88	L50	61.97	79.74	56.89	73.22
L12	89.11	>ULOQ	78.90	91.88		59.87	78.55	47.82	65.57
	92.14	>ULOQ	74.97	87.45	L56	n.a.	n.a.	n.a.	n.a.
L19	30.09	87.14	46.25	84.22	L57	93.90	>ULOQ	92.40	91.78
	36.02	89.20	44.50	85.08		92.34	>ULOQ	94.13	88.55
L22	94.41	>ULOQ	83.93	89.61	L58	>ULOQ	>ULOQ	93.10	93.90
L39	30.56	78.78	45.93	86.62		94.09	>ULOQ	94.71	91.50
	30.98	78.62	44.37	87.64	L59	>ULOQ	>ULOQ	94.16	91.47
L42	93.03	>ULOQ	>ULOQ	94.85		>ULOQ	>ULOQ	92.42	92.39
	91.80	>ULOQ	93.61	91.68					

Supplementary Table 44: MGMT enhancer K-M methylation status [%] of 4 CpGs, determined by PSQ (assay 1D). If possible, two replicates were used for calculation of arithmetic means. Values marked red not included in data evaluation. Values below 5% are marked <LLOQ and values over 95% are marked >ULOQ. n.a. = not available.

Sample	CpG 5	CpG 6	CpG 7	CpG 8	Sample	CpG 5	CpG 6	CpG 7	CpG 8
L02	74.33	80.06	89.10	78.96	L22	36.03	32.95	54.58	46.46
	68.60	79.83	89.00	82.09	L39	73.12	27.82	79.60	73.59
L04	81.28	85.86	92.30	86.42		72.16	34.07	83.41	82.06
	78.26	76.07	82.83	82.83	L42	72.88	68.06	79.84	72.86
	79.46	82.74	91.11	84.39		72.54	66.84	81.45	71.13
L07	17.54	15.16	71.29	59.57	L43	77.37	70.79	86.07	78.25
	27.52	19.97	67.94	65.09		76.63	66.36	85.05	84.60
	17.54	16.00	69.62	57.56	L44	40.25	32.20	70.74	34.34
L08	17.96	13.39	32.29	29.56	L46	79.39	77.93	88.21	81.90
	19.66	10.08	30.79	35.82		75.63	72.67	84.24	80.86
L12	40.02	45.21	70.52	63.45	L48	56.69	69.94	82.05	80.73
	48.62	36.94	75.66	62.02		68.46	73.18	85.13	76.28
L15	62.50	64.41	82.53	70.93		57.30	69.93	79.38	81.22
L18	62.43	59.11	64.19	46.01	L50	19.81	8.75	30.03	46.74
L19	60.61	29.49	53.18	65.97		16.13	7.61	25.17	44.54
	61.26	35.96	55.49	66.11	L54	44.20	46.45	55.65	56.19
L21	55.35	9.62	73.81	18.21	L56	64.43	48.50	79.66	65.39

Sample	CpG 5	CpG 6	CpG 7	CpG 8
L57	68.22	61.73	80.73	69.22
	66.14	64.82	75.73	71.56
L58	72.68	67.30	77.07	67.19
	67.49	61.64	73.18	70.04
L59	78.67	77.88	86.97	73.62
	79.12	78.20	89.04	79.56

Supplementary Table 45: MGMT enhancer K-M methylation status [%] of 8 CpGs, determined by PSQ (assay 2B). If possible, two replicates were used for calculation of arithmetic means. Values marked red not included in data evaluation. Values below 5% are marked <LLOQ and values over 95% are marked >ULOQ. n.a. = not available.

Sample	CpG 11	CpG 12	CpG 13	CpG 14	CpG 15	CpG 16	CpG 17	CpG 18
L02	85.41	71.76	81.89	52.71	91.06	71.13	91.93	85.78
	89.42	68.26	82.20	49.24	91.90	73.72	90.11	84.48
L04	85.83	85.30	62.88	69.37	92.05	68.46	92.09	87.36
	85.45	86.48	83.42	71.75	90.43	67.94	92.49	82.44
	85.61	90.52	84.56	71.07	89.81	59.19	90.40	75.01
L07	20.91	56.89	45.62	51.30	76.66	59.91	78.79	71.50
	18.22	51.50	48.14	47.34	72.21	60.94	83.15	67.87
L08	61.19	61.60	35.80	32.83	75.73	66.97	86.90	77.36
	60.71	61.11	36.84	33.64	78.09	69.78	87.63	80.03
L12	45.69	72.94	39.43	31.23	84.31	73.94	92.76	79.47
	48.37	72.13	34.88	29.79	75.98	75.36	90.32	80.21
L19	51.39	41.09	19.80	30.06	79.66	70.41	82.89	74.43
	53.97	38.39	16.00	29.19	77.41	70.61	83.53	77.83
L39	76.47	67.39	62.00	67.22	88.18	65.92	79.38	77.14
	77.42	63.85	57.31	62.68	86.28	67.11	86.61	83.44
L42	75.26	66.17	13.85	67.56	89.27	76.25	93.89	86.91
	86.84	72.35	16.67	73.66	89.61	81.12	92.88	85.84
L43	90.76	82.91	81.40	79.29	85.64	51.22	84.81	84.90
	90.99	80.41	85.60	86.81	94.32	58.82	92.54	88.86
L44	61.53	66.69	59.34	59.50	77.54	62.40	83.15	76.37
L46	82.29	83.05	17.50	17.26	85.98	70.17	89.89	75.52
	82.07	86.05	13.44	18.67	86.04	75.55	91.92	80.54
L48	37.06	60.18	37.82	27.06	87.57	71.21	85.42	79.25
	36.98	60.46	35.98	24.89	90.04	74.69	87.02	81.36
L50	39.12	41.12	33.60	24.95	54.61	49.00	62.65	55.33
	42.31	40.13	36.93	30.34	58.41	57.09	67.54	63.59
L56	67.60	46.97	45.15	58.41	83.21	65.19	85.94	76.93
L57	73.49	66.65	66.78	61.26	78.25	65.16	85.29	78.26
	75.11	74.79	75.80	65.73	87.33	69.40	89.89	81.83
L58	73.76	73.98	67.18	51.43	79.99	63.37	81.73	79.88
	83.12	84.00	70.21	67.09	86.16	68.75	86.75	82.83

	71.02	74.39	63.47	48.19	79.00	57.72	80.76	72.12
L59	83.92	80.60	76.09	74.77	87.40	64.93	88.04	84.76
	86.16	82.08	82.51	76.47	90.39	69.74	91.99	87.99

Supplementary Table 46: MGMT enhancer K-M methylation status [%] of 4 CpGs, determined by PSQ (assay 4H). If possible, two replicates were used for calculation of arithmetic means. Values marked red not included in data evaluation. Values below 5% are marked <LLOQ and values over 95% are marked >ULOQ. n.a. = not available.

Sample	**CpG 24**	**CpG 25**	**CpG 26**	**CpG 27**
L02	5.72	<LLOQ	24.90	65.29
	n.a.	<LLOQ	23.15	63.87
	<LLOQ	<LLOQ	24.77	66.43
L04	7.04	<LLOQ	5.85	<LLOQ
	n.a.	<LLOQ	7.87	5.27
L06	<LLOQ	39.63	45.23	65.35
	7.72	42.74	50.75	60.95
L07	18.20	20.01	<LLOQ	<LLOQ
	n.a.	<LLOQ	<LLOQ	<LLOQ
L08	<LLOQ	<LLOQ	23.58	35.53
	n.a.	<LLOQ	21.34	36.32
	<LLOQ	<LLOQ	21.56	38.35
L11	38.71	14.95	<LLOQ	<LLOQ
	39.93	14.62	<LLOQ	<LLOQ
L12	<LLOQ	<LLOQ	17.12	28.36
	n.a.	<LLOQ	12.76	22.00
	<LLOQ	<LLOQ	12.73	24.24
L15exp	40.10	<LLOQ	41.63	58.38
	24.40	<LLOQ	41.59	56.43
L16exp	21.22	16.99	35.39	36.39
	18.15	18.62	32.29	33.72
L19exp	40.88	33.62	21.27	6.78
	n.a.	40.27	22.88	6.44
	37.44	38.80	22.71	7.50
L21exp	<LLOQ	10.00	19.83	72.40
	<LLOQ	8.00	23.39	73.11
L22exp	<LLOQ	<LLOQ	18.86	25.33

	<LLOQ	5.96	21.83	28.37
L39exp	7.45	7.75	8.88	5.47
	n.a.	10.17	6.24	<LLOQ
L42exp	<LLOQ	5.88	5.99	<LLOQ
	n.a.	<LLOQ	5.55	<LLOQ
L43	23.77	19.08	23.29	9.64
	n.a.	20.59	26.89	11.41
	14.50	20.58	27.52	12.66
L45	<LLOQ	<LLOQ	60.03	42.50
	<LLOQ	<LLOQ	65.36	54.83
L46	<LLOQ	81.81	57.09	81.45
	n.a.	81.03	55.33	83.17
	11.53	80.73	57.21	84.11
L48	6.24	5.60	<LLOQ	<LLOQ
	n.a.	<LLOQ	<LLOQ	<LLOQ
L50	<LLOQ	<LLOQ	<LLOQ	<LLOQ
	n.a.	<LLOQ	<LLOQ	<LLOQ
L51	<LLOQ	28.29	<LLOQ	<LLOQ
	<LLOQ	28.15	<LLOQ	<LLOQ
L57exp	16.91	10.24	20.98	13.31
	n.a.	9.92	19.14	12.33
	18.21	10.20	19.39	13.56
L59exp	48.98	51.57	43.92	23.57
	n.a.	48.25	41.73	23.54
	42.51	46.17	40.17	25.16

Supplementary Table 47: MGMT enhancer K-M methylation status [%] of 3 CpGs, determined by PSQ (assay 5C). If possible, two replicates were used for calculation of arithmetic means. Values marked red not included in data evaluation. Values below 5% are marked <LLOQ and values over 95% are marked >ULOQ. n.a. = not available.

Sample	CpG 37	CpG 38	CpG 39	Sample	CpG 37	CpG 38	CpG 39	Sample	CpG 37	CpG 38	CpG 39
L02	81.98	71.66	46.58	L39	82.71	76.15	73.46	L57	78.30	73.94	64.72
	90.00	80.85	48.08		89.93	84.52	78.29		79.80	72.72	70.70
L04	83.12	72.40	75.71	L41	34.52	28.20	25.11	L59	84.94	79.44	79.67
	>ULOQ	76.35	90.42	L42	80.72	69.64	32.74		89.00	82.81	82.61
L05	68.55	75.82	57.68		86.39	84.54	42.85				
L07	77.32	70.32	57.26		81.50	72.16	36.22				
	78.88	72.55	54.54	L43	87.53	79.71	79.98				
L08	30.58	27.67	<LLOQ		86.07	72.16	75.45				
	42.30	28.59	<LLOQ	L46	82.48	77.23	80.68				
L12	<LLOQ	<LLOQ	<LLOQ		94.53	80.68	78.76				
	6.45	<LLOQ	<LLOQ	L48	91.59	75.13	21.63				
L15	65.92	60.70	48.40		79.78	66.98	32.92				
L16	26.76	21.34	19.82	L50	58.95	57.45	20.11				
	38.81	37.28	32.36		45.58	36.63	39.37				
L19	71.39	68.46	45.57		56.46	54.86	20.31				
	70.76	57.80	35.25		37.49	39.54	44.20				
L21	80.47	73.21	37.03	L55	75.59	75.44	21.17				

Supplementary Table 48: ABCB1 promoter methylation status [%] of 7 CpGs, determined by PSQ. If possible, two replicates were used for calculation of arithmetic means. Values marked red not included in data evaluation. Values below 5% are marked <LLOQ and values over 95% are marked >ULOQ. n.a. = not available.

Sample	CpG 1	CpG 2	CpG 3	CpG 4	CpG 5	CpG 6	CpG 7
L01	74.85	61.44	41.02	51.30	31.56	14.35	19.38
	75.13	61.89	42.24	49.77	34.87	13.03	21.09
L02	73.53	68.33	40.56	47.43	41.31	71.59	48.82
	72.07	69.83	42.67	49.23	40.21	69.78	50.48
L03	47.12	41.38	48.87	54.60	34.56	23.80	15.92
	48.85	43.14	49.01	54.05	34.67	22.93	16.13
L05	44.49	41.59	48.41	52.73	37.66	21.03	52.11
	47.93	45.93	52.93	57.45	39.61	19.79	56.29
L06	39.94	26.31	<LLOQ	5.76	6.12	6.57	8.91
	39.57	26.97	5.30	7.43	6.60	8.45	7.98
L07	38.64	12.91	5.55	11.41	15.84	12.47	13.63
	39.81	15.64	7.01	12.85	16.93	13.61	15.28
L08	79.16	73.88	59.67	85.28	62.53	22.13	52.02
	81.03	74.36	53.83	50.20	69.93	18.48	56.81
L11	84.68	75.44	71.41	71.75	71.57	70.66	89.73
	84.83	72.76	71.05	71.06	73.68	74.11	93.74
L12	88.34	79.99	89.49	>ULOQ	>ULOQ	>ULOQ	>ULOQ
	80.28	75.75	87.05	>ULOQ	>ULOQ	>ULOQ	>ULOQ
L14	82.82	68.98	32.96	39.49	22.78	<LLOQ	25.81
	79.28	68.02	39.15	44.52	24.04	8.40	25.47
L15	56.78	54.82	66.92	53.86	46.57	13.36	62.66
	57.44	58.65	67.27	51.97	42.45	10.08	62.87
L16	13.18	15.87	<LLOQ	<LLOQ	<LLOQ	<LLOQ	<LLOQ
	11.57	15.10	<LLOQ	<LLOQ	<LLOQ	<LLOQ	<LLOQ
L17	26.07	28.03	24.04	25.58	20.96	21.03	<LLOQ
	27.78	31.00	22.50	23.43	19.65	19.97	<LLOQ
L18	75.77	68.93	55.68	61.17	81.07	10.72	70.53
	79.35	74.56	53.00	58.31	85.88	11.57	71.36
L20	84.93	70.48	13.38	17.61	43.34	18.95	59.08
	86.10	71.39	14.56	19.80	42.96	17.23	55.90
L21	79.79	68.07	58.06	59.66	63.89	8.74	41.35
	78.85	67.58	59.02	59.29	63.60	7.26	39.04

L22	79.66	68.63	37.80	40.28	46.23	7.06	19.15
	81.19	70.63	38.09	42.18	43.80	5.99	17.72
L40	80.03	70.32	31.50	47.00	69.88	51.85	91.67
	79.83	68.85	32.81	47.81	73.97	51.05	92.71
L41	56.00	52.54	25.48	27.19	49.94	37.67	39.62
	50.28	45.39	21.80	24.90	50.30	38.37	37.30
L45	75.01	65.97	56.60	60.12	64.27	35.19	14.45
	67.57	60.26	58.78	61.47	63.94	38.70	13.53
L47	74.25	66.70	72.56	79.96	65.55	48.40	35.22
	77.60	69.47	74.57	81.91	67.82	52.34	35.65
L49	75.41	74.16	54.64	60.59	60.40	44.22	61.64
	78.46	74.86	55.70	61.77	61.71	46.59	60.83
L51	80.81	68.90	21.43	38.52	39.09	38.10	60.80
	84.71	72.48	22.62	38.92	40.86	41.81	63.01
L52	37.54	33.59	12.99	23.65	43.81	33.28	43.46
L53	10.03	13.52	<LLOQ	<LLOQ	13.23	<LLOQ	<LLOQ
	9.91	14.53	<LLOQ	<LLOQ	13.59	<LLOQ	<LLOQ
L54	<LLOQ	<LLOQ	<LLOQ	<LLOQ	<LLOQ	5.03	5.11
	<LLOQ	<LLOQ	<LLOQ	<LLOQ	<LLOQ	5.63	5.56
L55	63.05	68.05	63.86	38.85	58.45	40.59	58.47
	59.43	62.77	60.42	33.55	64.69	43.88	65.75

Supplementary Table 49: ABCG2 promoter methylation status [%] of 8 CpGs, determined by PSQ. If possible, two replicates were used for calculation of arithmetic means. Values marked red not included in data evaluation. Values below 5% are marked <LLOQ and values over 95% are marked >ULOQ. n.a. = not available.

Sample	CpG 1	CpG 2	CpG 3	CpG 4	CpG 5	CpG 6	CpG 7	CpG 8
L01	24.80	18.71	19.17	35.60	23.67	51.43	53.05	35.99
	25.29	20.81	20.29	36.21	27.24	49.32	49.69	36.24
L02	<LLOQ	<LLOQ	<LLOQ	<LLOQ	<LLOQ	<LLOQ	<LLOQ	<LLOQ
	<LLOQ	<LLOQ	<LLOQ	<LLOQ	<LLOQ	<LLOQ	<LLOQ	<LLOQ
L03	40.62	38.77	39.83	31.33	37.42	47.45	46.79	39.44
	44.67	42.77	41.47	33.32	40.95	50.53	48.84	43.67
L05	26.67	24.85	24.72	29.26	26.91	33.18	32.02	29.43
	23.68	23.47	25.62	29.46	24.73	32.02	30.82	25.65
L06	7.31	<LLOQ	<LLOQ	<LLOQ	6.64	7.35	6.73	<LLOQ
	7.31	<LLOQ	<LLOQ	5.65	7.79	8.73	7.65	<LLOQ
L07	75.42	77.25	46.89	52.58	51.80	58.15	59.49	49.00
	74.69	75.20	50.98	55.63	54.54	59.16	61.22	50.59
L08	33.24	35.09	39.23	41.57	37.21	41.88	45.31	37.19
	30.07	28.90	44.19	45.97	48.89	49.74	52.81	44.57
L11	54.60	46.61	84.40	77.85	48.96	93.96	>ULOQ	77.24
	54.13	46.38	86.13	81.96	49.33	>ULOQ	>ULOQ	79.03
L12	<LLOQ	<LLOQ	<LLOQ	<LLOQ	<LLOQ	<LLOQ	<LLOQ	<LLOQ
	<LLOQ	<LLOQ	<LLOQ	<LLOQ	<LLOQ	<LLOQ	<LLOQ	<LLOQ
L14	48.58	46.21	48.73	56.25	50.96	62.34	54.59	44.79
	47.51	46.18	50.68	59.57	53.48	63.91	54.90	47.59
L15	17.12	21.52	14.86	12.84	8.25	30.28	25.18	22.64
	16.45	21.62	14.59	11.44	7.94	29.74	21.70	21.60
L16	<LLOQ	<LLOQ	<LLOQ	<LLOQ	<LLOQ	<LLOQ	5.32	<LLOQ
	<LLOQ	<LLOQ	<LLOQ	<LLOQ	<LLOQ	<LLOQ	<LLOQ	<LLOQ
L17	71.23	84.68	71.34	72.70	47.23	53.88	56.44	45.20
	69.11	84.53	70.77	72.01	45.92	51.27	50.74	42.86
L18	69.20	79.32	79.02	84.58	84.74	86.89	86.87	54.38
	68.60	80.38	78.69	85.15	86.71	89.75	89.54	56.55
L20	42.42	23.89	41.31	47.13	44.17	48.74	52.37	44.14
	41.65	23.86	37.97	46.74	43.08	47.63	50.93	42.60
L21	91.23	91.94	>ULOQ	>ULOQ	>ULOQ	>ULOQ	>ULOQ	85.42
	91.43	90.62	94.93	>ULOQ	>ULOQ	>ULOQ	>ULOQ	82.64

L22	29.78	32.89	39.80	58.92	44.18	62.57	51.77	58.64
	29.90	31.70	39.58	61.10	46.84	65.61	54.09	59.99
L40	94.50	93.97	93.97	>ULOQ	>ULOQ	>ULOQ	>ULOQ	>ULOQ
	94.64	93.54	>ULOQ	>ULOQ	>ULOQ	>ULOQ	>ULOQ	>ULOQ
L41	5.86	<LLOQ	<LLOQ	15.63	6.12	27.73	20.29	6.93
	5.90	<LLOQ	<LLOQ	7.14	6.82	24.36	20.43	8.08
L45	43.36	39.60	44.79	47.33	43.28	47.81	50.84	41.13
	42.06	39.98	44.05	47.86	43.39	49.07	50.97	43.06
L47	44.44	37.23	47.50	55.01	49.41	70.63	61.18	92.52
	42.20	36.82	45.34	51.18	49.42	69.34	66.64	90.60
L49	<LLOQ	<LLOQ	<LLOQ	<LLOQ	<LLOQ	<LLOQ	<LLOQ	<LLOQ
	<LLOQ	<LLOQ	<LLOQ	<LLOQ	<LLOQ	<LLOQ	<LLOQ	<LLOQ
L51	93.38	90.67	>ULOQ	97.50	>ULOQ	>ULOQ	>ULOQ	56.30
	94.48	91.92	>ULOQ	97.50	>ULOQ	>ULOQ	>ULOQ	52.81
L52	33.89	32.32	42.52	22.37	34.51	45.73	48.86	40.08
L53	26.52	32.75	36.91	38.24	24.17	51.72	57.77	19.28
	26.49	35.18	37.50	39.81	22.89	54.37	59.87	21.72
L54	66.53	57.04	67.17	76.82	69.84	78.47	82.49	66.17
	67.39	53.50	64.77	74.33	70.32	77.74	80.84	66.36
L55	72.56	89.86	73.10	>ULOQ	>ULOQ	>ULOQ	>ULOQ	69.98
	73.57	89.60	69.78	>ULOQ	94.63	>ULOQ	>ULOQ	68.03

Supplementary Table 50: Methylation status [%] of 7 CpGs in the ABCA7 exon 5 / intron 5 region, determined by PSQ. If possible, two replicates were used for calculation of arithmetic means. Values marked red not included in data evaluation. Values below 5% are marked <LLOQ and values over 95% are marked >ULOQ. n.a. = not available.

Sample	CpG 1	CpG 2	CpG 3	CpG 4	CpG 5	CpG 6	CpG 7
L01	19.47	24.64	28.32	12.26	38.38	28.92	63.84
	13.93	27.96	24.47	8.62	27.34	33.86	78.64
L02	>ULOQ	>ULOQ	>ULOQ	91.28	64.65	83.80	84.29
	90.30	>ULOQ	>ULOQ	>ULOQ	>ULOQ	69.24	82.24
	94.09	92.25	93.57	>ULOQ	>ULOQ	87.27	78.24
L03	>ULOQ	>ULOQ	93.44	83.21	>ULOQ	>ULOQ	82.86
	>ULOQ	87.80	81.53	94.87	>ULOQ	80.47	83.47
L05	31.28	67.99	40.90	41.99	54.92	42.62	70.30
	53.76	88.38	30.95	27.71	42.09	50.40	81.07
	42.85	55.23	21.83	31.94	35.28	38.61	51.01
L06	64.06	72.07	60.71	44.83	62.64	42.89	52.79
	60.37	77.48	55.28	61.87	81.43	49.17	72.66
	65.77	88.93	76.79	59.47	86.39	60.32	68.27
L07	49.90	90.09	71.20	72.09	75.77	62.29	70.97
	69.93	81.43	82.24	68.33	82.07	57.17	68.87
	52.39	81.79	72.51	71.92	83.80	60.23	71.89
L08	79.42	79.51	76.46	77.24	80.73	89.32	66.86
	>ULOQ	94.65	>ULOQ	17.29	>ULOQ	88.76	85.03
L11	79.22	88.26	73.26	79.04	75.25	83.10	87.73
	>ULOQ	98.39	73.38	75.69	83.92	94.19	87.19
L12	>ULOQ	>ULOQ	>ULOQ	93.35	>ULOQ	75.74	86.17
	>ULOQ	>ULOQ	90.60	83.81	86.92	81.87	85.87
L14	5.73	9.06	29.53	<LLOQ	26.77	32.35	27.23
	<LLOQ	5.36	7.84	<LLOQ	9.03	22.78	28.02
	<LLOQ	6.37	<LLOQ	<LLOQ	14.52	25.13	27.95
L15	91.67	>ULOQ	>ULOQ	88.21	87.51	80.95	81.34
	>ULOQ	92.69	>ULOQ	87.34	>ULOQ	89.39	86.10
L16	12.32	13.39	9.99	8.32	46.91	8.04	10.42
	14.49	13.00	13.40	6.33	41.50	7.71	12.20
L17	>ULOQ	>ULOQ	83.06	94.40	>ULOQ	46.24	85.47
	>ULOQ	94.97	>ULOQ	90.15	>ULOQ	44.26	71.42

L18	43.30	71.89	61.55	18.40	76.01	54.05	43.61
	73.69	88.60	53.68	41.56	81.77	38.61	24.20
	53.45	69.69	50.89	36.29	72.03	44.71	34.31
L20	39.58	49.73	61.92	26.32	77.62	76.45	39.16
	13.39	30.70	73.01	24.74	76.17	55.64	57.37
	8.48	59.61	57.06	24.66	68.16	74.60	50.59
L21	80.93	94.64	90.08	84.03	>ULOQ	88.32	55.76
	>ULOQ	>ULOQ	89.03	88.48	>ULOQ	87.02	58.39
L22	67.87	80.09	93.97	62.64	>ULOQ	70.91	58.15
	79.35	>ULOQ	>ULOQ	81.89	94.97	86.20	48.76
	>ULOQ	>ULOQ	>ULOQ	90.68	80.12	87.98	60.14
L40	68.23	60.83	70.82	75.69	>ULOQ	74.13	75.07
	72.57	73.85	72.73	93.16	89.98	72.60	75.86
L41	44.34	80.64	58.96	21.42	63.11	68.51	76.80
	36.84	61.84	57.25	29.75	74.81	57.24	63.24
	69.63	81.74	63.99	59.64	68.31	58.55	56.12
L45	94.46	>ULOQ	88.09	52.12	93.61	83.38	87.68
	90.42	94.99	83.43	46.46	>ULOQ	87.64	80.41
L47	>ULOQ	>ULOQ	88.72	72.22	94.29	75.99	82.68
	89.78	>ULOQ	93.73	78.12	94.88	85.34	82.24
L49	12.49	20.03	15.04	<LLOQ	22.27	5.64	18.32
	5.45	17.76	21.02	<LLOQ	28.91	11.69	21.62
L51	>ULOQ	>ULOQ	91.32	94.88	>ULOQ	32.00	51.69
	>ULOQ	>ULOQ	87.34	87.25	94.95	34.59	48.57
L52	21.06	22.94	43.22	19.32	35.93	12.10	<LLOQ
L53	76.99	>ULOQ	30.66	87.96	68.77	46.83	85.93
	74.70	>ULOQ	27.58	56.38	59.71	35.62	74.90
	67.32	90.11	47.46	83.24	63.23	61.55	84.67
L54	63.63	60.53	73.90	27.55	76.24	45.87	56.52
	59.19	58.81	54.89	30.43	68.77	56.95	66.29
L55	81.13	92.79	90.28	56.12	77.75	74.31	69.34
	78.15	89.77	83.35	47.90	75.49	67.75	59.29

Supplementary Table 51: Methylation status [%] of 9 CpGs in the ABCA7 exon 6 / intron 6 region, determined by PSQ. If possible, two replicates were used for calculation of arithmetic means. Values marked red not included in data evaluation. Values below 5% are marked <LLOQ and values over 95% are marked >ULOQ. n.a. = not available.

Sample	CpG 1	CpG 2	CpG 3	CpG 4	CpG 5	CpG 6	CpG 7	CpG 8	CpG 9
L01	54.92	55.26	29.12	64.70	22.78	65.89	82.97	87.65	67.73
	56.10	52.44	31.48	63.28	22.89	68.65	82.95	85.22	67.00
L02	82.77	80.51	59.71	81.15	42.03	88.42	84.46	90.16	74.34
	85.44	80.39	59.69	82.11	41.28	88.72	84.08	91.45	74.33
L03	81.72	75.24	40.67	80.21	64.65	90.11	89.38	85.68	76.66
	82.94	72.51	37.70	80.54	63.65	92.37	90.61	85.64	76.31
L05	41.85	43.89	32.22	68.14	15.82	61.72	79.67	79.34	62.01
	49.40	44.95	33.38	74.83	21.07	60.09	84.75	86.01	66.12
L06	67.27	71.43	53.78	77.76	41.02	79.31	83.24	87.68	70.07
	67.74	69.46	51.45	76.32	40.01	80.02	83.55	86.92	68.24
L07	83.21	76.25	61.08	78.65	41.36	87.29	86.86	94.91	76.18
	82.29	77.36	63.26	79.55	45.20	88.33	87.91	94.92	74.50
L08	75.61	74.97	61.87	81.03	67.14	88.53	89.61	94.53	74.90
L11	83.15	75.86	72.33	79.74	61.86	90.71	89.58	>ULOQ	76.53
	85.03	74.53	72.49	79.34	60.77	90.66	91.07	>ULOQ	75.26
L12	88.36	82.83	77.70	83.76	63.33	92.76	89.71	>ULOQ	75.56
	78.60	79.44	70.31	82.21	68.06	92.76	90.82	>ULOQ	74.14
L14	45.87	51.07	18.96	50.53	13.12	67.55	86.54	91.27	74.18
	47.01	54.10	19.19	52.05	10.41	67.86	86.37	89.58	72.62
L15	83.12	76.56	77.63	81.86	72.63	92.92	89.06	>ULOQ	76.91
	84.27	76.73	81.04	82.22	75.12	94.34	90.43	>ULOQ	76.41
L16	39.20	54.85	34.59	72.29	40.49	66.78	79.11	78.86	64.26
	39.64	56.30	37.36	73.36	40.05	67.04	80.18	79.94	65.43
L17	71.28	76.26	56.70	80.16	75.45	91.25	84.52	>ULOQ	74.64
	75.07	77.01	69.53	81.53	83.85	93.67	90.69	>ULOQ	76.41
L18	44.27	63.05	36.38	66.46	19.58	65.84	71.39	74.77	54.79
	46.69	66.75	38.10	70.45	16.86	67.05	72.25	>ULOQ	50.77
L20	75.97	74.99	58.44	78.85	44.52	65.62	90.36	94.34	70.61
	79.33	74.63	61.34	78.83	46.98	72.45	90.52	93.57	71.13
L21	79.30	75.13	70.27	79.50	58.23	89.51	89.25	>ULOQ	73.65
	81.08	77.73	69.82	81.89	61.36	94.10	91.57	93.61	77.61

L22	79.15	76.10	77.42	80.13	51.67	89.39	90.45	>ULOQ	74.75
	79.48	78.17	76.56	80.85	51.17	91.35	91.17	>ULOQ	75.23
L40	77.46	77.88	63.39	80.71	68.28	91.21	90.90	85.10	76.01
	79.24	76.78	60.14	81.53	65.33	92.57	90.77	84.10	76.14
L41	84.82	76.36	52.76	80.75	52.85	82.00	88.49	94.43	75.72
	84.31	78.55	55.08	81.71	54.51	80.81	87.35	94.04	76.04
L45	87.50	75.72	42.14	81.84	39.17	90.26	80.23	85.53	74.18
	77.86	79.67	37.92	81.86	55.57	91.49	91.51	94.09	76.90
	74.94	80.70	42.26	81.84	50.04	89.00	90.85	94.23	75.36
L47	86.84	78.11	77.80	81.99	44.84	92.94	92.04	93.19	77.20
	85.47	77.26	78.08	81.33	44.58	90.09	91.43	94.61	76.02
L49	36.42	46.97	11.56	53.90	13.89	45.13	76.86	84.27	69.93
	38.01	48.84	12.32	56.25	13.33	48.33	80.15	84.95	69.59
L51	79.72	73.16	57.51	80.04	79.42	92.31	90.23	>ULOQ	74.79
	83.53	75.77	57.80	81.83	79.27	93.79	90.71	>ULOQ	75.96
L52	79.68	53.06	53.24	80.56	33.83	77.43	89.82	86.64	73.85
L53	72.71	75.53	58.02	79.34	36.40	77.80	91.11	94.16	76.98
	74.16	76.48	56.52	80.35	36.05	81.18	90.82	93.59	75.56
L54	67.81	74.09	52.00	79.93	31.58	76.19	86.24	93.01	76.65
	70.19	73.51	51.85	80.14	35.04	77.18	85.93	93.81	75.42
L55	49.80	48.66	32.69	76.53	23.03	60.87	83.36	84.84	68.53
	79.57	80.07	47.92	82.74	57.56	88.27	90.23	94.43	73.26
	78.10	79.24	48.08	82.24	55.04	88.17	90.37	>ULOQ	70.00

Supplementary Table 52: Methylation status [%] of the DNA standards (0%, 25%, 50%, 75%, and 100%) for 7 CpGs in the p16 promoter region, determined by PSQ. If possible, two replicates were used for calculation of arithmetic means. Values marked red not included in data evaluation. Values below 5% are marked <LLOQ and values over 95% are marked >ULOQ. n.a. = not available.

Sample	**CpG 1**	**CpG 2**	**CpG 3**	**CpG 4**	**CpG 5**	**CpG 6**	**CpG 7**
0%	<LLOQ	<LLOQ	<LLOQ	<LLOQ	<LLOQ	5.68	<LLOQ
25%	<LLOQ	<LLOQ	5.58	<LLOQ	<LLOQ	6.09	<LLOQ
50%	7.40	8.65	10.68	7.99	8.98	11.41	9.05
75%	13.38	19.40	17.83	16.33	15.89	19.47	16.96
100%	72.75	84.89	>ULOQ	89.05	83.08	92.89	78.58

Supplementary Table 53: Average methylation status [%] of 7 CpGs in the p16 promoter region, determined by HRM. If possible, two replicates were used for calculation of arithmetic means. Values marked red not included in data evaluation. Values below 5% are marked <LLOQ and values over 95% are marked >ULOQ. SF = standardized fluorescence, n.a. = not available.

Sample	SF [%]	Methylation status [%]	SD [%]
L05	2.95	22.51	1.65
	0.80	7.89	0.53
L08	1.60	17.78	6.42
	1.44	18.62	1.13
L11	2.82	21.88	1.42
	2.98	20.48	0.58
L12	1.50	18.10	6.90
L14	2.55	20.57	0.99
	1.96	15.26	0.57
L15	2.71	21.37	0.26
	1.97	15.35	0.34
L16	0.49	6.28	1.70
L17	0.78	8.69	3.62
	2.11	16.10	0.70
L21	0.77	8.61	3.67
	1.95	15.19	0.54
L22	1.04	11.15	0.26
	1.81	14.31	2.65
L47	2.13	18.29	0.21
	2.50	18.12	0.24
L52	2.67	18.91	2.38
	2.55	26.88	1.06
L53	2.15	18.38	0.74
	2.44	17.72	2.87
L54	1.40	13.75	1.28
	2.91	20.14	0.27
L57	0.37	6.43	0.17
	3.57	32.84	0.98
L59	0.68	10.98	2.33
	2.28	24.92	3.56

Supplementary Table 54: Methylation status [%] of 24 CpGs in p16 exon 2, determined by PSQ. If possible, two replicates were used for calculation of arithmetic means. Values marked red not included in data evaluation. Values below 5% are marked <LLOQ and values over 95% are marked >ULOQ. n.a. = not available.

Sample	CpG 1	CpG 2	CpG 3	CpG 4	CpG 5	CpG 6	CpG 7	CpG 8	CpG 9	CpG 10	CpG 11	CpG 12
L02	<LLOQ	<LLOQ	<LLOQ	2.50	<LLOQ	<LLOQ	<LLOQ	<LLOQ	<LLOQ	<LLOQ	<LLOQ	<LLOQ
L05	>ULOQ	>ULOQ	<LLOQ	>ULOQ	91.20	86.24	81.17	84.97	>ULOQ	>ULOQ	>ULOQ	>ULOQ
	>ULOQ	>ULOQ	<LLOQ	>ULOQ	94.29	91.04	87.33	84.54	>ULOQ	>ULOQ	>ULOQ	92.85
L08	>ULOQ	>ULOQ	<LLOQ	>ULOQ	93.23	88.46	87.16	79.43	93.44	>ULOQ	>ULOQ	>ULOQ
	>ULOQ	>ULOQ	<LLOQ	>ULOQ	93.58	85.35	81.34	81.49	>ULOQ	>ULOQ	>ULOQ	>ULOQ
	>ULOQ	>ULOQ	<LLOQ	>ULOQ	>ULOQ	90.03	86.99	83.20	93.11	>ULOQ	>ULOQ	>ULOQ
L11	>ULOQ	>ULOQ	<LLOQ	>ULOQ	93.86	90.39	89.35	88.41	94.85	>ULOQ	>ULOQ	61.90
	>ULOQ	>ULOQ	<LLOQ	>ULOQ	93.60	86.29	86.66	82.91	>ULOQ	>ULOQ	>ULOQ	63.39
L12	>ULOQ	>ULOQ	94.59	>ULOQ	>ULOQ	91.50	88.33	86.39	6.25	7.95	>ULOQ	>ULOQ
	>ULOQ	56.46	93.15	>ULOQ	>ULOQ	90.60	89.38	85.95	6.22	7.55	>ULOQ	>ULOQ
	>ULOQ	>ULOQ	93.32	>ULOQ	>ULOQ	86.26	87.36	88.26	6.78	7.15	>ULOQ	>ULOQ
L14	>ULOQ	>ULOQ	<LLOQ	>ULOQ	92.88	89.20	85.23	83.93	93.15	>ULOQ	>ULOQ	>ULOQ
	91.24	92.00	<LLOQ	>ULOQ	90.89	82.61	82.77	78.97	91.77	>ULOQ	>ULOQ	91.21
L15	>ULOQ	79.53	<LLOQ	>ULOQ	77.45	79.53	87.88	80.21	>ULOQ	>ULOQ	90.76	48.90
	>ULOQ	78.77	<LLOQ	>ULOQ	68.57	75.89	84.84	79.09	93.66	>ULOQ	91.68	51.28
L16	46.33	19.69	<LLOQ	64.66	32.08	24.56	26.70	30.32	11.60	38.33	16.78	6.88
	40.05	19.57	<LLOQ	60.49	37.88	25.34	26.17	32.90	11.33	41.65	17.60	8.55

Sample	CpG 1	CpG 2	CpG 3	CpG 4	CpG 5	CpG 6	CpG 7	CpG 8	CpG 9	CpG 10	CpG 11	CpG 12
L17	>ULOQ	72.59	<LLOQ	>ULOQ	94.60	78.79	88.06	83.99	79.19	>ULOQ	>ULOQ	39.97
	>ULOQ	73.96	<LLOQ	>ULOQ	94.19	77.25	84.10	81.80	77.39	>ULOQ	>ULOQ	42.12
L21	>ULOQ	84.01	<LLOQ	>ULOQ	94.36	87.54	84.56	80.55	88.25	>ULOQ	>ULOQ	97.50
	>ULOQ	79.97	<LLOQ	94.41	93.80	85.96	85.01	81.66	92.47	>ULOQ	>ULOQ	93.23
L22	>ULOQ	>ULOQ	<LLOQ	>ULOQ	85.96	81.34	73.41	74.54	77.30	>ULOQ	>ULOQ	64.07
	>ULOQ	>ULOQ	<LLOQ	>ULOQ	82.70	85.58	78.02	81.53	70.94	>ULOQ	>ULOQ	61.76
L47	57.87	47.94	<LLOQ	58.56	41.83	51.74	51.32	50.46	57.44	64.55	53.37	37.12
	54.54	47.93	<LLOQ	54.96	39.19	46.52	47.15	45.39	51.94	61.19	52.04	32.91
L52	>ULOQ	97.50	<LLOQ	>ULOQ	86.51	86.79	85.48	81.93	93.51	>ULOQ	>ULOQ	72.84
	>ULOQ	97.50	<LLOQ	>ULOQ	91.51	90.62	88.03	82.62	91.93	>ULOQ	>ULOQ	78.54
L53	66.05	58.47	<LLOQ	86.46	53.49	54.24	55.57	67.60	64.49	85.65	69.43	45.80
	65.30	62.65	<LLOQ	85.14	55.49	55.40	56.88	66.21	62.06	82.58	71.21	46.65
L57	46.70	25.59	<LLOQ	74.59	22.22	29.61	28.75	37.09	13.04	55.48	23.42	13.95
	46.33	25.63	<LLOQ	76.26	18.94	36.22	25.57	38.82	9.84	46.23	20.22	8.06
L59	17.36	9.65	<LLOQ	43.78	14.39	41.28	18.46	25.49	9.05	41.92	14.41	17.41
	19.84	15.90	<LLOQ	40.28	15.52	44.29	18.66	25.72	12.36	39.46	14.05	14.65

Sample	CpG 13	CpG 14	CpG 15	CpG 16	CpG 17	CpG 18	CpG 19	CpG 20	CpG 21	CpG 22	CpG 23	CpG 24
L02	>ULOQ	<LLOQ	<LLOQ	<LLOQ	5.60	<LLOQ	<LLOQ	<LLOQ	87.93	<LLOQ	9.34	<LLOQ
L05	>ULOQ	89.08	85.21	>ULOQ	>ULOQ	94.76	92.98	>ULOQ	>ULOQ	92.86	>ULOQ	87.47
	>ULOQ	90.60	92.36	>ULOQ	>ULOQ	92.22	94.84	>ULOQ	>ULOQ	90.90	>ULOQ	90.74
L08	>ULOQ	88.11	92.10	>ULOQ	>ULOQ	89.86	91.94	94.73	94.07	91.32	>ULOQ	>ULOQ
	>ULOQ	88.46	93.17	>ULOQ	>ULOQ	91.98	92.94	97.50	>ULOQ	91.87	>ULOQ	>ULOQ
	>ULOQ	90.84	89.61	93.53	>ULOQ	89.89	90.20	91.93	>ULOQ	88.98	94.27	>ULOQ
L11	>ULOQ	87.33	>ULOQ	59.08	>ULOQ	92.76	93.42	94.71	>ULOQ	94.11	>ULOQ	71.29
	>ULOQ	90.37	>ULOQ	57.60	>ULOQ	89.45	92.96	91.89	>ULOQ	90.26	>ULOQ	78.19
L12	18.24	9.55	>ULOQ	>ULOQ	>ULOQ	91.76	90.60	94.55	>ULOQ	46.73	>ULOQ	>ULOQ
	18.47	8.93	>ULOQ	>ULOQ	>ULOQ	94.51	94.10	>ULOQ	>ULOQ	92.87	>ULOQ	>ULOQ
	18.40	8.40	>ULOQ	>ULOQ	>ULOQ	93.55	92.91	>ULOQ	>ULOQ	92.34	>ULOQ	>ULOQ
L14	>ULOQ	78.90	>ULOQ	>ULOQ	>ULOQ	>ULOQ	93.30	>ULOQ	>ULOQ	93.08	>ULOQ	>ULOQ
	>ULOQ	77.96	>ULOQ	>ULOQ	>ULOQ	94.63	94.17	>ULOQ	>ULOQ	93.27	>ULOQ	>ULOQ
L15	>ULOQ	68.85	69.65	94.01	74.29	92.61	84.96	86.84	85.48	77.74	87.57	60.69
	>ULOQ	67.46	76.14	>ULOQ	78.00	90.93	89.20	82.03	83.84	78.30	87.36	59.97
L16	87.67	7.45	16.56	<LLOQ	14.98	10.35	13.12	22.10	31.28	11.33	29.60	23.28
	80.51	6.01	16.39	6.65	13.03	17.35	13.31	17.74	35.67	9.10	25.45	16.45

Sample	CpG 13	CpG 14	CpG 15	CpG 16	CpG 17	CpG 18	CpG 19	CpG 20	CpG 21	CpG 22	CpG 23	CpG 24
L17	>ULOQ	58.55	59.55	>ULOQ	>ULOQ	93.16	92.00	68.38	>ULOQ	86.99	>ULOQ	>ULOQ
	>ULOQ	63.69	69.56	>ULOQ	>ULOQ	90.04	92.13	66.76	>ULOQ	88.66	>ULOQ	>ULOQ
L21	>ULOQ	91.19	>ULOQ	>ULOQ	75.01	90.82	91.72	94.09	>ULOQ	90.63	94.47	63.24
	>ULOQ	89.20	>ULOQ	>ULOQ	69.34	89.42	93.55	94.35	>ULOQ	90.64	>ULOQ	61.56
L22	>ULOQ	82.89	94.09	>ULOQ	>ULOQ	92.83	94.02	79.66	92.77	68.82	92.17	89.09
	>ULOQ	86.11	92.89	90.75	>ULOQ	91.39	91.00	83.74	91.92	74.69	89.76	80.79
L47	69.73	50.39	59.74	60.61	61.31	56.35	58.30	59.71	58.61	55.71	49.35	67.58
	62.79	45.60	56.03	57.45	57.20	52.75	52.96	55.59	54.53	52.86	45.76	62.54
L52	>ULOQ	66.11	66.49	>ULOQ	75.21	81.37	92.59	75.07	94.15	73.55	80.44	75.61
	>ULOQ	69.18	69.32	94.90	77.52	84.65	90.68	78.31	93.92	79.88	82.20	68.49
L53	89.93	40.81	64.89	44.58	66.01	55.98	55.05	66.31	82.70	65.90	67.63	62.10
	92.26	40.66	59.63	45.19	66.26	57.89	54.81	62.15	80.08	66.01	69.04	54.52
L57	>ULOQ	8.50	23.80	<LLOQ	15.28	15.40	16.23	21.81	35.98	17.29	35.22	26.90
	>ULOQ	6.96	20.73	7.84	17.97	14.38	15.17	23.70	35.15	12.45	31.57	29.99
L59	87.78	5.09	8.30	<LLOQ	10.44	5.03	7.53	15.91	21.86	23.05	18.53	11.01
	89.72	<LLOQ	9.44	<LLOQ	10.93	6.64	7.33	15.26	17.71	27.78	20.40	13.58

7.3.3 Chemicals and kits

Supplementary Table 55: List of used chemicals and kits.

Name	Manufacturer
DNA Exitus Plus™ IF	AppliChem (Darmstadt, Germany)
ELGA water	Department of Analytical Chemistry, University of Vienna (AG Köllensperger)
EpiTect HRM PCR Kit	Qiagen (Hilden, Germany)
EpiTect PCR Control DNA Set	Qiagen (Hilden, Germany)
Ethanol (absolute)	Merck (Vienna, Austria)
HotStarTaq DNA Polymerase	Qiagen (Hilden, Germany)
MilliQ water	University of Vienna (in-house)
Nuclease-free water	Qiagen (Hilden, Germany)
Oligonucleotides (Primer)	Sigma-Aldrich (Vienna, Austria)
PyroMark Denaturation Solution	Qiagen (Hilden, Germany)
PyroMark Q24 Advanced CpG Reagents	Qiagen (Hilden, Germany)
PyroMark Wash Buffer 10x	Qiagen (Hilden, Germany)
RNase-free water	Qiagen (Hilden, Germany)
Streptavidin Sepharose High Performance	GE Healthcare (Vienna, Austria)
Type-it HRM PCR Kit	Qiagen (Hilden, Germany)
Zymo DNA standards 0/100% methylated	ZYMO research USA

7.3.4 Disposables

Supplementary Table 56: List of used consumable/disposable materials.

Name	Manufacturer
Biosphere Filter Tips (0.5-20 µL)	Sarstedt (Wiener Neudorf, Austria)
Biosphere Filter Tips (100-1000 µL)	Sarstedt (Wiener Neudorf, Austria)
Falcon Tubes (15 and 50 mL)	VWR International (Vienna, Austria)
Filter Tips (20-200 µL)	Brand (Vienna, Austria)
iCycler iQ 96-well PCR Plates	Bio-Rad Laboratories (Vienna, Austria)
Individual PCR Tubes, Flat Cap (0.2 mL)	Bio-Rad Laboratories (Vienna, Austria)
Microseal 'B' PCR Plate Sealing Film	Bio-Rad Laboratories (Vienna, Austria)
Microtubes (0.65 mL)	VWR International (Vienna, Austria)
PyroMark Q24 Cartridge	Qiagen (Hilden, Germany)
PyroMark Q24 Plate	Qiagen (Hilden, Germany)
Safe Lock Tubes (1.5, 2, and 5 mL)	Eppendorf GmbH (Vienna, Austria)

StarGuard sensitive, Nitrile Gloves	Starlab International GmbH (Hamburg, Germany)
Strip Tubes and Caps (0.1 mL)	Qiagen (Hilden, Germany)

7.3.5 Laboratory equipment

Supplementary Table 57: List of used laboratory equipment.

Name	Manufacturer
2511 Dry Vacuum and pressure pump	Welch (Fürstenfeldbrück, Germany)
Centrifuge Galaxy Mini	VWR International (Vienna, Austria)
Centrifuge Mini Star Silverline	VWR International (Vienna, Austria)
PCR working station	VWR International (Vienna, Austria)
PCR working station Pro	VWR International (Vienna, Austria)
Pipettes 0.5-10, 2-20, 20-200, 100-1000 µL	Eppendorf GmbH (Vienna, Austria)
Pipettes 2-20, 20-200, 100-1000 µL	Bio-Rad Laboratories (Vienna, Austria)
PyroMark Q24 advanced instrument	Qiagen (Hilden, Germany)
PyroMark Q24 Plate Holder	Qiagen (Hilden, Germany)
PyroMark Q24 vacuum workstation	Qiagen (Hilden, Germany)
Rotor-Gene® Q Thermocycler	Qiagen (Hilden, Germany)
Thermomixer Comfort	Eppendorf GmbH (Vienna, Austria)
Vortex genie 2 Digital	Scientific Industries (New York, USA)
Vortex mixer Classic Advanced	VELP Scientifica (Vienna, Austria)
Vortex mixer VF2	IKA (Staufen, Germany)
Vortex mixer W3	VWR International (Vienna, Austria)

7.3.6 Webtools and databases

Supplementary Table 58: List of used webtools and databases.

Name	Link
IDT OligoAnalyzer™ Tool	https://www.idtdna.com/pages/tools/oligoanalyzer
National Center for Biotechnology Information (NCBI)	https://www.ncbi.nlm.nih.gov/
Oligo Calc: Oligonucleotide Properties Calculator	http://biotools.nubic.northwestern.edu/OligoCalc.html
Primer Design and Search Tool	http://bisearch.enzim.hu/?m=genompsearch
Reverse Complement	https://www.bioinformatics.org/sms/rev_comp.html
RNAfold WebServer	http://rna.tbi.univie.ac.at/CGi-bin/RNAWebSuite/RNAfold.CGi

Transcriptional Regulatory Element Database (TRED)	https://cb.utdallas.edu/CGi-bin/TRED/tred.CGi?process=searchPromForm
UCSC Genome Browser	https://genome.ucsc.edu/
VISTA Enhancer Brower	https://enhancer.lbl.gov/

7.3.7 Software

Supplementary Table 59: List of used softwares.

Name	**Manufacturer**
ChemDraw 18.0	PerkinElmer (Waltham, USA)
Methyl Primer Express 1.0	Thermo Fisher Scientific (Vienna, Austria)
Microsoft Office 365	Microsoft (Redmond, USA)
OriginPro 2022b 9.95	OriginLab Corporation (Northampton, USA)
Paint 4.3.12	Microsoft (Redmond, USA)
PyroMark Assay Design Software 2.0	Qiagen (Hilden, Germany)
PyroMark Q24 Advanced Software 3.0.1	Qiagen (Hilden, Germany)
Rotor-Gene Q Series Software 2.3.1	Qiagen (Hilden, Germany)
IBM SPSS Statistics 28	IBM (Armonk, USA)

7.4 List of abbreviations

Supplementary Table 60: List of abbreviations used in this master's thesis.

Abbreviation	Meaning
%	Percent
°C	Degree(s) Celsius
µL	Microliter(s)
µM	Micromolar
5mC	5-methylcytosine
A	Adenine
AAG	Alkyl adenine DNA glycosylase
ABC-transporter	ATP-binding cassette transporter
ABCA7	ATP-binding cassette subfamily A member 7
ABCB1	ATP-binding cassette subfamily B member 1
ABCG2	ATP-binding cassette subfamily G member 2
adj	Adjuvant
ADP	Adenosine diphosphate
AIC	5-aminoimidazole-4-carboxamide
AMP	Adenosine monophosphate
APS	Adenosine-5'-phosphosulfate
ATP	Adenosine triphosphate
BER	Base excision repair
bp	Base pair(s)
C	Cytosine
CDK	Cyclin-dependent kinase
CDKN2A, p16	Cyclin-dependent kinase inhibitor 2A
CGI	CpG island
Ch-Th	Chemotherapy
CIMP	CpG island methylator phenotype
CpG	Cytosine-phosphate-guanine dinucleotide
Ct	Cycle threshold
Da	Dalton
dATP	Deoxyadenosine triphosphate
dATPαS	Deoxyadenosine α-thiotriphosphate
dCTP	Deoxycytidine triphosphate
dGTP	Deoxyguanosine triphosphate
DNA	Deoxyribonucleic acid

dNDP	Deoxynucleoside diphosphate
dNMP	Deoxynucleoside monophosphate
DNMT	DNA methyltransferase
dNTP	Deoxynucleoside triphosphate
DSB	Double-strand breaks
dsDNA	Double-stranded DNA
dTTP	Deoxythymidine triphosphate
EGFR	Epidermal growth factor receptor
FDA	United States Food and Drug Administration
Fw	Forward
G	Guanine
GBM	Glioblastoma
GBX2	Gastrulation brain homeobox 2
GLOBOCAN	Global Cancer Observatory
HRM	High resolution melting
IDH1	Isocitrate dehydrogenase 1
IHC	Immunohistochemistry
IL-6	Interleukin 6
kcal/mol	Kilocalorie per mole
KPS	Karnofsky performance status
LLOQ	Lower limit of quantification
MDR	Multi drug resistance
MGMT	O^6-methylguanine-DNA methyltransferase
min	Minute(s)
mL	Milliliter(s)
mM	Millimolar
MMR	Mismatch repair
mRNA	Messenger RNA
MTIC	Monomethyl triazene 5-(3-methyltriazen-1-yl)-imidazole-4-carboxamide
N^3-MeA	N^3-methyladenine
N^7-MeG	N^7-methylguanine
NBD	Nucleotide binding domains
NCBI	National Center for Biotechnology Information
No.	Number
NOS	Not otherwise specified

NTC	non-template controls
O^6-MeG	O^6-methylguanine
OS	Overall survival
PCR	Polymerase chain reaction
P_i	Phosphate
PP_i	Pyrophosphate
PSQ	Pyrosequencing
PTEN	Phosphate and tensin homologue
Rb	Retinoblastoma protein
R-Ch-Th	Chemoradiotherapy
Rev	Reverse
RNA	Ribonucleic acid
RNase	Ribonuclease
rpm	Rounds per minute
R-Th	Radiotherapy
SAM	S-adenosyl-methionine
sec	Second(s)
Seq	Sequencing
SNP	Single nucleotide polymorphism
ssDNA	Single-stranded DNA
T	Temperature
T_a	Annealing temperature
T_e	Elongation temperature
T_m	Melting temperature
TMD	Transmembrane domains
TMZ	Temozolomide
TRED	Transcriptional Regulatory Element Database
TSS	Transcription start site
ULOQ	Upper limit of quantification
UV	Ultraviolet
WHO	World Health Organization

7.5 List of figures

Figure 1: Prodrug activation of temozolomide and its effects on DNA. 3
Figure 2: MGMT repair mechanism of O^6-MeG. 4
Figure 3: Representative scheme of DNA repair mechanisms related to TMZ resistance. 5
Figure 4: Methylation of cytosine by DNA methyltransferases (DNMTs). 7
Figure 5: Methylation patterns in normal and cancer cells. White cycles represent unmethylated CpGs, black circles methylated CpGs. Transcription start site marked by a black arrow, which is repressed by hypermethylation. Modified from [53] 8
Figure 6: Bisulfite conversion of cytosine and 5-methylcytosine. 12
Figure 7: PCR amplification of bisulfite converted genomic DNA. 13
Figure 8: Principle of PCR. Modified from [137]. 14
Figure 9: Overview of the enzymatic cascade during pyrosequencing. Modified from [143]. 16
Figure 10: General workflow for DNA methylation analysis. 19
Figure 11: Assays for MGMT enhancer E employed in this thesis. 28
Figure 12: Representative pyrogram (top) and histogram (bottom) of assay 1D with 50% methylated standard DNA. 29
Figure 13: Assays for MGMT enhancer K-M employed in this thesis. 30
Figure 14: Representative pyrogram (top) and histogram (bottom) of assay 3 with 50% methylated standard DNA. 30
Figure 15: Assay ABCB1 (top) and ABCG2 (bottom) employed in this thesis. 31
Figure 16: Derivative HRM plot obtained for assay ABCB1 (left) and assay ABCG2 (right). UM = unmethylated standard DNA, 50% = 50% methylated standard DNA, M = methylated standard DNA, NTC = no-template control. 31
Figure 17: Assay ABCA7 ex 5 / in 5 and ex 6 / in 6 employed in this thesis. 32
Figure 18: Derivative HRM plot obtained for assay ABCA7 ex 5 / in 5 (left) and assay ABCA7 ex 6 / in 6 (right). UM = unmethylated standard DNA, 50% = 50% methylated standard DNA, M = methylated standard DNA, NTC = no-template control. 32
Figure 19: Assay p16 promoter (top) and p16 exon 2 (bottom) employed in this thesis. 33
Figure 20: Representative pyrogram (top) and histogram (bottom) obtained with the two newly designed sequencing primers of assay p16 exon 2 with 50% methylated standard DNA. 33
Figure 21: GBX2 assays employed in this thesis. 34
Figure 22: Genomic sequence of the GBX2 promotor region. Cyan highlighted and bold: binding sites of the forward and reverse primer, red and underlined: binding site of the sequencing primer, green highlighted: CpGs, pink highlighted: analyzed CpGs. 35
Figure 23: Amplification plot and derivative HRM plot obtained for GBX2 primer set 1. Primer concentration: 0.2 & 0.4 µM. T_a = 56.4 °C, T_e = 72 °C. UM = unmethylated standard DNA, M = methylated standard DNA, NTC = no-template control. 36
Figure 24: Genomic sequence of the GBX2 promotor region. Cyan highlighted and bold: binding sites of the forward and reverse primer, red and underlined: binding site of the sequencing primer, green highlighted: CpGs, pink highlighted: analyzed CpGs. 37
Figure 25: Amplification plot and derivative HRM plot obtained for GBX2 primer set 2. fw-C & rev-G = 0.2 µM, fw-T & rev-A = 0.4 µM. T_a = 60.5 °C, T_e = 72 °C. UM = unmethylated standard DNA, 50% = 50% methylated standard DNA, M = methylated standard DNA, NTC = no-template control. 39
Figure 26: Representative pyrogram (top) and histogram (bottom) of GBX2 primer set 2 with 50% methylated standard DNA. 40
Figure 27: Methylation status of twelve CpGs in the MGMT promoter region, ordered by sample. Blue plots: non-MGMT expressing samples, red plots: MGMT expressing samples, continuous lines: median, dashed lines: mean. 42

Figure 28: Methylation status of twelve CpGs in the MGMT promoter region, ordered by CpG. Blue plots: non-MGMT expressing samples, red plots: MGMT expressing samples, continuous lines: median, dashed lines: mean, ***: $p < 0.001$. 43
Figure 29: Methylation status of 14 CpGs in MGMT enhancer E, ordered by sample. Blue plots: non-MGMT expressing samples, red plots: MGMT expressing samples, continuous lines: median, dashed lines: mean. 45
Figure 30: Methylation status of 14 CpGs in MGMT enhancer E, ordered by CpG. Blue plots: non-MGMT expressing samples, red plots: MGMT expressing samples, continuous lines: median, dashed lines: mean, *: $p < 0.05$, **: $p < 0.01$, ***: $p < 0.001$. 46
Figure 31: Boxplot comparison of CpG 17 methylation status in MGMT enhancer K-M. Blue plot: non-MGMT expressing samples, red plot: MGMT expressing samples, continuous lines: median, dashed lines: mean. 49
Figure 32: Methylation status of 19 CpGs in MGMT enhancer K-M, ordered by sample. Blue plots: non-MGMT expressing samples, red plots: MGMT expressing samples, continuous lines: median, dashed lines: mean. 49
Figure 33: Methylation status of 19 CpGs in MGMT enhancer K-M, ordered by CpG. Blue plots: non-MGMT expressing samples, red plots: MGMT expressing samples, continuous lines: median, dashed lines: mean. 50
Figure 34: Boxplot comparison of CpG 14 methylation status in MGMT enhancer K-M. Blue plot: low Ki67 expressing samples, red plot: high Ki67 expressing samples, continuous lines: median, dashed lines: mean, *: $p < 0.05$. 51
Figure 35: Boxplot comparison of promoter methylation status of ABCB1 (marked blue) and ABCG2 (marked red) in 27 GBM samples, ordered by sample. Continuous lines: median, dashed lines: mean. 53
Figure 36: Promoter methylation status of ABCB1 (marked blue) and ABCG (marked red) in 27 GBM samples, ordered by CpG. Continuous lines: median, dashed lines: mean. 54
Figure 37: Amplification plot and derivative HRM plot obtained for the PSQ assay of ABCA 7 exon 5 / intron 5. Primer concentration = 0.2 µM, T_a = 58.3 °C, T_e = 72.0 °C. UM = unmethylated standard DNA, 50% = 50% methylated standard DNA, M = methylated standard DNA, NTC = no-template control. 55
Figure 38: Methylation status of seven CpGs in the ABCA7 exon 5 / intron 5 region in eight samples, ordered by sample. Continuous lines: median, dashed lines: mean. 55
Figure 39: Methylation status of nine CpGs in the ABCA7 exon 6 / intron 6 region in 27 GBM samples, ordered by sample. Continuous lines: median, dashed lines: mean. 56
Figure 40: Methylation status of nine CpGs in the ABCA7 exon 6 / intron 6 region in 27 GBM samples, ordered by CpG. Continuous lines: median, dashed lines: mean. 57
Figure 41: Amplification plot and derivative HRM plot obtained for the PSQ assay of the p16 promoter. Primer concentration = 0.4 µM, Ta = 59.5 °C, Te = 72.0 °C. UM = unmethylated standard DNA, 50% = 50% methylated standard DNA, M = methylated standard DNA, NTC = no-template control. 58
Figure 42: Representative pyrogram (top) and histogram (bottom) of seven CpGs in the p16 promoter region with 75% methylated standard DNA. 58
Figure 43: Normalized melt curves of the employed DNA standards (0%, 25%, 50%, 75%, and 100%) and polynomial calibration curve (0%, 25%, 50%, and 75%) for the p16 promoter region. 59
Figure 44: Average methylation status of seven CpGs in the p16 promoter region, determined by HRM. Mean values of two technical replicates (except for L12 and L16) and standard deviation. 60
Figure 45: Amplification plot and derivative HRM plot obtained for the PSQ assay of p16 exon 2. Primer concentration = 0.4 µM, Ta = 62.1 °C, Te = 72.0 °C. NTC = no-template control, UM

= unmethylated standard DNA, 50% = 50% methylated standard DNA, M = methylated standard DNA. 61
Figure 46: Methylation status of 24 CpGs in p16 exon 2 of 16 samples, ordered by sample. Continuous lines: median, dashed lines: mean. 62
Figure 47: Methylation status of 24 CpGs in p16 exon 2 of 16 samples, ordered by CpG. Continuous lines: median, dashed lines: mean. 62

7.6 List of tables

Table 1: GBM samples analyzed as part of this study. The 40 listed samples were provided by our cooperation partner Sabine Spiegl-Kreinecker from the Kepler University Hospital (Department of Neurosurgery) in Linz. They consist of DNA extracts from primary cell line samples, which were isolated from GBM tumor tissue. Clinical data of the patients is listed, along with MGMT promoter methylation, expression levels of MGMT (determined via Western blotting), and Ki67 (determined via Immunohistochemistry). f = female, m = male, GBM = Glioblastoma multiforme, GS = Gliosarcoma, wt = wildtype, mut = mutant, UM = unmethylated, M = methylated, R-Ch-Th = chemoradiotherapy, R-Th = radiotherapy, Ch-Th = chemotherapy, adj. = adjuvant, OS = overall survival, KPS = Karnofsky performance status. Not specified data is indicated with a n.s. 20
Table 2: *PyroMark Assay Design* software settings used for automatic primer design. 23
Table 3: General PCR reaction setup – *EpiTect HRM PCR Kit*[147] 24
Table 4: Modified thermal cycling program using the *EpiTect HRM PCR Kit*[147]. Annealing and elongation temperatures are method dependent. 25
Table 5: Master mix setup used for pyrosequencing using the *PyroMark Q24 Advanced CpG Reagents Kit*[148]. 26
Table 6: Characteristics of primer set 1 for the GBX2 promoter. 35
Table 7: Characteristics of primer set 2 for the GBX2 promoter. Green-highlighted: CpG site. 38
Table 8: Two-tailed Spearman-Rho test for correlations between MGMT promoter methylation and MGMT expression. r_S = Spearman-Rho correlation coefficient, ***: $p < 0.001$. 41
Table 9: Characteristics of patients and their MGMT promoter methylation status in 40 GBM samples. 44
Table 10: Two-tailed Spearman-Rho test for correlations between MGMT enhancer E methylation and MGMT expression. r_S = Spearman-Rho correlation coefficient, *: $p < 0.05$, **: $p < 0.01$. 45
Table 11: Two-tailed Spearman-Rho test for correlations between MGMT enhancer K-M methylation and MGMT expression, applied to all 40 GBM samples. r_S = Spearman-Rho correlation coefficient. 47
Table 12: Two-tailed Spearman-Rho test for correlations between MGMT enhancer K-M methylation and MGMT expression, applied to the 19 MGMT expressing samples. r_S = Spearman-Rho correlation coefficient. 48
Table 13: Comparison of MGMT enhancer K-M methylation between samples with low and high Ki67 expression. *: $p < 0.05$. 51